University of Alberta

Aspects of Excitation-Contraction Coupling and Wound Healing in Striated Muscles of the Hydromedusa, *Polyorchis penicillatus* - and Labelling of the Nervous System Using a Monoclonal Antibody

by

Yi-Chan James Lin ©

A thesis submitted to the Faculty of Graduate Studies and Research in partial fulfillment of the requirements for the degree of Doctor of Philosophy

in

Physiology and Cell Biology
Department of Biological Sciences

Edmonton, Alberta
Fall 1999

National Library
of Canada

Acquisitions and
Bibliographic Services

395 Wellington Street
Ottawa ON K1A 0N4
Canada

Bibliothèque nationale
du Canada

Acquisitions et
services bibliographiques

395, rue Wellington
Ottawa ON K1A 0N4
Canada

Your file Votre référence

Our file Notre référence

The author has granted a non-exclusive licence allowing the National Library of Canada to reproduce, loan, distribute or sell copies of this thesis in microform, paper or electronic formats.

L'auteur a accordé une licence non exclusive permettant à la Bibliothèque nationale du Canada de reproduire, prêter, distribuer ou vendre des copies de cette thèse sous la forme de microfiche/film, de reproduction sur papier ou sur format électronique.

The author retains ownership of the copyright in this thesis. Neither the thesis nor substantial extracts from it may be printed or otherwise reproduced without the author's permission.

L'auteur conserve la propriété du droit d'auteur qui protège cette thèse. Ni la thèse ni des extraits substantiels de celle-ci ne doivent être imprimés ou autrement reproduits sans son autorisation.

0-612-46874-7

Canada

University of Alberta

Library Release Form

Name of Author: Yi-Chan James Lin

Title of Thesis: Aspects of Excitation-Contraction Coupling and Wound Healing in Striated Muscles of the Hydromedusa, *Polyorchis penicillatus* - and Labelling of the Nervous System Using a Monoclonal Antibody

Degree: Doctor of Philosophy

Year this Degree Granted: 1999

Permission is hereby granted to the University of Alberta Library to reproduce single copies of this thesis and to lend or sell such copies for private, scholarly, or scientific research purposes only.

The author reserves all other publication and other rights in association with the copyright in the thesis, and except as hereinbefore provided, neither the thesis nor any substantial portion thereof may be printed or otherwise reproduced in any material form whatever without the author's prior written permission.

63, Chaung Shin St. Tainan
Taiwan, R. O. C.

Date: September 30, 1999

University of Alberta

Faculty of Graduate Studies and Research

The undersigned certify that they have read, and recommend to the Faculty of Graduate Studies and Research for acceptance, a thesis entitled Aspects of Excitation-Contraction Coupling and Wound Healing in Striated Muscles of the Hydromedusa, *Polyorchis penicillatus* submitted by Yi-Chan James Lin in partial fulfillment of the requirements for the degree of Doctor of Philosophy in Physiology and Cell Biology.

Dr. A.N. Spencer, supervisor

Dr. W.J. Gallin, examiner

Dr. J.P. Chang, examiner

Dr. R.B. Campenot, examiner

Dr. G.G. Goss, examiner

Dr. R.E. Steele, external examiner

Sept. 29, 1999

Date of approval by committee

Abstract

The impetus for the studies described in this thesis evolved from a wish to examine differentiation events in inexcitable precursors that produce excitable cell types in a cnidarian. Experimental systems were developed to examine the morphology and physiology of de- and re-differentiation in striated muscle cells.

In situ subumbrellar muscle cells of the hydromedusa *Polyorchis penicillatus* have a distinct polarity with the somata forming the outer epithelium and interdigitating contractile feet below forming a muscle sheet. After wounding, the muscle cells at the wound margin absorbed their feet, removed ion channels from the cell membrane, developed lamellipodia, and migrated centripetally. Migration ceased when cells met at the centre of the wound whereupon cells regained their former morphology with fully functional contractile feet. Cell migration did not require protein synthesis or an extracellular source of calcium, unlike contraction of the intact muscle where calcium influx through voltage-gated channels was shown to be required. Whole-cell patch clamp recordings from "heat fixed" muscle cells showed that calcium influx was via T-type calcium channels. Localisation of these channels by fluorescence-labelled dihydropyridines showed that these channels were distributed in the membrane of the myofibrillar region in a higher density than in the somal region. Reduction of the contractile force of isolated muscle strips by caffeine demonstrated that a proportion of the calcium used to initiate contraction was also derived from intracellular sources, possibly through a calcium-induced calcium release mechanism. The presence of

calcium stores in muscle cells just beneath the sarcolemma was confirmed by both cytohistochemical localisation of Ca^{2+}-ATPase and ultrastructural localisation of calcium using both transmission electron microscopy and electron energy-loss spectroscopy.

A monoclonal antibody was developed as an adjunct to the main thrust of the studies constituting this thesis. This antibody labelled all known neurons and their precursors in one single preparation which previously could only be labelled or stained using several techniques. In addition several new features of the hydromedusan nervous system were revealed using this antibody. Such a general neuronal labelling antibody will be extremely valuable for both tracing neuronal lineage studies in culture and *in vivo* and as an adjunct to studies of the neuronal basis of behaviour.

Acknowledgements

I like to thank the following people for their help: My supervisor, Dr. A. N. Spencer for his guidance and inextinguishable patience in my program; my supervisory committee members, Dr. J. P. Chang, Dr. W. J. Gallin, and Dr. R. B. Campenot for their valuable suggestions, especially Dr. J. P. Chang and Dr. W. J. Gallin for letting me use their laboratory facilities; my friend, Dr. N. Grigoriev for teaching me patch-clamp techniques and setting up my first perfusion system (chapter 3, 4, 5), valuable discussion, and encouragement; Mr. G. Braybrook for carrying out the SEM (chapter 3); Mr. R. Bhatnagar and Mr. R. Mandryk for their technical support in histology, TEM, and confocal microscopy (chapter 2, 3, 4, and 5); Dr. D. Bazzet-Jones and Mr. M. Herfort in the University of Calgary for helping on the calcium EELS (chapter 5); staff members at Bamfield Marine Station for collecting and shipping jellyfish; Dr. C. Wang, Dr. S. Buckinghan, Mr. J. Johnson, and Ms. B. Hepperle for reading and correcting my manuscripts; Dr. J. Goldberg for letting me use his laboratory computer from time to time.

I also like to thank the Department of Biological Sciences and NSERC (operating grants to Dr. A. N. Spencer) for providing financial support.

On a personal side I like to thank my parents for their continued support both financially and emotionally; my wife for her company and emotional support throughout this program.

Table of Contents

Chapter 1 - General introduction 1
Anatomy of a cnidarian nervous system 3
Wound healing 4
Striated swimming muscle in jellyfish 7
Voltage-gated calcium currents in Cnidaria 8
Sarcoplasmic reticulum in excitation-contraction coupling 10

REFERENCES 13

Chapter 2 - The anatomy of the nervous system of the hydrozoan jellyfish, *Polyorchis penicillatus*, as revealed by a monoclonal antibody 20

INTRODUCTION 20

MATERIALS AND METHODS 22
Production of monoclonal antibodies 22
Immunofluorescence microscopy and laser scanning confocal microscopy.. 23

RESULTS 24
Subumbrella and peduncle 25
Radii 26
Marginal region 27
Ocelli and ocellar nerves 28
Tentacles 29
Gonads and manubrium 30

DISCUSSION 31
Swimming motor neuron network 32
Peduncle, manubrium and gonads 34
Tentacles 35
Marginal region ("B" and "O" systems) 36
Endodermal systems 37
General conclusions 37

REFERENCES 52

Chapter 3 - Scarless wound healing in jellyfish striated muscle involves rapid switching between two modes of cell motility 54

SUMMARY 54

RESULTS AND DISCUSSION 55

METHODS 62
    Wounding procedure 62
    Electron microscopy and laser confocal microscopy 62
    Pharmacology of muscle contraction 63
    Electrophysiology 64

REFERENCES 73

Chapter 4 - Characterization and localisation of a T-type calcium channel from a hydrozoan jellyfish, *Polyorchis penicillatus* 75

INTRODUCTION 75

MATERIALS AND METHODS 78
    Cell dissociation and electrophysiology 78
    Solutions 79
    Pharmacology of muscle contraction 80
    Localisation of calcium channels 81

RESULTS 83
    Cell dissociation 83
    Calcium-selective inward current 83
    Permeability to divalent cations 84
    Electrical and Kinetic properties 84
    Pharmacology 85
    Localisation of T-channels by fDHP 86

DISCUSSION 87
    Cell dissociation channel localisation 87
    Channel kinetics 88
    Pharmacology 89
    Possible function of T-type calcium channels in jellyfish striated muscle cells 90
    Implications for channel evolution 91

REFERENCES 93

Chapter 5 - Localisation of intracellular calcium stores putatively involved in excitation-contraction coupling 107

INTRODUCTION 107

MATERIALS AND METHODS 110
  Field stimulation of muscle strips 110
  Localisation of Ca^{2+}-ATPase 111
  Ultrastructural localisation of calcium 112
  Electron energy-loss spectroscopy (EELS) 112

RESULTS 114
  Field stimulation of muscle strips 114
  Localisation of Ca^{2+}-ATPase 115
  Ultrastructural localisation of calcium 116

DISCUSSION 118

REFERENCES 137

Chapter 6 - General conclusion 141

  Neuroanatomy 141
  Wound healing 142
  T-type calcium currents in muscle contraction 146
  Putative calcium stores involved in excitation-contraction coupling 149
  Calcium dependence of cell migration 150
  Conclusion 151

REFERENCES 153

Appendix - Isolation and culture of interstitia cells 157

REFERENCES 162

List of Tables

Appendix

Table A1- Components of the jellyfish culture medium........................160, 161

List of Figures

Chapter 2

Figure 2.1 - Diagram of *Polyorchis penicillatus*..........39

Figure 2.2 - Whole-mount preparation of the subumbrellar area near the peduncular region labelled with the monoclonal antibody 5C6..........40, 41

Figure 2.3 - Whole-mount of a portion of the radial canal region with an inset showing a transverse section of the same region labelled with the monoclonal antibody 5C6..........42, 43

Figure 2.4 - Marginal region and the nerve-rings labelled with the monoclonal antibody 5C6..........44, 45

Figure 2.5 - An ocellus labelled with the monoclonal antibody 5C6..........46, 47

Figure 2.6 - Whole-mount of a tentacle labelled with the monoclonal antibody 5C6..........48, 49

Figure 2.7 - Whole-mounts of the manubrium and gonad and a section of the gonad labelled with the monoclonal antibody 5C6..........50, 51

Chapter 3

Figure 3.1 - Changes in cell morphology during the wound-healing process in jellyfish striated muscle cells..........66, 67

Figure 3.2 - Migrating cells generate traction forces and maintain gap junctional connections..........68, 69

Figure 3.3 - Effect of different pharmacological agents on muscle contraction and migration..........70, 71

Figure 3.4 - Diagram of the wound healing process..........72

Chapter 4

Figure 4.1 - Dissociation of striated muscle cells from *Polyorchis penicillatus* at different temperatures and their associated membrane currents..........93, 94

Figure 4.2 - T-type current recorded from a muscle cell dissociated at 30°C..............95

Figure 4.3 - Voltage dependence of time to peak (upper panel) and inactivation time constant (lower panel) of the T-type current..96

Figure 4.4 - Steady-state inactivation and recovery from inactivation of the T-type current..97

Figure 4.5 - Effect of various dihydropyridines and verapamil on swimming muscle contraction..98

Figure 4.6 - Effect of two dihydropyridines on the T-type calcium current of swimming muscle...99

Figure 4.7 - Labelling of striated muscle cells dissociated at room temperature (a) and 30°C (b) with RH414 and fDHP..100, 101

Chapter 5

Figure 5.1 - Force-frequency relationship of the swimming muscle..................123, 124

Figure 5.2 - Ultrastructure of the swimming muscle...125, 126

Figure 5.3 - Ca^{2+}-ATPase in the soma of swimming muscle.............................127, 128

Figure 5.4 - Ca^{2+}-ATPase in the myofibrils of swimming muscle......................129, 130

Figure 5.5 - Negative control for the Ca^{2+}-ATPase activity..............................131, 132

Figure 5.6 - Localisation of calcium in the swimming muscle...........................133, 134

Figure 5.7 - Electron energy loss spectroscopy of calcium localisation..........135, 136

List of Symbols, Nomenclature, and Abbreviations

AgaIVA - agatoxin.

A-type - fast inactivated potassium channels.

ASW - artificial seawater.

"B" systems - a group of neurons showing bursts of action potentials, located in the outer nerve-ring of *Polyorchis*.

BODIPY FL phalloidin - 4,4-difluoro-4-bora-3a,4a-diaza-s-indacene conjugated phalloidin for labelling actin.

BrdU - bromodeoxyuridine.

Ca^{2+}-ATPase - a large class of enzymes that transports calcium by the hydrolysis of adenosine 5'-triphosphate.

CTx - conotoxin.

C_m - membrane capacitance.

DABCO - diazabicyclo{2.2.2}octane.

DHPRs - voltage-gated, dihydropyridine-sensitive calcium channels.

DMSO -dimethy sulfoxide.

EDTA - ethylenediaminetetraacetic acid.

EELS - electron energy loss spectroscopy.

EGF - epidermal growth factor.

EGTA - ethylene glycol-bis(β-aminoethyl ether)-N,N,N',N'-tetraacetic acid.

eV - electron volt; the energy an electron receives when accelerated by a voltage of 1 V.

fDHP - fluorescent dihydropyridine-BODIPY.

FITC - fluorescein isothiocyanate.

FTX - funnel-web spider toxins.

GABA$_A$ - γ-aminobutyric acid receptor type A.

GABARAP - GABA$_A$-receptor-associated protein.

HEPES - N-2-hydroxyethylpiperazine-N'-2-ethanesulfonic acid.

HVA - high-voltage-activated.

Hz - hertz.

IgG - immunoglobulin.

I_{max} - maximum current.

I-V - current-voltage relationship.

kHz - kilohertz.

kV - kilovolt; accelerating voltage.

L-type - high-voltage-activated calcium channels, sensitive to dihydropyridines.

LVA - low-voltage-activated.

"O" systems - a group of neurons showing a slowly oscillating membrane potential, identified in the outer nerve ring of *Polyorchis*.

mAb - monoclonal antibody.

mg - milligram.

Min - minute.

mM - millimolar.

ms - millisecond.

mV - millivolt.

MΩ - megaohm.

μm - micrometer.

μM - micromolar.

μs - microsecond.

N-type - high-voltage-activated calcium channels, sensitive to conotoxin.

nA - nanoampere.

NMG - N-methyl-D-glucamine.

P-type - high-voltage-activated calcium channels, sensitive to funnel-web spider toxins.

pA - picoampere.

P_{Ba}, P_{Ca}, P_{Sr} - permeability, expressed in 1/s, calculated using the Goldman-Hodgkin-Katz constant-field equation.

PBS - phosphate-buffered saline.

PBST - phosphate-buffered saline with 0.25% Tween 20 or Triton X-100.

Q-type - high-voltage-activated calcium channels, sensitive to agatoxin.

R-type - high-voltage-activated calcium channels, no antagonists available.

RH414 -a styryl dye.

RN - radial nerve.

R_s - series resistance.

RyRs - ryanodine receptors.

s - second.

S5, S6 - alpha-helical, hydrophobic, transmembrane segments.

S.E. - standard error.

SEM - scanning electron microscopy.

SMN - swimming motor neuron.

SR - sarcoplasmic reticulum.

TEA - tetraethylammonium.

TEM - transmission electron microscopy.

TGF-α - transforming growth factor α.

T-type - a calcium current activating at low voltage range.

T-tubules - transverse tubules in muscle cells.

τ - time constant.

Vg - voltage-gated.

V_h - voltage of half-activation.

Chapter 1

General introduction

Cnidarians are composed of two epithelia, an epidermis and a gastrodermis derived from ectoderm and endoderm, respectively during embryogenesis, and mesoglea, the extracellular matrix between these two layers of tissues (Hyman 1940). Muscular structures are usually formed from differentiated myoid processes at the basal portion of epithelia, both epidermal and gastrodermal (Hyman 1940, Chapman 1974). These myoid processes can be either smooth or striated. The nervous system is embedded among the basal portions of epithelial cells and is made up of only three or four basic cell types, including sensory cells, ganglion cells, and neurosecretory cells (Thomas and Edwards 1991). The relatively "simple" nervous systems (in terms of neuronal types) make cnidarians attractive animals for neurobiologists. Many of the advances in the cellular-level neurophysiology in cnidarians have come from studies on hydromedusae and scyphomedusae (Anderson 1987, 1989, Mackie and Meech 1985, 1989, Spencer et al. 1989, Przysiezniak and Spencer 1992, 1994, Meech and Mackie 1993a, b, Grigoriev et al. 1996, Spafford et al. 1996), since these cnidarians contain "giant" neurons which make better accessibility for electrophysiological study (Mackie 1990). These studies revealed that the mechanism of membrane excitability in cnidarians does not differ from other animal systems. The generation and shape of action potentials are governed by the balance among sodium, calcium, and potassium currents. However, the development of cellular excitability during cell differentiation and the regulation of ion channel expression are still largely unknown.

The objective of this thesis was to study the development of cellular excitability and the regulation of their expression in cnidarians. Two experimental systems were intended to develop for this study. The first one is the differentiation of nerve cell. Nerve cells were chosen because the presence of large amount of information regarding their cellular excitability. Nerve cells in cnidarians are derived from a group of pluripotent cells, interstitial cells (Thomas and Edwards 1991). Interstitial cells are present during embryogenesis and throughout the life span of the adult animals. The derivatives of interstitial cells include nerve cells, gland cells, gametes, and cnidocytes (Thomas and Edwards 1991). Interstitial cells can be identified by their relative large nuclear and basophilic cytoplasm (Thomas and Edwards 1991). The approach for this experimental system was to isolate interstitial cells, culture them *in vitro*, and trigger them differentiate into nerve cells. The development of cellular excitability would be monitored by using whole-cell patch-clamping recording techniques. Interstitial cells were isolated by using PERCOLL step gradient and kept *in vitro* (Appendix). However, cultured interstitial cells were not able to be driven into the differentiation of nerve cells, even after trying several chemicals which were known to trigger neuronal differentiation (Appendix). Therefore this direction was abandoned.

The second experimental system to develop was the wound-healing process of striated muscle cells of medusa. It was noticed that these striated muscle cells dedifferentiated immediately when dissociated in culture (the term "dedifferentiation" used in this thesis is defined as the removal or down-regulation of voltage-gated ion channels, since the presence of voltage-gated ion channels is a functional requirement for excitability). Another noticed phenomena was that small wounds in the swimming muscle, where cells had been abraded from the mesoglea, healed very rapidly with no trace of scarring. Preliminary investigations suggested that denuded areas were covered by muscle cells migrating from the wound margin to cover the wound. It therefore seemed likely that these two phenomena were linked in that contractile muscle cells had to convert to a phenotype that was capable of migration. Since both muscle contraction and cell motility involve mobilisation and sequestration of calcium but, presumably, with very different kinetics and compartmentalisation I decided to investigate both excitation contraction coupling and the wound-healing process in more depth.

Anatomy of a cnidarian nervous system

An important experimental tool for examining the differentiation of neurons *in vivo* and in culture would be the ability to label all neuronal cell precursors, that is interstitial cells, and their descendents using specific markers. Previous studies used . a variety of histological techniques, such as vital methylene blue staining and silver staining (Jha and Mackie 1967), immuno-labelling against transmitters (Grimmelikhuijzen and Spencer 1984, Mackie et al. 1985, Grimmelikhuijzen et al. 1986), Lucifer yellow and carboxyfluoroscein iontophoresis (Spencer 1981, Spencer and Arkett 1984), and TEM ultrastructure examination (Jha and Mackie 1967, Singla 1978a, b, Spencer 1979, Anderson and Grunert 1988) to study nerve systems of medusae. However, none of the above methods has provided a complete picture of the anatomy of the nervous system, nor applicable to the intended *in vitro* study.

The hybridoma technique (Kohler and Milstein 1975, 1976) has been used successfully to generate monoclonal antibodies against hydra neurons (Dunne et al. 1985, Yaross 1986, Sakaguchi et al. 1996). Thus, this method was used to generate monoclonal antibodies against nerve cells in jellyfish and these antibodies were used to elucidate the anatomy of the nervous system. I have isolated a monoclonal antibody that labels all known nerve elements of the hydromedusan *Polyorchis penicillatus* and some previously undescribed nerve elements (Chapter 2). Labelling with this monoclonal antibody revealed that the swimming motor neurons form a continuous network encircling each quadrant of swimming muscle to synchronise excitation of the muscle sheet.

Wound healing

Striated muscles of the jellyfish, *Polyorchis penicillatus*, are capable of migration and participate in wound healing *in vivo* when the nearby muscles are damaged. The striated muscle cells involved in wound healing first de-differentiate (removal of ion channels), migrate, and then re-differentiate (reappearance of ion channels). In contrast, terminally differentiated adult mammalian striated muscles (skeletal and cardiac) are irreversibly withdrawn from the cell cycle (Zak 1974, Nadal-Ginard 1978), and do not undergo dedifferentiation, proliferation and migration as do smooth muscle cells in primary culture (Campbell et al. 1971, Campbell and Campbell 1995). Wound-healing in mammalian striated muscle consists of a cascade of highly orchestrated events involving migration, proliferation, and differentiation of inflammatory cells, fibroblasts, endothelial cells, and matrix remodelling (Schaffer and Nanney 1996, Witte and Barbul 1997). In adult skeletal muscle, a small pool of quiescent, undifferentiated myogenic stem cells, termed satellite cells can proliferate, differentiate, and fuse into multinucleated myofibres to restore muscle function (Megeney et al. 1996, Schultz 1996). In cardiac tissue no such undifferentiated stem cell population exists and necrosis leads to a functional loss after healing (Weber et al. 1996).

Despite the large amount of information regarding regeneration and morphogenesis in cnidarians, particularly in *Hydra* (Hyman 1940, Tardent 1965, Gierer et al. 1972, Bode et al. 1988, Shimizu et al. 1993, Shimizu and Sugiyama 1993), the cellular mechanism regulating the wound-healing process is still not clear (Campbell and Bibb 1970, Bibb and Campbell 1973, Campbell 1985). The process of re-epithelialization during wound-healing in vertebrate systems (Stenn and DePalma 1988) will be reviewed briefly here, since this process resembles wound-healing in jellyfish. Re-epithelialization involves cellular dedifferentiation, migration, proliferation, and differentiation of each cell. At the border of the wound, cells are induced to migrate. The signal that induces the cells to become migratory is not clear, although the change in the concentration of extracellular calcium is known to be associated with the beginning of migration (Grzesiak and Piershbacher 1995). Different integrins are expressed as cells become migratory (Cavani et al. 1993). Epithelial cells first retract tonofilaments and dissolve hemidesmosomes and desmosomes which link them to basal lamina and each other, respectively. At the same time, they lose their cuboidal, polarized shape, flatten out, and form lamellipodia with actin filaments on the side facing the wound to provide the motor apparatus for migration (Gabbiani et al. 1978). Cells either migrate as a whole cell sheet in which marginal cells lead the sheet and pull it along, or by marginal cells rolling over one another (Stenn and DePalma 1988). Cell proliferation does not occur in the migratory population at the wound edge but happens some distance from the wound margin. However, migration is not altered even when proliferation is inhibited (Schaffer and Nanney 1996). Cytokines, for example EGF and TGF-α, are known to be involved in both migration and proliferation of epithelial cells (Lawrence 1998). Cells migrate until a confluent cell layer covers the wounded area. When contact inhibition halts migration. Cells then re-differentiate into polarised morphology with separated soma and feet.

Thus, the wound-healing process in jellyfish represents a unique case in which striated muscles are capable of migration and participate in wound healing and deserve further study to elucidate the underlying mechanisms. Chapter 3 describes the wound-healing process in a jellyfish striated muscle sheet. The wound-healing process involves the transformation of polarised myoepithelial cells which have separate somal and myofibrillar regions into lamellipodia-bearing, keratocyte-like, migratory cells. Accompanying the cellular transformation, calcium channels are removed and cell motility then depends on intracellular calcium stores whereas normal muscle contraction depends on the availability of extracellular calcium.

The calcium dependence of muscle contraction was further characterised by examining the voltage-gated calcium channels on the cell membrane and the presence of a sarcoplasmic reticulum in the striated muscles as the putative source of intracellular calcium for muscle contraction in the subsequent two chapters (Chapter 4 and 5).

Striated, swimming muscle in jellyfish

Jet propulsion (swimming) in jellyfish is produced by contraction of the subumbrellar swimming muscle (Gladfelter 1972). This group of muscles is under neuronal control (Spencer and Satterlie 1981, Spencer 1982). The striated swimming muscle sheets of hydromedusae are formed by a single layer of cells which also face the seawater, and hence they are termed "myoepithelial cells" or "epithelio-muscular cells" (Chapman 1974). Myoepithelial cells are considered a "primitive" type of muscle cell and are widely distributed among several animal phyla, including cnidarians, ctenophores, annelids, echinoderms, and vertebrates (Paniagua et al. 1996). Myoepithelial cells can be subdivided into smooth and striated, based on the organization of thin and thick filaments in the myofibrils. Striated myoepithelial cells are only found in the subumbrellar area in medusae where they produce the phasic contractions associated with swimming (Chapman et al. 1962, Thomas and Edwards 1991). These cells generally possess somal and myofibrillar regions. The somal region contains vacuoles, Golgi complexes, and mitochondria whereas the basal region or foot contains striated myonemes. Most of the mitochondria are concentrated in the perimyofibrillar cytoplasm which is just basal to the somal region. Like other striated muscles the myofibrils are composed of thick and thin filaments and arranged into sarcomeres with A, I, H, and Z bands (Keough and Summers 1976, Singla 1978a, b). However, unlike vertebrate striated muscle where many myofibrils are confined within the same sarcoplasmic membrane, each myofibril in medusae is segregated by sarcoplasmic membrane. Myofibres are joined end-to-end by desmosomes and side-by-side by gap junctions (Keough and Summers 1976, Singla 1978a, b, Spencer 1979). A well-defined T-tubular system has not been reported in hydromedusae, except some membrane-bound vesicles and tubules have been found in the sub-sarcolemma cytoplasm in *Aglantha digitale* (Singla 1978a) and *Halocordyle disticha* (Keough and Summers 1976).

Voltage-gated calcium currents in Cnidaria

Based on their voltage-activation range, voltage-gated calcium channels can be categorized into high voltage activated (HVA) channels and low voltage activated (LVA) channels. In general, HVA calcium channels activate at > -40 mV. Further classification of HVA channels depends on their sensitivity to different pharmacological agents: dihydropyridines (L-type; Fox et al. 1987), ϖ-conotoxin (CTx)-GVIA (N-type; McCleskey 1987), funnel-web spider toxins FTX and low concentrations (2 nM) of ϖ-Agatoxin (AgaIVA) (P-type; Llinas et al. 1989, Mintz et al. 1992), and high concentrations (200 nM) of AgaIVA (Q-type; Sather et al. 1993). The R-type channels are a class of HVA channels that are resistant to dihydropyridines, ϖ-conotoxin (CTx)-GVIA, ϖ-CTx-MVIIC, and ϖ-Agatoxin (AgaIVA) (Randall and Tsien 1995).

LVA channels activate at around -70 to -40 mV, inactivate rapidly, and are sensitive to Ni^{2+} and mibefradil (Akaike et al. 1989, Huguenard 1996, Ertel 1997). Only one type of channel, T-type channel has been described for LVA channels (Tsien 1998). The recording traces of T-type currents show a distinct pattern which is in a manner reminiscent of classical sodium currents which with progressively stronger depolarisation, successive currents activate and inactivate faster (Randall and Tsien 1997).

Both HVA and LVA calcium currents have been described in various cnidarians, including *Cyanea*, *Obelia*, *Calliactis*, *Polyorchis,* and *Aglantha* (Anderson 1987, Dunlap et al. 1987, Holman and Anderson 1991, Przysiezniak and Spencer 1992, Meech and Mackie 1993b). The HVA currents of *Polyorchis* neurons are apparently responsible for transmitter release at the pre-synaptic terminal (Anderson 1987, Spencer et al. 1989) and those in anemone myoepithelial cells with muscle contraction. The LVA current in *Aglantha* giant axons produces low-amplitude and low-threshold calcium spikes which control slow swimming, while in the same axon a sodium current produces high-amplitude and high-threshold action potentials responsible for escape swimming (Mackie and Meech 1985). In *Obelia* epithelial cells the LVA current serves as a source of calcium for regulating bioluminescence in neighbouring photocytes (Dunlap et al. 1987).

Contraction of striated muscle in the hydromedusa *Polyorchis penicillatus* depends on the availability of extracellular calcium, presumably through voltage-gated calcium channels (Spencer and Satterlie 1981, and Chapter 3). The depolarisation phase of the action potential depends on both extracellular sodium and calcium ions (Spencer and Satterlie 1981), indicating the possible involvement of LVA (T-type) channels in the initiation of action potentials. However, prior to or during migration calcium channels are removed from cell membrane (Chapter 3) which contrasts to the vertebrate systems where T-type calcium channels up regulate in injured tissue (Sen and Smith 1994, Nuss and Houser 1993).

Tight-seal, whole-cell patch clamp recording was used to examine the ion currents in membranes of acutely dissociated muscle cells (Chapter 4). The only inward component of the total ionic current was found to be a T-type calcium current and no sodium current was dectected. Chapter 4 also describes the electro-kinetics and pharmacology of this T-type current. This channel was localised by using a fluorescence-labelled calcium antagonist, dihydropyridine, and confocal microscope. These images show that the sarcolemma has a higher intensity of fluoresence, suggesting a differential distribution of this channel.

Sarcoplasmic reticulum in excitation-contraction coupling

The sequence of excitation-contraction coupling in vertebrate muscle cells starts with a propagated depolarisation invading the plasma membrane. This change in potential across the membrane activates voltage-gated, calcium channels (DHPRs), which either leads to a direct increase in intracellular Ca^{2+} or to the release of Ca^{2+} from internal calcium stores in the sarcoplasmic reticulum (SR) through Ca^{2+} release channels (Winegrad 1965, Inui et al. 1987). The mechanism of calcium release via ryanodine-sensitive channels (RyRs) in the sarcoplasmic reticulum differs for skeletal and cardiac muscles. In skeletal muscle, Ca^{2+} influx through DHPRs is not required to initiate Ca^{2+} release from the SR (Nabauser et al. 1989) since DHPRs interact directly with RyRs at a molecular level (Flucher and Franzini-Armstrong 1996). In contrast, cardiac muscle requires Ca^{2+} influx through DHPRs in cardiac muscle to activate Ca^{2+} release from the SR through a process known as calcium-induced calcium release (Fabiato 1983). Calcium-induced calcium release is generally accepted as the major source of calcium for regulation of contraction in cardiac muscle, although there may be some contribution from Ca^{2+} influxing through DHPRs (Bers et al. 1993).

The development of sarcoplasmic reticulum in striated muscle can be as elaborate and sophisticated as vertebrate skeletal muscle where SR and T-tubule form triads which are precisely positioned above the Z line in each sarcomere (Fawcett 1986). In cases like this, muscle contraction is completely dependent on calcium released from sarcoplasmic reticulum. At the other extreme, where a sarcoplasmic reticulum is absent, such as the striated muscles of the tunicate *Doliolum nationalis*, muscle contraction depends on calcium influx through the sarcolemma (Bone 1997). Other striated muscles showing varying degrees of development of the sarcoplasmic reticulum, including vertebrate cardiac and invertebrate muscles, calcium influx is essential for muscle contraction and triggering the release of calcium from sarcoplasmic reticulum. Thus, it appears that the requirement for extracellular calcium influx for muscle contraction is inversely correlated with the development of the sarcoplasmic reticulum (Bers 1991, Ashley et al. 1993, Palade and Györke 1993, Paniagua et al. 1996).

For *Polyorchis* striated swimming muscle, facilitation in the amplitude of contraction tension was observed during a train of stimuli (Spencer and Satterlie 1981). Here we demonstrated that the amplitude of contractile tension was suppressed in the presence of caffeine (Chapter 3 and 5). These physiological data indicate the possible presence of calcium stores, possibly the sarcoplasmic reticulum, and the presence of a calcium induced calcium release mechanism. However, no sarcoplasmic reticulum network resembling that of vertebrates was observed in our ultrastructural studies. However, we did observe several large, membrane-bound, electron-lucent vesicles at the perimyofibrillar region (Singla 1978a, Spencer 1979, Chapter 5). To examine if these membrane vesicles are sarcoplasmic reticulum or functionally equivalent to sarcoplasmic reticulum, cytochemical methods were chosen to examine if Ca^{2+}-ATPase activity and calcium were present in these vesicles (Chapter 5). Results from this cytochemical study indicate the presence of Ca^{2+}-ATPase activity and calcium in these vesicles. Therefore these vesicles are functionally equivalent to sarcoplasmic reticulum.

REFERENCES

Akaike, N., Kanaide, H., Kuga, T., Nakamura, M., Sadoshima, J., and Tomoike, H. (1989). Low-voltage-activated calcium current in rat aorta smooth muscle cells in primary culture. *J. Physiol.* **416**, 141-60.

Anderson, P. A. V. (1987). Properties and pharmacology of a TTX-insensitive Na^+ current in neurons of the jellyfish, *Cyanea capillata*. *J. Exp. Biol.* **133**, 233-248.

Anderson, P. A. V. (1989). Ionic currents of the Scyphozoa. *In* Evolution of the First Nervous Systems, vol. 188 (ed. P. A. V. Anderson). New York: Plenum Press.

Anderson, P. A. and Grunert, U. (1988). Three-dimensional structure of bidirectional, excitatory chemical synapses in the jellyfish *Cyanea capillata*. *Synapse* **2**, 606-13.

Ashley, C. C., Griffiths, P. J., Lea, T. J., Mulligan, I. P., Palmer, R. E., and Simnett, S. J. (1993). Barnacle muscle: Ca^{2+}, activation and mechanics. *Rev. Physiol. Biochem. Pharm.* **122**, 149-258.

Bers, D. M. (1991). Excitation-contraction coupling and cardiac contractile force. Boston: Kluwer Academic.

Bers, D. M., Bassani, J. W. M., and Bassani, R. A. (1993). Competition and redistribution among calcium transport systems in rabbit cardiac myocytes. *Cadioves. Res.* **27**, 1772-1777.

Bibb, C. and Campbell, R. D. (1973). Tissue healing and septate desmosoome formation in hydra. *Tiss. Cell* **5**, 23-35.

Bode, P. M., Awad, T. A., Koizumi, O., Nakashima, Y., Grimmelikhuijzen, C. J., and Bode, H. R. (1988). Development of the two-part pattern during regeneration of the head in hydra. *Development* **102**, 223-35.

Bone, Q., Inoue, I., and Tsutsui, I. (1997). Contraction and relaxation in the absence of a sarcoplasmic reticulum: muscle fibers in the small pelagic tunicate *Doliolum*. *J. Mus. Res. Cell Motil.* **18**, 375-80.

Campbell, G. R. and Campbell, J. H. (1995). Development of vessel wall: overview. *In* The vascular smooth muscle cell: molecular and biological responses to the extracellular matrix (eds. S. M. Schwartz and R. P. Mecham). San Diego: Academic Press, Inc.

Campbell, G. R., Uehara, Y., Mark, G. E., and Burnstock, G. (1971). Fine structure of smooth muscle cells grown in tissue culture. *J. Cell Biol.* **49**, 21-34.

Campbell, R. D. (1985). Tissue architecture and hydroid morphogenesis: the role of locomotory traction in shaping the tissue. *In* The cellular and molecular biology of invertebrate development (ed. R. H. Sawyer and R. M. Showman). University of South Carolina Press.

Campbell, R. D. and Bibb, C. (1970). Transplantation in coelenterates. *Transpl. Proc.* 2(2): 202-201.

Cavani, A., Zambruno, G., Marconi, A., Manca, V., Marchetti, M., and Gianetti, A. (1993). Distinctive integrin expression in the newly forming epidermis during wound healing in humans. *J. Invest. Dermatol.* **101**, 600-604.

Chapman, D. M. (1974). Cnidarian Histology. *In* Coelenterate biology: review and new perspectives (ed. L. Muscatine and H. M. Lenhoff). New York: Academic Press, Inc.

Chapman, D. M., Pantin, C. F. A., and Robson, E. A. (1962). Muscle in coelenterates. *Rev. Canad. Biol.* **21**, 267-278.

Dunlap, K., Takeda, K., and Brehm, P. (1987). Activation of a calcium-dependent photoprotein by chemical signaling through gap junctions. *Nature* **325**, 60-62.

Dunne, J. F., Javois, L. C., Huang, L. W., and Bode, H. R. (1985). A subset of cells in the nerve net of *Hydra oligactis* defined by a monoclonal antibody: its arrangement and development. *Dev. Biol.* **109**, 41-53.

Ertel, S. I., Ertel, E. A., and Clozel, J. P. (1997). T-type Ca^{2+} channels and pharmacological blockade: potential pathophysiological relevance. *Cardiovas. Drugs Ther.* **11**, 723-39.

Fabiato, A. (1983). Calcium-induced release of calcium from the cardiac sarcoplasmic reticulum. *Am. J. Physiol.* **245**, C1-14.

Fawcett, D. W. (1986). A textbook of histology. Philadelphia: Saunders.

Flucher, B. E. and Franzini-Armstrong, C. (1996). Formation of junctions involved in excitation-contraction` coupling in skeletal and cardiac muscle. *Proc. Natl. Acad. Sci. USA* **93**, 8101-8106.

Fox, A. P., Nowycky, M., and Tsien, R. W. (1987). Kinetic and pharmacological properties distinguishing three types of calcium currents in chick sensory neurons. *J. Physiol. (London)* **394**, 149-172.

Gabbiani, G., Chapponnier, C., and Huttner, I. (1978). Cytoplasmic filaments and gap junctions in epithelial cells and myofibroblasts during wound healing. *J. Cell Biol.* **76**, 561-580.

Gierer, A., Berking, S., Bode, H., David, C. N., Flick, K., Hansmann, G., Schaller, H., and Trenkner, E. (1972). Regeneration of hydra from reaggregated cells. *Nature New Biol.* **239**, 98-101.

Gladfelter, W. B. (1972). Structure and function of the locomotory system of *Polyorchis montereyensis* (Cnidaria, Hydrozoa). *Helgol Wiss Meeresunters* **23**, 38-79.

Grigoriev, N. G., Spafford, J. D., Przysiezniak, J., and Spencer, A. N. (1996). A cardiac-like sodium current in motor neurons of a jellyfish. *J. Neurophysiol.* **76**, 2240-2249.

Grimmelikhuijzen, C. J. and Spencer, A. N. (1984). FMRFamide immunoreactivity in the nervous system of the medusa *Polyorchis penicillatus*. *J. Comp. Neurol.* **230**, 361-71.

Grimmelikhuijzen, C. J. P., Spencer, A. N., and Carre, D. (1986). Organization of the nervous system of physonectid siphonophores. *Cell Tiss. Res.* **246**, 463-479.

Grzesiak, J. J. and Pierschbacher, M. D. (1995). Shifts in the concentrations of magnesium and calcium in early porcine and rat wound fluids activate the cell migratory response. *J. Clin. Invest.* **95**, 227-233.

Holman, M. A. and Anderson, P. A. V. (1991). Voltage-activated ionic currents in myoepithelial cells isolated from the sea anemone *Calliactis tricolor*. *J. Exp. Biol.* **161**, 333-346.

Huguenard, J. R. (1996). Low-threshold calcium currents in central nervous system neurons. *Ann. Rev. Physiol.* **58**, 329-48.

Hyman, L. (1940). The invertebrates, vol. 1. New York: McGraw-Hill.

Inui, M., Saito, A., and Fleischer, S. (1987). Isolation of the ryanodine receptor from cardiac sarcoplasmic reticulum and identity with the feet structure. *J. Biol. Chem.* **262**, 15637-15642.

Jha, R. K. and Mackie, G. O. (1967). The recognition, distribution and ultrastructure of hydrozoan nerve elements. *J. Morph.* **123**, 43-61.

Keough, E. M. and Summers, R. G. (1976). An ultrastructural investigation of the striated subumbrellar musculature of the anthomedusan, *Pennaria tiarella*. *J. Morph.* **126**, 211-248.

Kohler, G. and Milstein, C. (1975). Continuous cultures of fused cells secreting antibody of predefined specificity. *Nature* **256**, 495-497.

Kohler, G. and Milstein, C. (1976). Derivation of specific antibody-producing tissue culture and tumor lines by cell fusion. *Eur. J. Immuno.* **6**, 511-519.

Lawrence, W. T. (1998). Physiology of the acute wound. *Clin. Plast. Surg.* **25**, 321-40.

Llinas, R., Sugimori, M., Lin, J.-W., and Cherskey, B. (1989). Blocking and isolation of a calcium channel from neurons in mammals and cephalopods utilizing a toxin fraction (FTX) from funnel-web spider poison. *Proc. Natl. Acad. Sci. USA* **86**, 1689-1693.

Mackie, G. O. (1990). The elementary nervous system revisited. *Am. Zool.* **30**, 907-920.

Mackie, G. O. and Meech, R. W. (1985). Separate sodium and calcium spikes in the same axon. *Nature* **313**, 791-793.

Mackie, G. O. and Meech, R. W. (1989). Potassium channel family in axons of the jellyfish *Aglantha digitale. J. Physiol. (London)* **418**, 14P.

Mackie, G. O., Singla, C. L., and Stell, W. K. (1985). Distribution of nerve elements showing FMRFamide-like immunoreactivity in Hydromedusae. *Acta Zool. (Stockholm)* **66**, 199-210.

McCleskey, E. W., Fox, A. P., Feldman, D. H., Cruz, L. J., Olivera, B. M., Tsien, R. W., and Yoshikami, D. (1987). ω-conotoxin: direct and persistent blockade of specific types of calcium channels in neurons but not muscle. *Proc. Natl. Acad. Sci. USA* **84**, 4327-4331.

Meech, R. W. and Mackie, G. O. (1993a). Potassium channel family in giant motor axons of *Aglantha digitale*. *J. Neurophysiol.* **69**, 894-901.

Meech, R. W. and Mackie, G. O. (1993b). Ionic currents in giant motor axons of the jellyfish, *Aglantha digitale*. *J. Neurophysiol.* **69**, 884-893.

Megeney, L. A., Kablar, B., Garrett, K., Anderson, J. E., and Rudnicki, M. A. (1996). MyoD is required for myogenic stem cell function in adult skeletal muscle. *Genes Develop.* **10**, 1173-1183.

Mintz, I. M., Venema, V. J., Swiderek, K. M., Lee, T. D., Bean, B. P., and Adams, M. E. (1992). P-type calcium channels blocked by the spider venom toxin ω-Aga-IVA. *Nature* **355**, 827-829.

Nabauer, M. G., Callewart, L., Cleemann, L., and Morad, M. (1989). Regulation of calcium release is gated by calcium current, not gating charge, in cardiac myocytes. *Science* **244**, 800-803.

Nadal-Ginard, B. (1978). Commitment, fusion, and biochemic differentiation of a myogenic cell line in the absence of DNA synthesis. *Cell* **15**, 855-864.

Nuss, H. B. and Houser, S. R. (1993). T-type Ca^{2+} current is expressed in hypertrophied adult feline left ventricular myocytes. *Circ. Res.* **73**, 777-782.

Palade, P. and Györke, S. (1993). Excitation-contraction coupling in crustacea: do studies on these primitive creatures offer insights about EC coupling more generally? *J. Mus. Res. Cell Motil.* **14**, 283-287.

Paniagua, R., Royuela, M., Garcia-Anchuelo, R. M., and Fraile, B. (1996). Ultrastructure of invertebrate muscle cell types. *Histol. Histopathol.* **11**, 181-201.

Przysiezniak, J. and Spencer, A. N. (1992). Voltage-activated calcium currents in identified neurons from a hydrozoan jellyfish, *Polyorchis penicillatus*. *J. Neurosci.* **12**, 2065-2078.

Przysiezniak, J. and Spencer, A. N. (1994). Voltage-activated potassium currents in isolated motor neurons from the jellyfish *Polyorchis penicillatus*. *J. Neurophysiol.* **72**, 1010-1019.

Randall, A. D. and Tsien, R. W. (1995). Pharmacological dissection of multiple types of Ca^{2+} channel currents in rat cerebellar granule neurons. *J. Neurosci.* **15**, 2995-3012.

Randall, A. D. and Tsien, R. W. (1997). Contrasting biophysical and pharmacological properties of T-type and R-type calcium channels. *Neuropharmacology* **36**, 879-893.

Sakaguchi, M., Mizusina, A., and Kobayakawa, Y. (1996). Structure, development, and maintenance of the nerve net of the body column in *Hydra*. *J. Comp. Neurol.* **373**, 41-54.

Sather, W. A., Tanabe, T., Zhang, J.-F., Mori, Y., Adams, M. E., and Tsien, R. W. (1993). Distinctive biophysical and pharmacological properties of class A (BI) calcium channel alfa1 subunits. *Neuron* **11**, 291-303.

Schaffer, C. J. and Nanney, L. B. (1996). Cell biology of wound healing. *Intl. Rev. Cytol.* **169**, 151-81.

Schultz, E. (1996). Satellite cell proliferative compartments in growing skeletal muscles. *Dev. Biol.* **175**, 84-94.

Sen, L. and Smith, T. W. (1994). T-type Ca2+ channels are abnormal in genetically determined cardiomyopathic hamster hearts. *Circ. Res.* **75**, 149-155.

Shimizu, H., Sawada, Y., and Sugiyama, T. (1993). Minimum tissue size required for hydra regeneration. *Dev. Biol.* **155**, 287-296.

Shimizu, H. and Sugiyama, T. (1993). Suppression of head regeneration by accelerated wound healing in hydra. *Dev. Biol.* **160**, 504-11.

Singla, C. L. (1978a). Locomotion and neuromuscular system of *Aglantha digitale*. *Cell Tiss. Res.* **188**, 317-27.

Singla, C. L. (1978b). Fine structure of the neuromuscular system of *Polyorchis penicillatus* (Hydromedusae, Cnidaria). *Cell Tiss. Res.* **193**, 163-174.

Spafford, J. D., Grigoriev, N. G., and Spencer, A. N. (1996). Pharmacological properties of voltage-gated Na+ currents in motor neurons from a hydrozoan jellyfish *Polyorchis penicillatus*. *J. Exp. Biol.* **199**, 941-948.

Spencer, A. N. (1979). Neurobiology of *Polyorchis*. II. Structure of effector systems. *J. Neurobiol.* **10**, 95-117.

Spencer, A. N. (1981). The parameters and properties of a group of electrically coupled neurons in the central nervous system of a hydrozoan jellyfish. *J. Exp. Biol.* **93**, 33-50.

Spencer, A. N. (1982). The physiology of a coelenterate neuromuscular synapse. *J. Comp. Physiol.* **148**, 353-363.

Spencer, A. N. and Arkett, S. A. (1984). Radial symmetry and the organization of central neurons in a hydrozoan jellyfish. *J. Exp. Biol.* **110**, 69-90.

Spencer, A. N., Przysiezniak, J., Acosta-Urquidi, J., and Basarsky, T. A. (1989). Presynaptic spike broadening reduces junctional potential amplitude. *Nature* **340**, 636-8.

Spencer, A. N. and Satterlie, R. A. (1981). The action potential and contraction in subumbrellar swimming muscle of *Polyorchis penicillatus* (Hydromedusae). *J. Comp. Physiol.* **144**, 401-407.

Stenn, K. S. and DePalma, L. (1988). Re-epithelialization. *In* The molecular and cellular biology of wound repair (ed. R. A. F. Clark and P. M. Henson). New York: Plenum Press.

Tardent, P. (1965). Developmental aspects of regeneration in coelenterates. *In* Regeneration in animals and related problems (ed. V. Kiortsis, and Trampusch, H. A. L.). Amsterdam: North-Holland Publishing Company.

Thomas, M. B. and Edwards, N. C. (1991). Cnidaria: Hydrozoa. *In* Placozoa, Porifera, Cnidaria, and Ctenophora, vol. 2 (ed. F. W. Harrison and J. A. Westfall). New York: Wiley-Liss, Inc.

Tsien, R. W. (1998). Key clockwork component cloned. *Nature* **391**, 839-841.

Weber, K. T., Sun, Y., and Katwa, L. C. (1996). Wound healing following myocardial infarction. *Clin. Cardiol.* **19**, 447-455.

Winegrad, S. (1965). Autoradiographic studies of intracellular calcium in frog skeletal muscle. *J. Gen. Physiol.* **48**, 455-479.

Witte, M. B. and Barbul, A. (1997). General principles of wound healing. *Surg. Clin. North Am.* **77**, 509-28.

Yaross, M. S., Westerfield, J., Javois, L. C., and Bode, H. R. (1986). Nerve cells in *Hydra*: monoclonal antibodies identify two lineages with distinct mechanisms for their incorporation into head tissue. *Dev. Biol.* **114**, 225-37.

Zak, R. (1974). Development and proliferative capacity of cardiac muscle cells. *Circ. Res. (Suppl)* **2**, 17-26

Chapter 2

The anatomy of the nervous system of the hydrozoan jellyfish, *Polyorchis penicillatus*, as revealed by a monoclonal antibody

INTRODUCTION

From the earliest days of comparative physiology there has been considerable attention given to the histology and organization of the nervous system in medusae, especially the hydromedusae (eg. Hertwig and Hertwig, 1878; Mackie, 1960, 1971; Mackie and Singla, 1975; Spencer, 1979; Singla, 1978a, b; Grimmelikhuijzen and Spencer, 1984). This interest is well founded as the Cnidaria represent a pivotal, early step in the evolution of the metazoan nervous system. Certainly, these are not the earliest evolutionary experiments in nervous system organization, which for the time remain hidden with undiscovered ancestors of the Cnidaria and Platyhelminthes. Nevertheless, cnidarian nervous systems do show us important general trends in the organization of metazoan nervous systems, particularly in radially symmetrical animals. For example, within this phylum it is possible to identify several, separate nerve-nets (Spencer and Arkett, 1984), and the condensation and formation of a centralised portion of the nervous system (nerve-rings) with the formation of distributed ganglia and neuropile (Mackie, 1971). The more recent ultrastructural and immunohistochemical studies referred to above have often been undertaken by behavioural neurobiologists who wish to understand the neuronal circuitry associated with recorded electrical activity. Often the cellular substrates responsible for a particular type of spike train activity is in doubt until such studies are completed. Despite the use of a range of histological techniques, such as vital methylene blue staining, silver staining, immuno-labelling against transmitters (amines and peptides), Lucifer yellow and carboxyfluoroscein iontophoresis, investigators have not yet been able to identify all elements of the nervous system simultaneously. This study describes the production of a monoclonal antibody against all known neurons in the hydromedusan jellyfish, *Polyorchis penicillutas*, which helps us appreciate the subtleties of nervous system organization in the Cnidaria.

MATERIALS AND METHODS

Medusae of *Polyorchis penicillatus* were collected in either Bamfield Inlet or Pachena Bay, near Bamfield, B.C., Canada and maintained in an aquarium with recirculating seawater at 12-14°C at the University of Alberta, Edmonton, Alberta, Canada.

Production of monoclonal antibodies

Bell margins of jellyfish were dissociated using 1000 units/ml of collagenase type I (Sigma) in artificial seawater (ASW - NaCl: 376 mM, $Na_2(SO_4)$: 26 mM, $MgCl_2$: 41.4 mM, $CaCl_2$: 10 mM, KCl: 8.5 mM, and HEPES (hemisodium salt): 10 mM), for 1 to 2 h at room temperature (Przysieziak and Spencer, 1989). In some later experiments tissue was dissociated with 1 mg/ml of Pronase (Boehringer Mannheim) in ASW at 308C for 30 min. Dissociated cells were layered onto a 33% Percoll solution (Pharmacia, LKB, Biotechnology) and centrifuged at 2000 x *g* for 30 min at 12°C to remove cnidocytes. The Percoll solution was prepared by diluting pure Percoll 9:1 with 10 x ASW. The 10 x ASW was NaCl: 3760 mM, $Na_2(SO_4)$: 260 mM, $MgCl_2$: 414 mM, $CaCl_2$: 100 mM, KCl: 85 mM, and HEPES (hemisodium salt): 100 mM. After centrifugation, cells were collected from the top layer, washed with ASW, and then fixed with 4% paraformaldehyde in ASW at room temperature for 2 h. Fixed cells were washed with phosphate-buffered saline (PBS) three times and used as immunogens to innoculate Balb/C mice at a density of 10^7-

10^8 cells/ ml in 0.25 ml PBS without adjuvant. Production of hybridomae followed the protocol outlined by Acheson and Gallin (1992). Culture suspensions were used for immunofluorescent screening for hybridomae labelling relevant cell types.

Immunofluorescence microscopy and laser scanning confocal microscopy

Paraffin sections and whole-mount preparations were used for both conventional fluorescence microscopy and laser-scanning confocal microscopy. Jellyfish were fixed overnight at 4°C with a solution containing 4% paraformaldehyde, 50% ethanol, and 25% acetic acid. Paraffin sections were processed using standard procedures for paraffin embedding and sectioning. Rehydrated sections or pieces of tissue were washed with phosphate-buffered saline with 0.25% Tween 20 or Triton X-100 (PBST), blocked with 3% bovine serum albumin and 3% goat serum in PBST for 1 h and then incubated with primary antibodies at 4°C overnight. After incubation with primary antibody, sections were washed 3 times with PBST and then incubated with secondary antibody (FITC-conjugated goat anti-mouse IgG) for another 2 h at room temperature. After secondary antibody incubation, samples were washed with PBST three times and mounted in Monitol with the addition of 2.5% DABCO (Sigma). Samples were examined using a Molecular Dynamic laser-scanning confocal microscope. Adobe Photoshop v.4.0 (Adobe Systems, Inc.) software was used to process confocal images.

RESULTS

Since we were interested in producing antibodies against neurons we had to ensure that the fixed cell suspensions we used as immunogens were enriched with neurons. This required removal of a large percentage of the cnidocytes which are prevalent in the margin as this is a zone for maturation of cnidocytes. Enrichment was achieved using a Percoll step gradient which isolated the more dense cnidocytes and cnidoblasts to the bottom layer. Examination of the upper layer using phase contrast optics showed that no cnidocytes or cnidoblasts were present in the innoculum.

From two successful cell fusions we isolated 156 wells of hybridomae secreting antibodies of interest. We used limiting dilution to isolate a clone secreting antibodies that recognise neurons which we designated, 5C6. This antibody appeared to label all interstitial cells and their progeny which are both neurons and cnidocytes. Fortunately cnidocytes and their precursors, the cnidoblasts, did not label as heavily as neurons and their precursors.

All the discrete nerve-nets previously identified in hydromedusae and specifically of *Polyorchis penicillatus* could be readily discerned using 5C6. In addition we were able to extend the distribution of neurons in these nets because of the sensitivity of the antibody and its apparent ability to label all neural elements. We assume that this was possible because, unlike other techniques used in hydromedusae, this antibody produced general labelling of all known neuronal elements. The only tissues that did not show labelling, and hence appear to lack neurons, were the exumbrella epithelium, the subumbrellar ectodermal muscle sheets (except near their peripheries), the endodermal lamellae and the tentacular endoderm. The gross anatomy of *Polyorchis* is illustrated in Fig. 2.1 to aid interpretation of the nervous systems described.

Subumbrella and Peduncle

Figure 2.2a is a montage from ten confocal images of a whole-mount preparation showing the distribution of 5C6 positive cells in the upper portion of one of the subumbrellar quadrants and the associated peduncular region. This montage shows the anastomosing network of large bi- and multipolar neurons that formed the radial nerve (RN) networks running up either side of the radial smooth muscle bands which lie above the radial canals (Fig. 2.3 inset). These networks ran in the ectoderm at the junction of the circular, striated, swimming muscle sheets and the radial smooth muscle and were contiguous with the swimming motor neuron (SMN) network which lay circularly in the inner nerve-ring (see Fig. 2.4b). As can be seen in Fig. 2.2a the RNs from adjacent radii formed an interconnected arch at the margin of the subumbrellar muscle sheets with the peduncle, thus creating a contiguous network at the periphery of each of the four quadrants of swimming muscle. The largest neurons, with somal diameters of 10 to 20 μm, were found in portions of the RNs that formed the arches and the nerve bundles running along either side of the radial muscle band (Fig. 2.2c and Fig. 2.3). These neurons were mostly multipolar with occasional bipolar neurons present, and their processes were thick, from 2 to 4 μm wide. Some neurons close to the swimming muscle sheets were seen to have processes which innervate the swimming muscle (Fig. 2.2d). Each RN network branched where the radial smooth muscle bands diffused at their apical terminii to form the radial muscle sheets of the peduncular wall beneath the gonads and then the manubrium itself (Fig. 2.2a,b). These two branches of immunoreactive neurons formed the arches of adjacent quadrants while between them a central network ran in association with the radial muscle underlying the gonads and then spread laterally into the radial muscle sheet of the manubrium. Neurons of this central branch became progressively smaller, decreasing to a somal diameter of 5 µm. In the triangular area between the arch network and the bases of the gonads, the ectodermal epithelium contains relatively sparse, isolated neurons (Fig. 2.2a,e) that do not appear to form a continuous network, unless the interconnecting neurons are too fine to be resolved. No labelling was seen in the endodermal lamella.

Radii

Most of the 5C6 labelling of the radii was restricted to the ectoderm with a far less dense network in the endodermal radial canal and its lateral diverticula (Fig. 2.3). Each RN could be traced as large bipolar and multipolar neurons on the lateral margins of the smooth muscle bands (Fig. 2.3 and inset). Some of the RN multipolar neurons were linked by their processes forming an orthogonal network of neurons with the "rungs of the ladder" running just below the radial muscle bands on the ectodermal face of the mesoglea. These neuronal processes appeared quite faint in the micrographs as they were seen through the thick radial muscle band. Other ectodermal processes projected around the radial canal and partly into the diverticula. The orthogonal network was contiguous with the central branch mentioned in the previous section and also extended a short way into the lateral diverticula, once again at the base of the ectoderm (Fig. 2.3). Isolated neuronal somata could be seen embedded in the radial muscle (Fig. 2.3). A more diffuse endodermal network could also be seen in both the radial canal and diverticula from sections (Fig. 2.3 inset) and whole-mounts (Fig. 2.3). Sections did not provide any evidence of connectivity between endodermal and ectodermal nerve elements in this region.

Marginal Region

Monoclonal antibody labelling of radial sections of the margin revealed numerous neuronal profiles in both the inner and outer nerve-rings (Fig. 2.4a). Careful examination of sections of the inner nerve-ring revealed that several very large diameter profiles were labelled in the position of the swimming motor neuron network (Spencer, 1979, 1981). In whole-mounts the SMN network is discernable but is not heavily labelled (Fig. 2.4b,c), nevertheless it was possible to see where the RN joined the SMN network (Fig. 2.4b). On the outer edge of the SMN network an accessory network of small neurons projected a short way onto the subumbrellar surface of the velum (Fig. 2.4c). Not only did the outer nerve-ring proper show extensive labelling but the whole of the ectoderm from the mesogleal tri-radius to the beginning of the exumbrella, especially at the bases of the tentacles, showed immunoreactivity (Fig. 2.4a). These immunoreactive neurites consisted of both neuronal and sensory somata, and relatively thin neurites. Towards the velum many of the labelled neurons had a radial orientation and their processes appeared to extend into the radial muscle sheet on the exumbrellar side of the velum (Fig. 2.4d). On the opposite side of the outer nerve-ring, at the bases of tentacles, a fairly dense array of large neurons projected to the exterior surface of the ectodermal epithelium (Fig. 2.4d). These cells had bottle-shaped somata about 10 to 15 µm long with a central cilium surrounded by a circlet of short microvilli (Fig. 2.4e, f). In more central regions of the outer nerve-ring were smaller (5 µm long) ciliated neurosensory cells which also projected to the exterior. Networks of circularly aligned processes could be seen in less superficial regions of the outer nerve-ring (Fig. 2.4d). The larger neurons in these networks had poorly defined somata and the average neurite width was 2 to 5 µm, and we presume that this is the "B" system, which was shown by Spencer and Arkett (1984) to be located in the outer nerve-ring as a condensed network and to extend up into the tentacles as a more diffuse network. The architecture of this network, and the thickness of neurites that was revealed using 5C6 labelling was very similar to that reported by Spencer and Arkett (1984) using Lucifer-yellow iontophoresis. A second network of smaller neurons with thin processes (< 1µm) was present in the outer nerve-ring and extended up into the tentacles towards the ocelli as a pair of nerves. This network is almost certainly the "O" system (Spencer and Arkett, 1984), as these authors had shown the existence of a second outer nerve-ring network formed by smaller neurons that innervated the ocelli. Scattered neurites were found in the endodermal ring canal and were more prevalent opposite the nerve-rings (Fig. 2.4a).

Ocelli and Ocellar nerves

Whole-mounts of the proximal portion of tentacles, as shown in figure 2.5, clearly showed the paired ocellar nerves crossing the bases of the tentacles and descending into the outer nerve-ring. These tracts of mostly neurites were set in a background of neurosensory cells (described in the previous and following sections) connected by a reticulum of neurites. The ocelli were formed by evenly spaced, immunoreactive photoreceptors approximately 15 μm long (Fig. 2.5. insert). The apical surface of each receptor cell carried a short central cilium.

Tentacles

Two ectodermal, neuronal networks were present in the tentacles (Fig. 2.6). One was a network formed from multipolar, ganglionic cells with thick processes which in more distal parts of the tentacles was formed from mostly bipolar neurons that had a distinctly longitudinal bias (Fig. 2.6b, c). We assumed that this network which extended back into the outer nerve-ring and was connected to the thicker, circularly oriented processes seen in figure 4b was the "B" system (Spencer and Arkett, 1984). Elements of this network did not project to the ectodermal surface. The second ectodermal network of bipolar and multipolar neurons had finer processes with ciliated neurosensory cells that projected to the ectodermal surface (Fig. 2.6b). The longitudinally oriented, finer processes of this second network were often beaded, and we assumed that this network was synonymous with the RF-amide immunoreactive network (Grimmelikhuijzen and Spencer, 1984). In addition to neurons, the tentacular ectoderm had a high density of, cnidoblasts and cnidocytes which either did not label or were all lightly immunoreactive. In the proximal portion of the tentacles there were no cnidocyte-battery cell complexes so that neurosensory cells, cnidocytes and their precursors were evenly distributed (Fig.

2.6a). In more distal regions of tentacles where most cnidocytes were associated with battery complexes (Fig. 2.6c) there were usually 3 to 15 immunoreactive sensory cells embedded in the complexes and connected to the neuronal network by basal processes (Fig. 2.6d).

Gonads and Manubrium

The four central branches of the RN networks of each radius continued beneath each gonad towards the manubrium (Fig. 2.7a). These networks became increasingly composed of bipolar neurons with their fine processes radially oriented so that in the manubrium proper they aligned with the smooth muscle sheet (Fig. 2.7b). The cell bodies (5 μm long) usually lay with their long axes at right angles to the network and with their apices projecting to the surface (Fig. 2.7c). The neurites were very fine with numerous varicosities, giving a beaded appearance. Sections showed that neurons of two types were also present in the endoderm (Fig. 2.7d). One type, located at the base of the endoderm close to the mesogloea, had small somata (5 μm) which were similar to the ectodermal neurons, while a second type had long, rod-shaped somata that contained numerous vesicles. Neurons in the ectoderm of the gonads were both bi- and multipolar but were not obviously connected to one another (Fig. 2.7e).

DISCUSSION

Although it is impossible to prove that any histological method labels every neuronal element in a nervous system we are reasonably certain that we have discovered a generalized neuronal labelling technique. Our reasons for believing this are:

1. The 5C6 antiserum labelled a population of neurons that included all neurons identified by all other techniques.

2. The antiserum also stained sub-popualtions of neurons not labelled by other techniques.

3. The antiserum labels interstitial cells which are known to be neuronal precursors in hydrozoans.

Of course there may be neuron-like cells that are descended from non-interstitial cell precursors, or there may be neurons that lose expression of this antigen.

In this discussion we will associate each of the neuronal systems identified using 5C6 with systems previously described using a variety of other histological and electrophysiological techniques. The following identified nerve nets have been previously described in *Polyorchis*: swimming motor neuron network (SMN), accessory neurons, oscillating system ("O" system), burster system ("B" system), RF amide immunoreactive neurons (Singla 1978b; Spencer, 1979; Grimmelikhuijzen and Spencer, 1984; Spencer and Arkett, 1984). Homologous networks have also been described in *Sarsia* (Mackie, 1971) and *Stomotoca* (Mackie and Singla, 1975).

Swimming Motor Neuron Network

Although it was suspected that this system formed a continuous network at the periphery of each subumbrellar muscle quadrant this study shows that continuity is maintained by the arches at the apex of each sheet, in addition to the continuous circular network in the inner nerve-ring. Connection of adjacent radial nerves had previously been noted for *Stomotoca* (Mackie and Singla, 1975). We are therefore able to confirm the adaptational interpretation given by Spencer (1981, 1982) for this symmetrical pattern of motor innervation of each swimming muscle sheet whereby motor spikes are propagated rapidly through electrical coupling to all member neurons. Conduction delay is compensated by changes in motor spike duration which in turn modulates synaptic delay (Spencer, 1982). Also, since muscle action potentials propagate inwards from the periphery through each triangular muscle sheet, a peristaltic pump is created since the narrower portion of the muscle sheet at the apex (within the SMN arch) is fully contracted before the wider region of the muscle sheet at the margin. This study also extends our understanding of how the muscle sheets are innervated at each radius since lateral extensions of the RN could be seen running out at right angles a short distance onto the muscle sheets. Labelling with 5C6 also confirmed the connection of the radial portion of the SMNs running down the radii with the circular network in the inner nerve-ring and the presence of an accessory network of neurons that lay along the velar margin of the SMN network. These latter neurons have only been described from one reduced methylene blue preparation (Spencer, 1982).

Of considerable interest are the connections made between the radial nerves on each side of the radial canal. This is the first time an orthogonal arrangememt of neurons has been described in a cnidarian showing that there are developmental programs in this radially symmetrical phylum for what is presumed to be an architecture more typical of the Bilateria (Bullock and Horridge, 1965). Although it may be attractive to assume that these lateral connections play a role in maintaining coordination of motor spikes for swimming by connecting the RNs on either side of each radial canal, two lines of evidence suggest that this may not be the case. First, the orthogonal network is continuous with the network that emerges between the radial nerves and extends along the gonads and up into the manubrium. Along its length it is associated with smooth muscle. Second, it is not possible to say whether the ladder-like network is connected to neurons that form the radial portion of the SMN network or whether there is another net with other functions. The reason for this uncertainty is that King and Spencer (1981) reported synapses between elements of the radial nerve and the smooth muscle. It is possible, therefore, that the radial nerves carry neurons, other than SMNs, that are associated with control of the radial smooth muscle. This cannot be determined unless separation of a swimming motor network and a smooth muscle network is shown by dye coupling or electrical coupling experiments. These techniques have been used previously to show that all the systems so far examined in this way (SMN, "O", and "B") are electrically isolated from one another (Spencer and Arkett, 1984) which appears to be a general rule for hydrozoan nervous system organization.

Peduncle, Manubrium and Gonads

In the area above the arches and between adjacent gonads there are scattered labelled cells which do not appear to be connected as a network, we have assumed they are neurons or at least neuronal precursors carrying the 5C6 antigen. Their function is unknown. As they are not connected they cannot be a motor network nor are they likely to be local multimodal neurons as there are no obvious effectors in this region. It is also possible that they form a reserve of non-differentiated neurons that migrate into either the SMN network or the radial networks of the gonad and manubrium to replace senescent neurons. Isolated, immunofluorescent, neuron-like cells are also found in the gonads. It is possible that these neurons are associated with the direct photosensitivity of gonads whereby gametes are released a few hours after dawn in isolated gonads (Ikegami et al., 1978). The organization of the 5C6 labelled neurons and their neurites in the manubrium is identical to that seen with anti RF-amide labelling (Grimmelikhuijzen and Spencer, 1984). These authors found a network of triangular shaped cell bodies with an apical projection to the surface connected by fine neurites running parallel to the smooth muscle fibres. This is a common pattern seen in similar structures in other hydrozoans, such as the RF-amide immunoreactive network of the gastrozooid in physonectid siphonophores (Grimmelikhuijzen et al., 1986). We assume that the network in the ectoderm of the manubrium is a local senosory/motor network innervating the longitudinal muscle which can also be activated remotely via the network that runs back to each radius. The small varicosities seen on neurites are unlikely to be fixation artefacts since they are also seen with anti RF-amide labelling. It is likely that they are synaptic boutons for muscle activation.

Tentacles

The ectodermal, neuronal networks that label with 5C6 antibody in the tentacles consist of neurosensory and ganglionic cells and their processes. We assume that these two networks are not electrically coupled to one another since dissimilar neuronal types have never been seen to be in electrical continuity in *Polyorchis* (Spencer and Arkett, 1984). Indeed, preliminary experiments in which tentacles were double-labelled using 5C6 and anti RF-amide antibody showed the discreteness of these two networks. The ganglionic cells lie deep in the ectoderm with neurites that project along the axis of the tentacles without projecting to the surface. At the tentacle base this network runs seamlessly into an ectodermal network at the outer edge of the margin and we believe that it is the same network as the "B" system (see below). The neurosensory network matches the anti RF-amide network (Grimmelikhuijzen and Spencer, 1984) with ciliated sensory cells projecting to the surface of the ectoderm and thin neurites running longitudinally. The labelling pattern in the tentacles is complicated by the presence of numerous isolated cnidoblasts and cnidocytes, and by cnidocyte battery complexes. In more terminal parts of the tentacle where these complexes are abundant the tentacular network develops a stronger longitudinal bias with thick processes that appear to be for rapid propagation. Most of the sensory functions are therefore restricted to the complexes where local reflex networks may regulate cnidocyte discharge thresholds.

Marginal Region ("B" and "O" systems)

Based on transmission electron microscopy the outer nerve-ring contains at least 800 neuronal profiles in radial sections with diameters between 0.2 and 1.4 µm, and 60 to 75 profiles with diameters between 1.4 and 6.8 µm (Spencer, 1979). Labelling with the mAb 5C6 confirms that there is a high density of neurons throughout the outer nerve-ring. This density is so high that even using confocal microscopy for optical sectioning it was often difficult to separate networks. In a previous study Spencer and Arkett (1984) identified two networks, the "B" and "O" systems, in the outer nerve-ring by both electrophysiological characterization and by simultaneous dye injection. We believe that the thicker processes seen running circularly in the outer nerve-ring using 5C6 antiserum are "O" neurons while the thinner processes are probably part of the "B" system. Lucifer-yellow injection shows that the "O" system projects to the ocelli via the ocellar nerves, the ocellar nerves can also be visualised using anti RF-amide labelling (Grimmelikhuijzen and Spencer, 1984). Until now it was not known whether these are two different sets of neuronal elements making up the ocellar nerve, however, the 5C6 labelling does not show significantly more parallel fibres in the ocellar nerves than either one of the other methods so, for now, we must assume that there is only one system present. This may be a system of "second order" neurons carrying photic information to the contiguous "O" system of the outer nerve-ring (Singla and Weber, 1982; Spencer and Arkett, 1984). The large evenly spaced ciliated cells seen in the ocellus with 5C6 labelling are presumably the first order photoreceptors. It will be necessary to examine for dye coupling between these supposed first and second order photic neurons to be certain that both are not part of the same electrically coupled network. Monoclonal antibody labelling revealed a group of large receptor-like cells on the exumbrellar side of the outer nerve-ring that have not been described before. One cannot be sure of their modality. If they are photoreceptors they could represent the extra-ocellar photoreceptors reported by Satterlie (1985) and suspected from physiological studies where ablation of the ocelli did not abolish the light-off response (Anderson and Mackie, 1977; Spencer and Arkett, 1984). Other features of the neuro-anatomy of the outer nerve-ring using 5C6 that were not apparent using other techniques were the radially aligned neurons at the velar side of the ring. These are probably neurons that innervate the radial muscles of the velum and control velar steering.

Endodermal Systems

The presence of diffusely distributed 5C6 immunoreactive neurons in the endoderm of the ring and radial canals and the manubrium confirms previous findings using other techniques (Singla, 1978b; Spencer, 1979; King and Spencer, 1981). As for these other methods, 5C6 labelling failed to show a continuous network. The function of these neurons is unknown.

General Conclusions

This antiserum has provided us with the most global visualisation of a nervous system in any cnidarian. Thus it has provided details of the nervous system of *Polyorchis* that were unknown, such as the contiguity of the swimming motor neuron network around each muscle sheet and the presence of orthogonal networks associated with the radial canals. Antisera, such as 5C6, which are able to stain "all" neurons and their precursors, will be extremely valuable tools for studies that involve tracing this phenotype during development and regeneration in the Cnidaria.

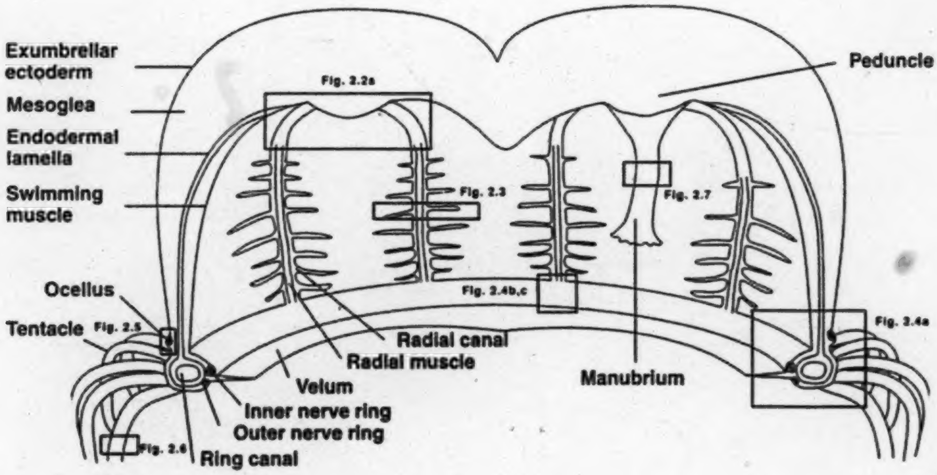
Exumbrellar ectoderm
Mesoglea
Endodermal lamella
Swimming muscle
Fig. 2.2a
Peduncle
Fig. 2.3
Fig. 2.7
Ocellus
Fig. 2.4b,c
Tentacle
Fig. 2.5
Fig. 2.4a
Radial canal
Radial muscle
Manubrium
Velum
Inner nerve ring
Outer nerve ring
Fig. 2.6
Ring canal

Fig. 2.1. Diagram of the medusa of *Polyorchis penicillatus* showing the gross anatomy and positions of subsequent figures. Animal is cut opened through the margin and bell.

Fig. 2.2. Whole-mount preparation of the subumbrellar area near the peduncular region abelled with the monoclonal antibody 5C6. a) A montage of 10 confocal images showing the radial nerve (RN) network from adjacent radii forming an arch at the apex of the subumbrellar muscle. A central branch (CB) from each radius runs at the bases of the gonads (G) to the manubrium (M). The area between the arch and the bases of the gonads is the peduncle (P). b) Enlarged view of the location where the radial nerve network branches into three groups. Arrow indicates the direction of branching to form the arches of adjacent quadrants. c) Part of the arch network. d) A neuron with processes invading the swimming muscle sheet at the edge of the arch network. e) Scattered neurons in the peduncle ectoderm. Scale bars in µm.

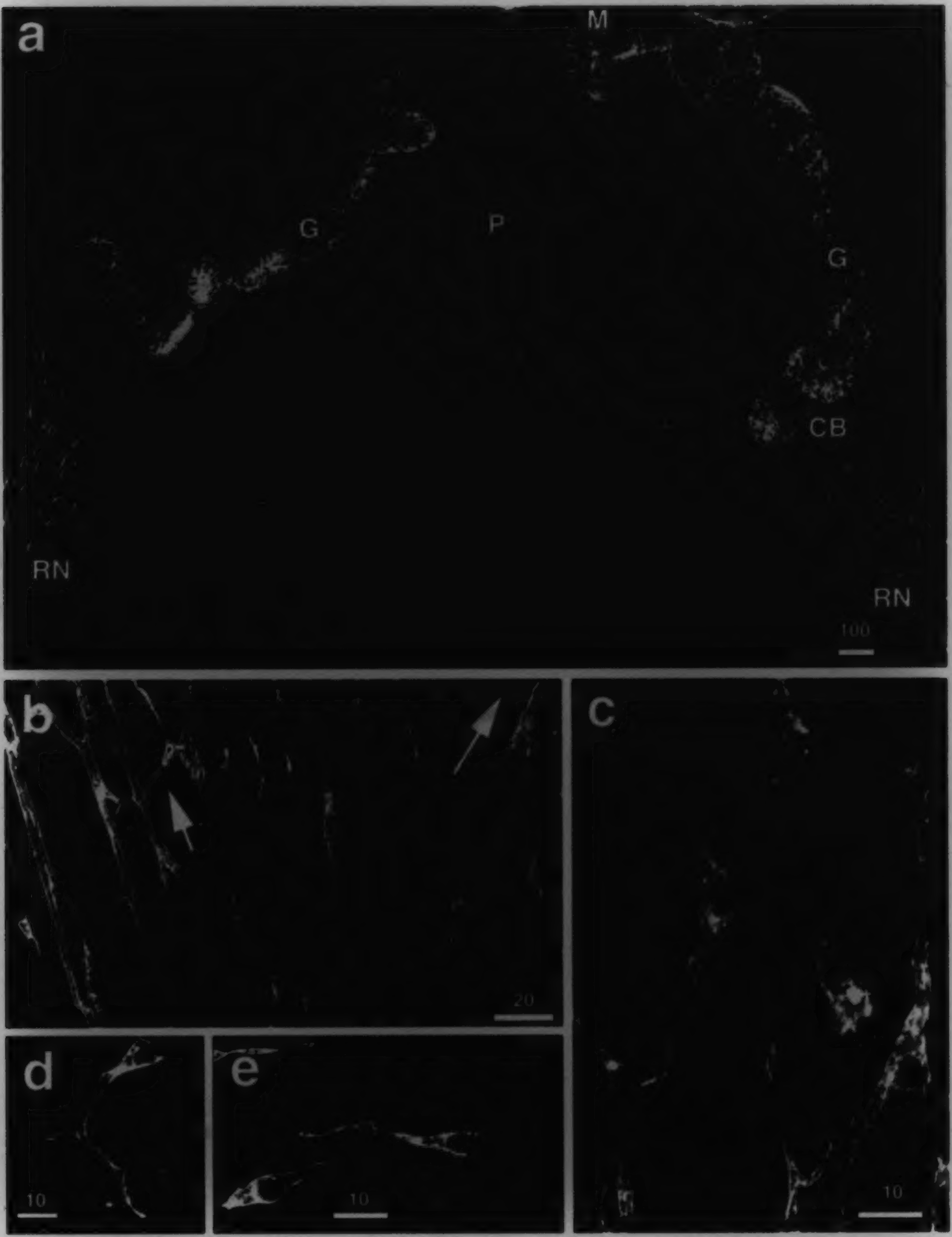
a
M
G
P
G
CB
RN
RN
100
b
20
c
10
d
10
e
10

Fig. 2.3. Whole-mount of a portion of the radial canal region with an inset showing a transverse section of the same region labelled with the monoclonal antibody 5C6. The radial nerves (RN, single arrows) can be seen running either side of the radial smooth muscle band (RM) in both whole-mounts and sections (inset). Processes from multipolar neurons of the RN form an orthogonal, ectodermal network (closed triangles) between the two RNs from each side and also project around the radial canal and partly into the diverticula. Isolated neuronal somata can be seen embedded in the ectodermal, radial muscle (open arrows). E - endodermal lamella, RC - radial canal, S – ectodermal swimming muscle. Scale bars in μm.

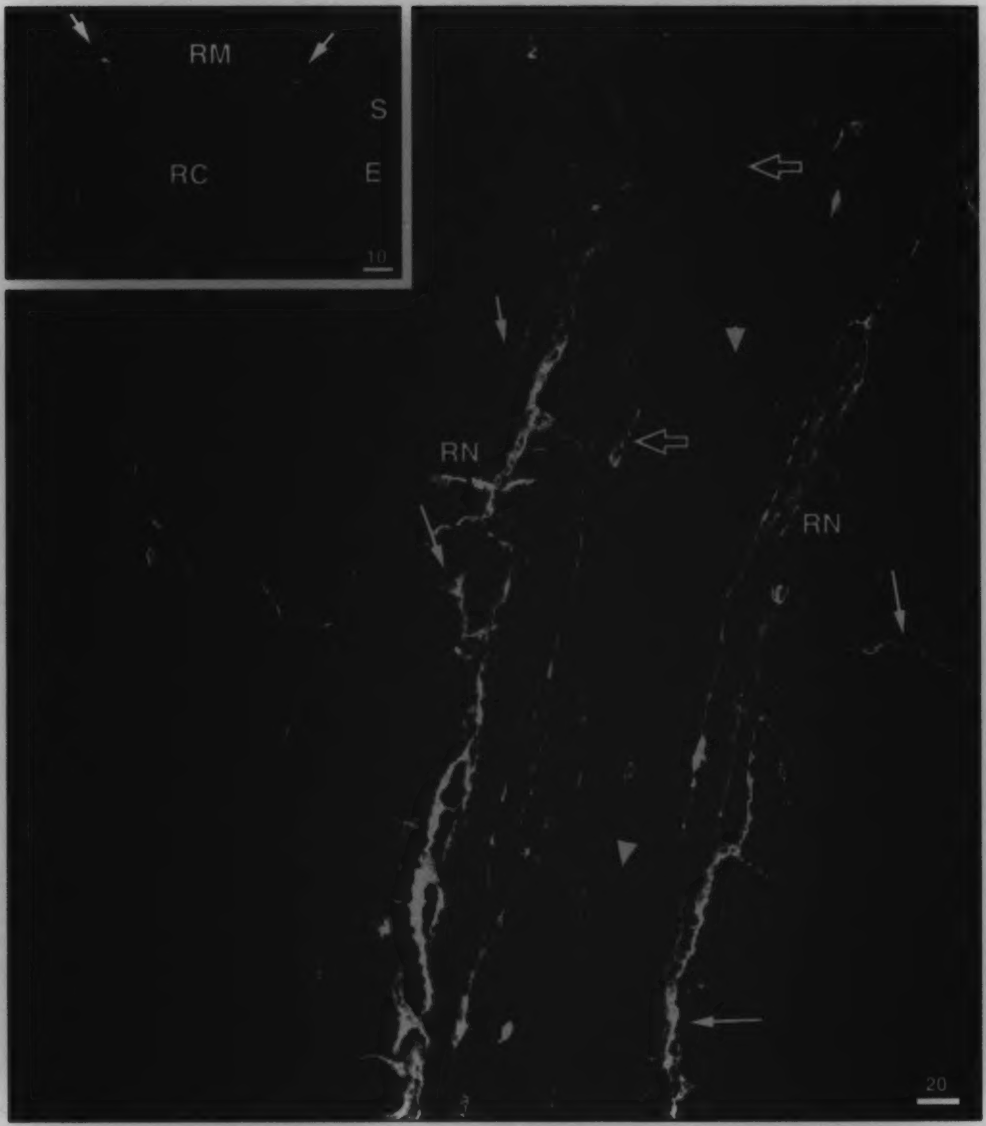
RM
S
RC
E
10
RN
RN
20

Fig. 2.4. Marginal region and the nerve-rings labelled with the monoclonal antibody 5C6. a) A radial section of the margin at the base of a tentacle (T) showing numerous profiles of immunoreactive neurons and neurosensory cells in the inner (INR) and outer (ONR) nerve-rings. The two nerve-rings are divided by the thin mesogleal tri-radius which is dark. The whole of the ectoderm from the outer nerve-ring proper (ONR) to an ocellus (arrow) contains immunoreactive cells, the cnidocytes appear as dark profiles. Three fluorescent endodermal neurites can be seen in the ring canal endoderm close to the tri-radius. EE - exumbrellar ectoderm, RC - ring canal, V - velum. b) Whole-mount of the inner side of the margin at the junction of a radial canal showing the radial nerves (RN) joining the swimming motor neuron (SMN) network in the inner nerve-ring. c) Whole-mount of velar edge of the inner nerve-ring showing accessory neurons (arrow) of the SMN running down onto the swimming muscle of the velum. d) Whole-mount of the outer side of the margin at the junction of a tentacle showing the intense labelling of numerous neurons and sensory cells throughout the outer nerve-ring (ONR) and the ectodermal networks of the tentacle (see Fig. 5). e) Enlarged view of the outer nerve-ring. he looping processes on the tentacular side of the outer nerve-ring are presumptive elements of the "B" (closed triangle) and "O" systems (open triangle). Radially directed neurites (open arrow) are seen running into the radial muscle of the velum. Much of the surface of the outer nerve-ring is covered by smaller sensory cells (SS). On the tentacular side of the ONR there are a number of large, bottle-shaped neurosensory cells (closed arrow) having a radial orientation. These cells are shown enlarged in f) (as indicated by the closed arrow in e) to show the filamentous processes at their apices. Scale bars in μm.

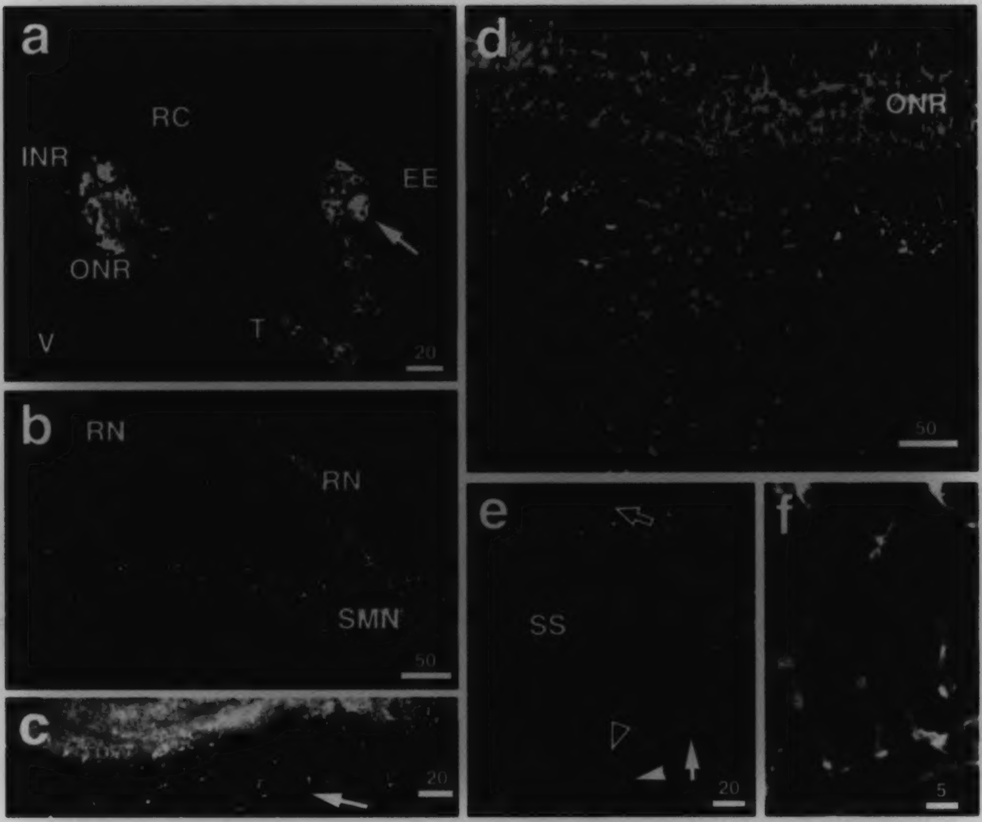
a
RC
INR
EE
ONR
V
T
20
b
RN
RN
SMN
50
c
20
d
ONR
50
e
SS
20
f
5

Fig. 2.5. a) Whole-mount of the base of a tentacle labelled with the monoclonal antibody 5C6 showing an ocellus (OC) and the paired ocellar nerves (arrows) running down into the outer nerve-ring (ONR) b) Enlarged view of an ocellus showing immunoreactive photoreceptor cells which are regularly distributed throughout the ocellus and separated by supporting epithelial pigment cells which do not label. c) Further enlargement of the photoreceptors showing the central cilium (closed arrow) and surrounding circlet of microvilli (open arrow). Scale bars in µm.

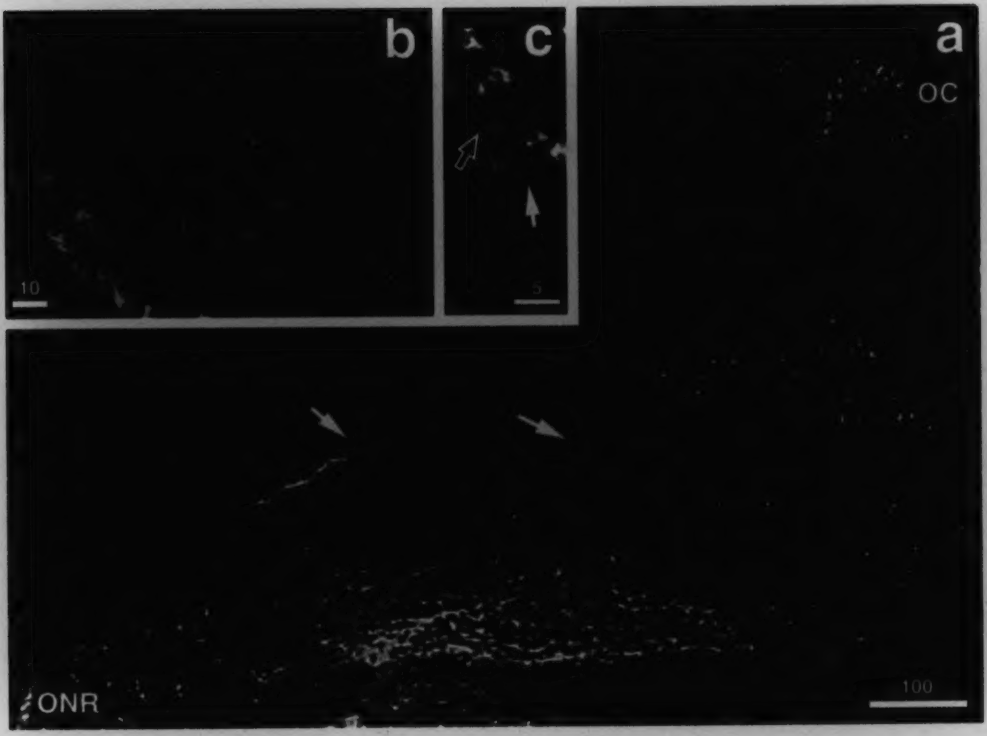
b
c
a
OC
10
5
ONR
100

47

Fig. 2.6. Whole-mount of a tentacle labelled with the monoclonal antibody 5C6. a) Proximal portion of a tentacle where cnidocyte battery complexes are absent showing both the presumed "B" system network of ganglionic cells and the RF-amide network with sensory cells projecting to the surface. b) Enlarged view of the region shown in a). Larger multipolar, ganglionic neurons form a network (presumed "B" system) of thick processes (closed arrow). This system does not project to the ectodermal surface. Neurosensory cells (triangles) which project to the surface are connected by a network of fine, beaded processes (open arrow) which run parallel to the longitudinal muscle fibres. The rounded, unlabelled areas (marked by x) between processes of the ganglionic net are stenotele cnidocytes. c) Distal region of a tentacle showing several cnidocyte-battery cell complexes (arrow) and the ganglionic network running between them. The larger labelled cells in the batteries are neurosensory cells while the punctate labelling is of the cnidocils of the cnidocytes. d) Enlargement of one cnidocyte-battery cell complex containing stenoteles (arrow) and surrounded by 9 neurosensory cells (triangles) which have a central cilium surrounded by microvilli. Scale bars in µm.

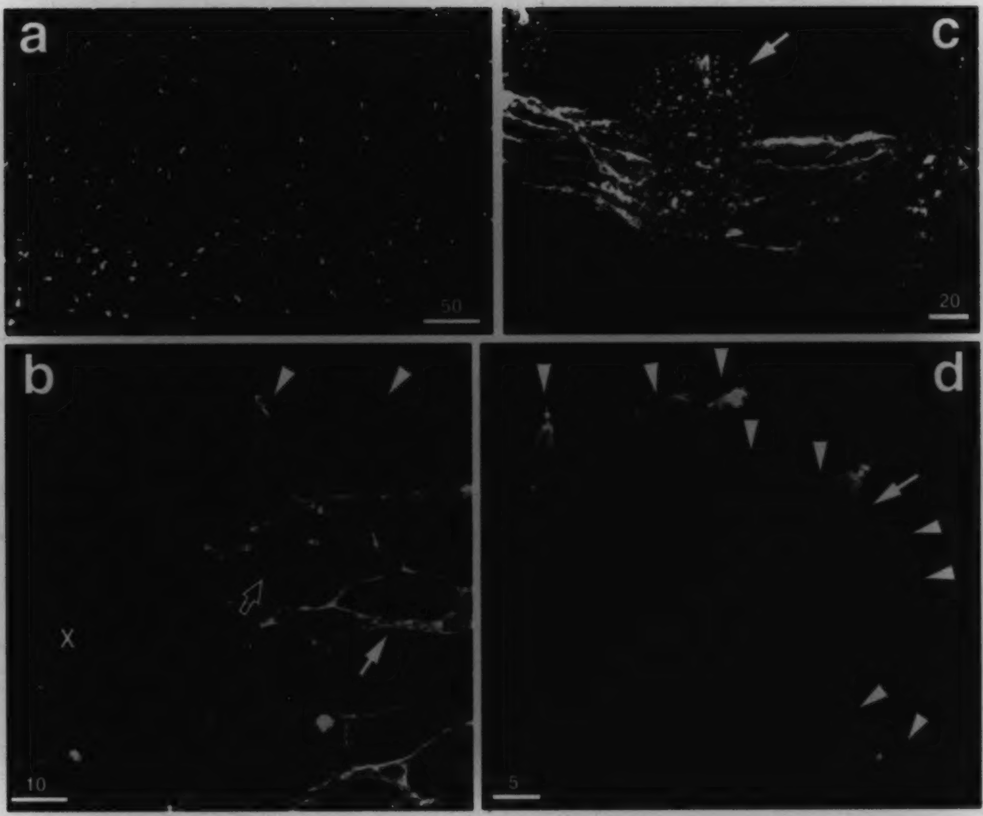
a
50
c
20
b
X
10
d
5

Fig. 2.7. Whole-mounts of the manubrium and gonad and a section of the gonad labelled with the monoclonal antibody 5C6. a) The central branch of the radial nerve network as it approaches the manubrium (M) with neurites parallel to the radial smooth muscle. b) Ectodermal nerve plexus in the manubrium with somata that project to the surface and an underlying radially oriented network of fine, beaded processes. c) Enlarged view of this manubrial network. d) Section of the manubrium showing immunoreactivity in both the ectoderm (Ec) and endoderm (E). d) Scattered immunoreactive neurons in the gonadal ectoderm that do not appear to make connections with one another. Scale bars in μm.

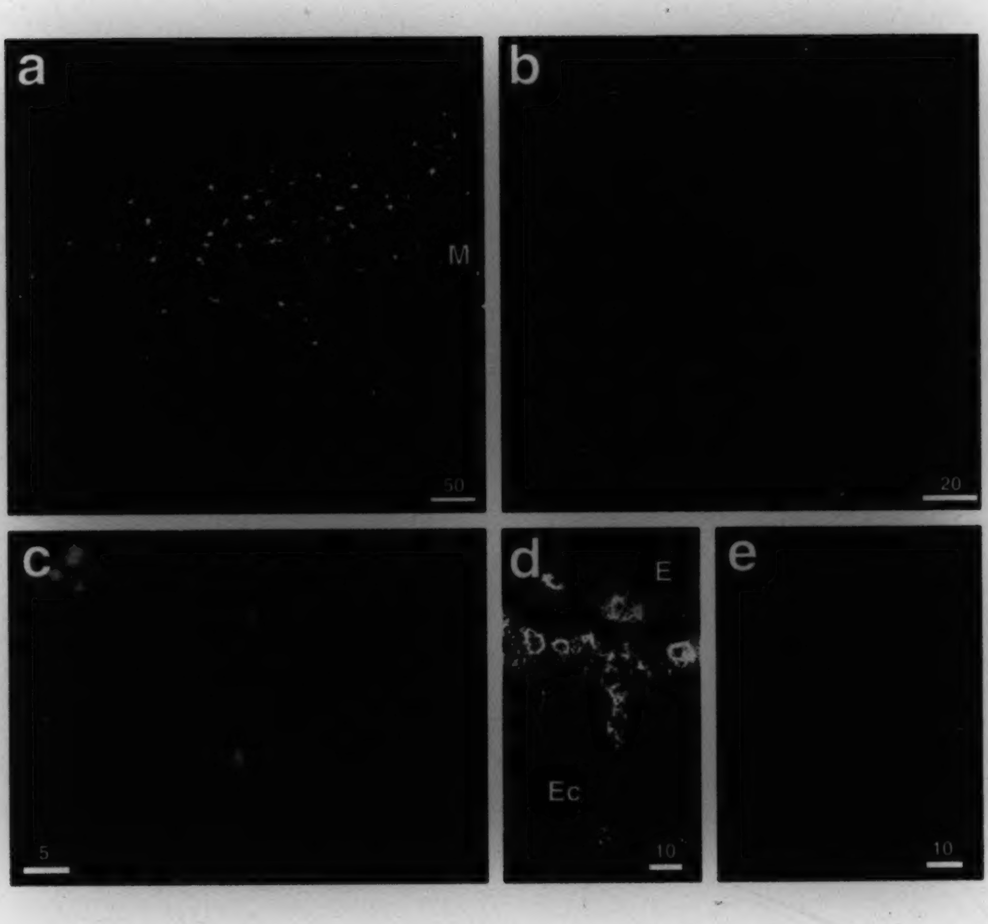
a
M
50
b
20
c
5
d
E
Ec
10
e
10

REFERENCES

Acheson, A. and Gallin, W. J. (1992). Generation and characterization of function blocking anti-cell adhesion molecule antibodies. *In* Cell-cell Interactions: a Practical Approach (ed. B. R. Stevenson, W. J. Gallin, and D. L. Paul). New York: Oxford University Press.

Anderson, P. A. and Mackie, G. O. (1977). Electrically coupled, photosensitive neurons control swimming in a jellyfish. *Science* **197**, 186-188.

Bullock, T. H. and Horridge, G. A. (1965). Coelenterata and Ctenophora. *In* Structure and Function in the Nervous Systems of Invertebrates, Vol. 1 (ed. T. H. Bullock, and G. A. Horridge). San Francisco: W. H. Freeman.

Grimmelikhuijzen, C. J. and Spencer, A. N. (1984). FMRFamide immunoreactivity in the nervous system of the medusa *Polyorchis penicillatus*. *J. Comp. Neurol.* **230**, 361-71.

Grimmelikhuijzen, C. J. Spencer, A. N., and Carré, D. (1986). Organization of the nervous system of physonectid siphonophores. *Cell Tiss. Res.* **246**, 463-479.

Ikegami, S., Honji, N., and Yoshida, M. (1978). Light-controlled production of spawning-inducing substance in jellyfish ovary. *Nature* **272**, 611-612.

King, M. G. and Spencer, A. N. (1981). The involvement of nerves in the epithelial control of crumpling behaviour in a hydrozoan jellyfish. *J. Exp. Biol.* **94**, 203-218.

Mackie, G. O. (1960). The structure of the nervous system in *Velella*. *Q. J. Micrsc. Sci.* **101**, 119-131.

Mackie, G. O. (1971). Neurological complexity in medusae: a report of central nervous system organization in *Sarsia*. *Actas del 10 Simp. Intl. Zoof., Salamanca* 269-280.

Mackie, G. O. and Singla, C. L. (1975). Neurobiology of *Stomotoca*. I. Action systems. *J. Neurobiol.* **6**, 339-56.

Przysiezniak, J. and Spencer, A. N. (1989). Primary culture of identified neurons from a cnidarian. *J. Exp. Biol.* **142**, 97-113.

Satterlie, R. A. (1985). Putative extraocellar photoreceptors in the outer nerve-ring of *Polyorchis penicillatus*. *J. Exp. Zool.* **233**, 133-139.

Singla, C. L. (1978a). Locomotion and neuromuscular system of *Aglantha digitale*. *Cell Tiss. Res.* **188**, 317-327. Singla, C. L. (1978b). Fine structure of the neuromuscular system of *Polyorchis penicillatus* (Hydromedusae, Cnidaria). *Cell Tiss. Res.* **193**, 163-174.

Singla, C. L. and Weber, C. (1982). Fine structure studies of the ocelli of *Polyorchis penicillatus* (Hydrozoa, anthomedusae) and their connection with the nerve ring. *Zoomorphology* **99**, 117-129.

Spencer, A. N. (1979). Neurobiology of *Polyorchis*. II. Structure of effector systems. *J. Neurobiol.* **10**, 95-117.

Spencer, A. N. (1981). The parameters and properties of a group of electrically coupled neurons in the central nervous system of a hydrozoan jellyfish. *J. Exp. Biol.* **93**, 33-50.

Spencer, A. N. (1982). The physiology of a coelenterate neuromuscular synapse. *J. Comp. Physiol.* **148**, 353-363.

Spencer, A. N. and Arkett, S. A. (1984). Radial symmetry and the organization of central neurons in a hydrozoan jellyfish. *J. Exp. Biol.* **110**, 69-90.

Chapter 3

Scarless wound-healing in jellyfish striated muscle involves rapid switching between two modes of cell motility

SUMMARY

Jet propulsion during jellyfish swimming is analogous to the pumping action of the vertebrate heart; indeed, early experiments with jellyfish contributed to the development of the myogenic theory of the heart beat (Romanes 1876, 1877, 1880, Fye 1987). Wound healing in heart tissue, such as after an infarction, involves multiple cell types and does not normally result in full functional recovery (Weber et al. 1996). In contrast, wound-healing in jellyfish swimming muscle does result in full functional recovery. This study demonstrates that striated muscle cells in a hydrozoan jellyfish are able to switch rapidly (within hours) from muscular motility that provides phasic contraction during swimming, to a non-muscular mode of motility that is responsible for cell migration and wound closure. During migration into the wound, the myofibrillar apparatus of jellyfish striated muscles is non-functional and is condensed around the nucleus. After wound closure, the contractile apparatus is realigned prior to functional recovery. This morphological and functional transformation is accompanied by changes in the dependency of cell motility on extracellular calcium: muscular motility depends on an extracellular source of calcium

whereas cell migration depends on an internal source, likely caffeine-sensitive and thapsigargin-sensitive calcium stores.

RESULTS AND DISCUSSION

The subumbrellar muscle sheets of the jellyfish, *Polyorchis penicillatus*, are formed by a layer of homogenous, mononucleated, striated muscle cells, about 10 μm thick. Distinct muscle "feet", where the contractile apparatus is formed, project from the soma (Fig. 3.1a, b). Muscle feet of neighbouring cells interdigitate and are connected end-on by desmosomes[6]. They attach to the underlying mesoglea (jelly) by hemi-desmosomes and are aligned concentrically so that by contracting they reduce the internal diameter of the bell cavity to expel water out of the bell opening (Spencer 1979). Like vertebrate cardiac muscles, gap junctions are present between cells in hydromedusan swimming muscles providing the electrical continuity required for myoid conduction (Spencer and Satterlie 1981). The convergence of the cellular apparatus used by hearts and jellyfish has presumably arisen to meet the similar mechanical demands of phasic fluid pumps. We noticed that specimens of this jellyfish collected from the wild are capable of healing small wounds in the muscle sheet in just a few days without the formation of scars. Scarless wound healing is common in vertebrate embryos but is not normally possible in adult tissues (Martin 1997).

To examine the wound-healing process in the swimming muscle layer of *Polyorchis*, we made circular wounds of about 1.2 mm in diameter in the centre of a swimming muscle sheet by scraping off the muscle sheet from the mesoglea. We then allowed the animals to recover in artificial seawater. Within one hour after wounding, undamaged striated muscle cells at the margin of the wound flattened and lost their polarised cellular morphology as muscle feet were withdrawn into the soma. Ruffled lamellipodial projections formed at the margin of cells that faced the wound (Fig. 3.1c). These lamellipodia-bearing cells then migrated in concert across the vacant mesogleal surface towards the wound centre. Myofibrils shortened and condensed, wrapping around the nucleus (Fig. 3.1d). The centripetally migrating cell front was followed by several rows of submarginal cells whose lamellipodia were tucked under the row in front. When the migrating front converged in the centre of the denuded area, cell migration stopped, with the whole area being covered by flattened cells, some 3 to 4 µm thick (Fig. 3.1e, f). After migrating cells met at the centre of the wound, they became elevated and it was at this stage that the muscle feet began to re-extend (Fig. 3.1g, h). Finally, feet became fully extended and the somata flattened again, returning the tissue to its undamaged state (Fig. 3.1i, j). Cells normally migrated as a continuous sheet, but occasionally some cells at the migrating edge broke free, revealing their individual morphology resembled moving keratocytes (Fig. 3.1k, l). This is the first reported case of differentiated striated muscle cells changing their phenotype to become migratory and participating in a wound-healing process. The phenomenon of cell migration described is similar to the "sliding model" of re-epithelialisation (Stenn and DePalma 1988).

To further examine the physiological changes involved in phenotype switching and in particular if contractility of the myofibrillar apparatus was preserved, we challenged the migrating cells with a depolarising stimulus (KCl). Addition of 100 mM KCl failed to elicit contractions from migrating cells but did cause contractions of intact muscle cells. Since gap junctions are involved in myoid conduction in undamaged muscle (Spencer 1979, Spencer and Satterlie 1981), we examined if gap junctions were maintained in the migrating muscle sheet. Dye coupling, following Lucifer Yellow injection, revealed that migrating muscle cells maintained their gap junction connections (Fig. 3.2a, b). TEM examination of migrating cells also revealed the presence of gap junctions (Fig. 3.2c) suggesting the possible involvement of gap junctions in co-ordinating migration (Wolburg and Rohlmann 1995). Like other migratory cells (Mitchison and Cramer 1996). jellyfish muscle cells use actin-based machinery for migration, since diffuse actin staining with phalloidin could be observed in the lamellipodia (Fig. 3.1l), and the actin-depolymerising agent cytochalasin B (5 $\mu g\ ml^{-1}$) inhibited cell migration.

In most systems studied to date, wound-healing involves the participation of myofibroblasts which are the contractile elements used to bring the wounded margins together and reduce wound size (Schmitt-Graff et al. 1994). However, in this jellyfish, migrating muscle cells themselves are capable of exerting tonic traction forces during both migration and repositioning of muscle feet. Figure 3.3d shows that the force generated by migrating muscle cells created strain marks in undamaged areas. These strain marks ran parallel to the long axis of the muscle feet. Due to the pliability of the mesoglea (Schmid

1976) the tonic forces generated during lamellipodial locomotion could help to close the wound by reducing the area that needs to be covered by migrating cells.

It takes about 8 to 10 h for muscle cells to migrate and cover a denuded mesogleal surface of about 1.2 mm in diameter and another 24 to 48 h for the migrating cells to resume their polarity and contractility. Although closure of the wound appears to be achieved by muscle cell migration and mesoglea retraction, we sought a possible contribution of cell proliferation. During the wound-healing process we treated whole jellyfish with 1 mM bromodeoxyuridine (BrdU)(Plickert and Kroiher 1988) for 72 h, by means of which we detected no cell proliferation in the muscle layer of 6 wounded jellyfish. However, cell proliferation was detected at the base of tentacles where no wound-healing was occurring, suggesting that, at least for small wounds, mitosis is not necessary for wound closure.

To determine whether transformation to a migratory phenotype required synthesis of new proteins, we treated whole jellyfish with 40 µM cycloheximide 4 h before inflicting the wound. Cycloheximide did not significantly affect either the ability of muscle cells to de-differentiate or to migrate (Fig. 3.3a). These data suggest that neither phenotype switching nor migration require the synthesis of new proteins. However, if jellyfish were treated with cycloheximide 4 h before wound closure, re-differentiation did not take place and the cells remained flat without muscle feet extension. When cycloheximide was removed, re-differentiation to a fully polarised state resumed, suggesting that re-differentiation does require protein synthesis.

Since normal phasic contraction of jellyfish muscle during swimming depends on influx of extracellular calcium (Spencer and Satterlie 1981), through voltage-gated calcium channels, we examined the role played by calcium and calcium channels in cell migration. Jellyfish muscle sheets in artificial seawater containing either a low concentration of calcium ions (1 μM free calcium) or the calcium channel blocker, nitrendipine, did not contract when directly stimulated (Fig. 3.3a). However, under either of these conditions, cells were able to migrate and cover the wound area at the same rate as under control conditions (Fig. 3.3b).

To determine the fate of voltage-gated channels during cell migration, we used whole-cell patch clamp recordings to compare the density of voltage-gated channels in differentiated cells and migrating cells. Figure 3.3c shows that contractile muscle cells possessed both outward potassium currents (A-type and delayed rectifier) and inward currents, whereas only the delayed rectifier current, albeit at a reduced amplitude, was present in migrating cells. The predominant inward current in intact striated myocytes is carried by calcium ions and channels passing this current resemble T-type vertebrate channels as they are activated at low-voltages (Chapter 4). Therefore, it appears that the de-differentiation of contractile muscle cells into migrating cells is accompanied by a down-regulation of voltage-gated channels, especially those responsible for inward currents, and this can explain the insensitivity of migrating cells to nitrendipine. Moreover, an up-regulation of voltage-gated ion channels following migration and before restoration of muscle contractility would explain the block of re-differentiation by cycloheximide.

Since cell migration was not affected by a reduction of extracellular calcium, we examined whether cell migration required an intracellular source of calcium. The strength of phasic contraction in swimming muscle increases with the stimulation (Chapter 5, Fig. 5.1a, b). A similar phenomenon in vertebrate heart muscles is due to redistribution of calcium ions from intracellular store(s) to cardiomyoplasm (Bers 1991). In jellyfish administration of 10 mM caffeine completely abolished the development of frequency-dependent augmentation, suggesting a contribution of intracellular stores to the excitation-contraction mechanism (Chapter 5, Fig. 5.1c, d). In the presence of caffeine, the migration rate slowed to 0.2 $\mu m\ min^{-1}$, compared to 1.2 $\mu m\ min^{-1}$ in ASW (Fig. 3.2b). To control for possible non-specific effects of caffeine (Butcher et al. 1962), the dependence of cell migration on an intracellular store of calcium was confirmed in a separate experiment by addition of 10 μM thapsigargin. This significantly reduced migration speed from $1.03 \pm 0.09\ \mu m\ min^{-1}$ to $0.46 \pm 0.08\ \mu m\ min^{-1}$ (mean ± S.E., n = 12 muscle strips, $p< 0.05$, paired T-test).

This study is the first demonstration that well-differentiated striated muscle cells can rapidly change their motility from phasic contraction to lamellipodial locomotion so as to cover a wounded area in a sheet of homogenous cells (Fig. 3.4). The tractive forces that are associated with migration act on the mesoglea and aid in wound closure by reducing the area that has to be covered by migrating cells. The switch from phasic contraction to lamellipodial migration is associated with a change in the required source of calcium from extracellular to intracellular and is accompanied by a down-regulation of certain voltage-gated ion channels. This phenotype switching does not require the synthesis of new proteins. Moreover, scar tissue, which could interfere with both the spread of excitation in the muscle sheet and contractility, is absent. Therefore, a full functional recovery could be achieved. Such a wound-healing mechanism exhibits obvious advantages when compared with post-traumatic changes in the cardiac muscle since the absence of scar tissue virtually eliminates the danger of ectopic electrical oscillations, analogous to post-infarct cardiac arrhythmias (Weber 1996).

METHODS

Wounding procedure

A radial cut of the bell of medusae (*Polyorchis penicillatus*) exposed the subumbrellar striated muscle sheets and a Pasteur pipette was used to mark an area 1.2 mm in diameter for cell removal. A surgical blade was used to gently scrape away muscle cells within the marked area. Digital images of the wound-healing process were acquired through a JVC CCD video camera mounted on a dissecting microscope using SigmaScan image software (Jandel Scientific, Inc.). The speed of migration was calculated by measuring the movement of the cell front at 3, 4 and 5 h post wounding. Jellyfish were immersed in artificial seawater (ASW, pH 7.5) containing: NaCl: 376mM, $Na_2(SO_4)$: 26 mM, $MgCl_2$: 41.4 mM, $CaCl_2$: 10 mM, KCl: 8.5 mM, and N-[2-Hydroxyethyl]piperazine-N′-[2-ethanesulfonic acid] (HEPES, hemisodium salt): 10 mM, at 10-12°C for all experiments.

Electron microscopy and laser confocal microscopy

For transmission electron microscopy, jellyfish were fixed with 4% paraformaldehyde and 2% glutaradehyde in phosphate buffered saline (pH 7.5) and postfixed with 1% osmium tetroxide and processed as described previously (Spencer 1979). For scanning electron microscopy, jellyfish were fixed with 0.01% osmium tetroxide in ASW, dehydrated, coated with gold and examined using a JEOL scanning electron microscope. For laser scanning confocal microscopy, jellyfish were fixed with 4% paraformaldehyde in ASW, washed with PBS, and double stained with BODIPY FL phalloidin and propidium iodide (Molecular Probes, Inc.).

Pharmacology of muscle contraction

Preliminary study indicated that both muscle strips from bell regions and vela had similar pharmacologies. Due to the thickness and elastic property of mesoglea in the bell region, recordings from muscle strips obtained from this region were extremely variable and it was difficult to measure contractile amplitude. Therefore, only muscle strips from vela were used in this study. The vela of medusae, anaesthetized in 1:1 isotonic $MgCl_2$ (0.33M) and artificial seawater (ASW), were excised so as to provide continuous strips of maximal width. Artificial seawater (pH 7.5) consisted of NaCl: 376 mM, $Na_2(SO_4)$: 26 mM, $MgCl_2$: 41.4 mM, $CaCl_2$: 10 mM, KCl: 8.5 mM, and HEPES (hemisodium salt): 10 mM. To avoid any contamination by nervous tissue, each velar strip was bisected lengthwise into two strips and only the strip free from any tissue from the inner nerve-ring was used in the study. The free ends of each velar strip were pinned to the Sylgard base of a 35 mm Petri dish which also contained a pair of embedded $Ag/AgCl_2$ stimulating electrodes connected to a Grass S44 stimulator. The velar strip ran between the two stimulating electrodes and around a small hook attached to a capacitative force transducer (Kent, Inc.). The tension on the strip was adjusted using a micromanupulator so as to remove any slack in the preparation and maximize tension excursions. The threshold for contraction was determined by increasing the stimulation voltage until a measurable contraction occurred. The rate of perifusion was controlled by a peristaltic pump at 1.5 ml/min and the perifusate was removed by a vacuum pump. All perifusates were kept at 12-14°C during the whole experiment by running the perfusion tubing through an ice bucket. The transduced tension was recorded on a digital Dash-IV pen-recorder (Astro-Med Inc.). The amplitude of contractile tension for each condition (control, drug effect, and washed) was calculated from averaging 30 contractile tensions. Low calcium ASW was prepared by adding 2 mM of 8-bromoBAPTA into ASW to create a free calcium concentration of 1 μM.

Electrophysiology

The protocol for whole-cell, patch-clamp recording was described previously (Grigoriev 1996). Normal muscle cells were dissociated by applying 1 mg ml^{-1} Pronase in ASW at 30°C for 15 min. Migrating cells were prepared by grafting a piece of jellyfish muscle onto a mesoglea coated Petri dish (Freeman 1981) and gently pressing it with a coverslip. This sandwich was kept immersed in ASW at 12°C before recording. Recordings were made within 6-12 h after grafting when muscle cells migrated onto the prepared mesoglea and formed a monolayer. Single cell recordings were achieved by selectively removing unwanted cells. Dye coupling was evaluated by adding 1 mM Lucifer Yellow to the recording electrode solution and iontophoresing it with repetitive hyperpolarising current injection. The bath solution for recording was artificial seawater (ASW). The electrode solution (pH 7.5) contained: NaCl: 50 mM, $MgCl_2$: 2 mM, $CaCl_2$:

1 mM, ethylene glycol-bis(β-aminoethyl ether)-N,N,N′,N′-tetraacetic acid: 11 mM, KCl: 350 mM, KOH: 30 mM, HEPES-free acid: 10 mM.

Fig. 3.1. Changes in cell morphology during the wound-healing process in jellyfish striated muscle cells. a) TEM section of undamaged muscle cells shows their polarised morphology with a superficial layer of somata and a deeper layer of attached contractile feet. b) Confocal laser image of undamaged muscle cells showing the ordered arrangement of striated myofibres, stained by BODIPY conjugated phalloidin (green) and nuclei stained with propidium iodide (red). c) SEM image of cells at the migrating wound margin 1 h after wounding showing ruffled lamellipodia at the leading edge. d) Confocal laser image taken 1 h after wounding showing that muscle feet were retracted at the wound margin. Myofibres lose their alignment and envelop the nuclei. e) SEM image of flattened migrating cells as the wound approaches closure 6 h after wounding. f) Migrating cells at the same stage as e) showing the contractile apparatus bundled around the nuclei. g) and h), SEM and fluorescent images of cells just after wound closure (18 h after wounding) as they begin to re-differentiate by rounding up, thickening and reorganising the muscle feet. i) SEM image of a healed area 60h after wounding showing that cells are no longer elevated. j) Fluorescent image at the same stage as i) showing that myofibres have re-extended but they are not yet completely re-aligned. k) and l) SEM and fluorescent images of isolated migrating cells (4 h after wounding) showing the loose arrangement of actin filaments in the ruffled lamellipodium and the non-functional myofibrillar apparatus wrapped around the nucleus. All pairs of images are of different cells or cell populations but they are fixed at the same time after wounding. Scale bars are 5 _m in a) and 10 _m for all other images.

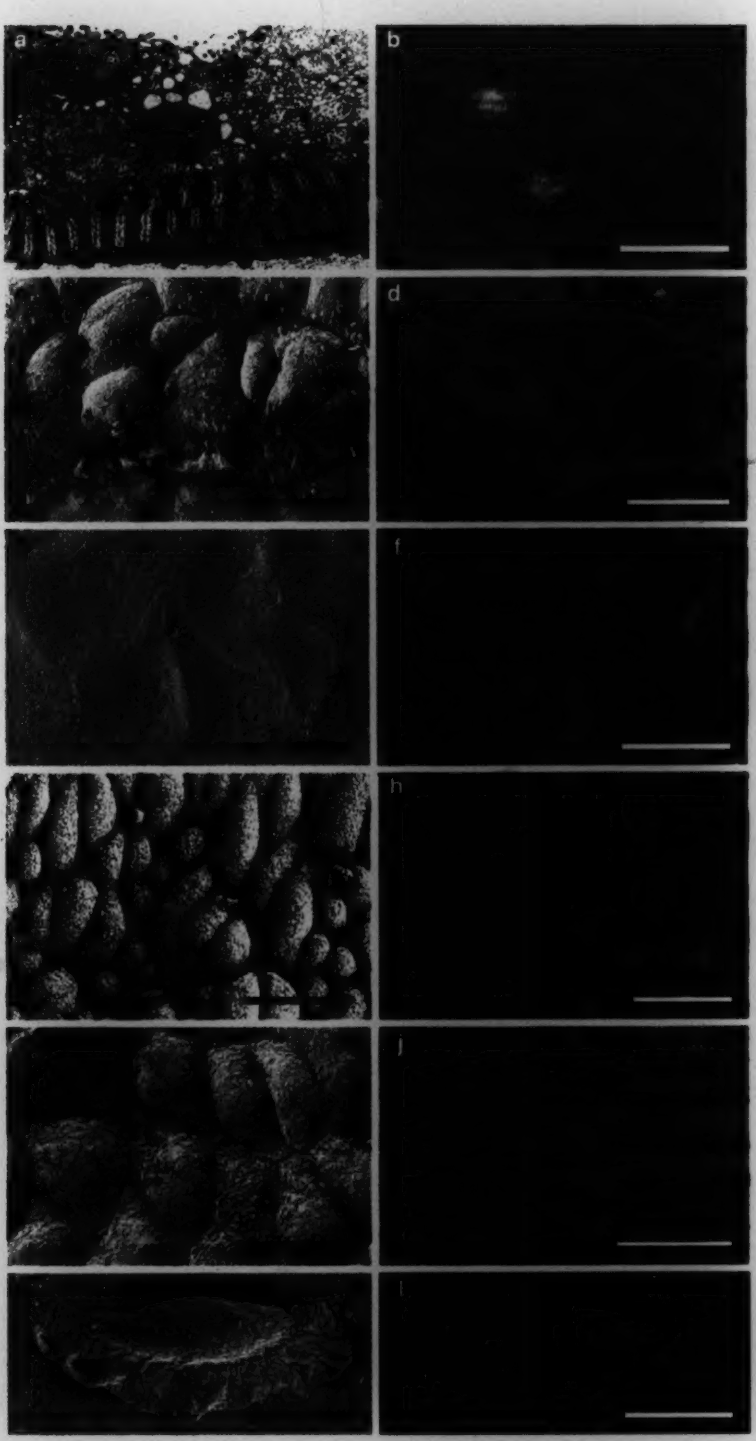
a
b
d
f
h
j
l

Fig. 3.2. Migrating cells maintain gap junction connections and generate traction forces. a) Phase contrast image of a population of migrating cells in which Lucifer Yellow was iontophoresed into one cell (arrow). b) Fluorescent image of the same region 5 min. after iontophoresis showing dye-coupling to neighbouring cells. c) A TEM image of migrating cells showing a section of gap junction (arrow). d) The force generated by migrating cells creates strain marks in the undamaged muscle (8 h after wounding). The uncovered mesoglea is shown by an asterisk, and the migrating cell front by an arrow. Scale bars are 10 _m in b), 200 nm in c), and 400 _m in d).

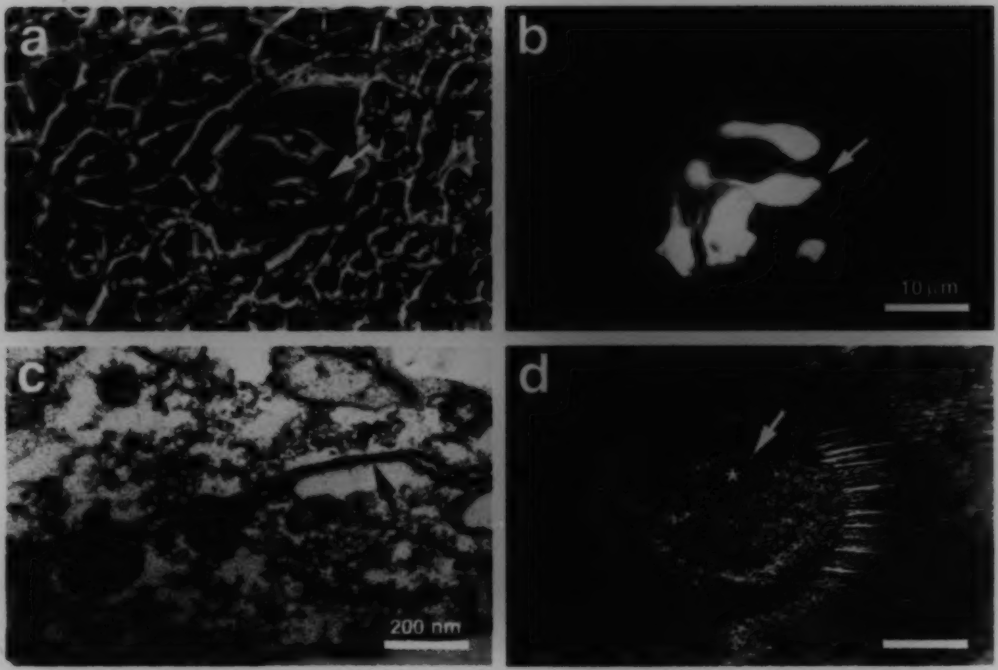
a
b
10 µm
c
200 nm
d

Fig. 3.3. Effects of different pharmacological agents on muscle contraction and migration. a) Trace from force transducer of stimulated muscle contractions and the inhibitory effect of addition of 40 _M nitrendipine in Asw (closed arrow) and subsequent wash (opened arrow). b) Effects of various drugs on the contractile force of normal muscle and their migratory velocity. The upper panel shows the maximal contractile force generated with each contraction when treated with the drugs shown when compared with the control in artificial seawater (ASW). The absence of contractions with nitrendipine and low calcium seawater indicates a requirement for an external source of Ca^{2+}. The lower panel shows that cell migration is significantly slowed by caffeine. The speed of cell migration was estimated from the advance of the wound margin at measured time intervals. Significant differences are indicated by asterisks (ANOVA test followed by PLSD test, $p < 0.05$). $N = 9$ for each treatment group. c) Whole-cell currents recorded from normal, contractile muscle cells (upper traces, average current traces of 15 cells) and migrating cells (lower traces, average current traces of 5 cells). The amplitudes of both inward and outward components are significantly reduced in migrating cells when compared with normal muscle cells, indicating that there is a down-regulation of ion channels prior to or during migration. Scale bars are 200 pA for the vertical bar and 5 ms for the horizontal bar.

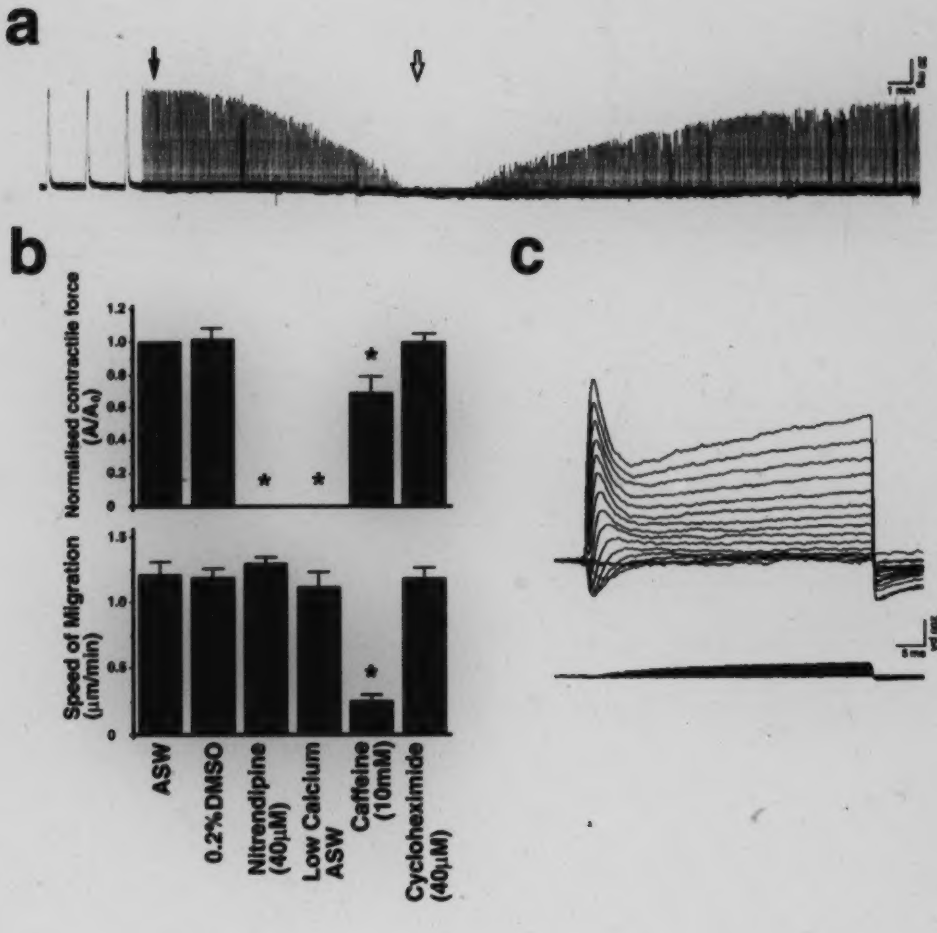
a
1 min
b
c
Normalised contractile force (A/A₀)
0
0.2
0.4
0.6
0.8
1.0
1.2
*
*
*
Speed of Migration (µm/min)
0
0.5
1.0
1.5
*
ASW
0.2%DMSO
Nitrendipine (40µM)
Low Calcium ASW
Caffeine (10mM)
Cycloheximide (40µM)
5 ms
200 pA

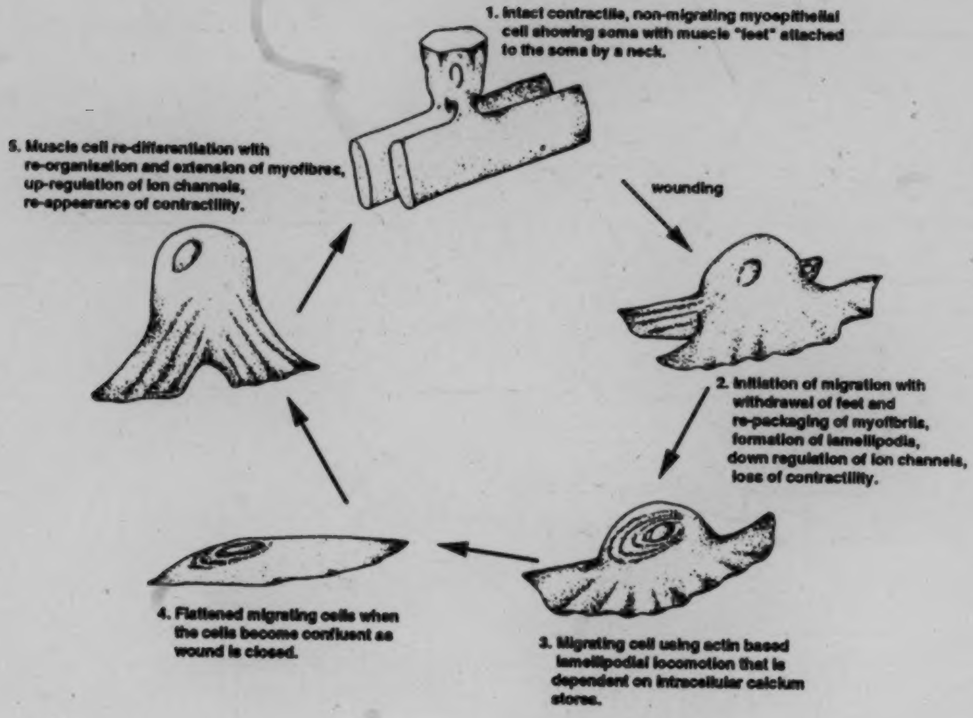
1. Intact contractile, non-migrating myoepithelial cell showing soma with muscle "feet" attached to the soma by a neck.
wounding
2. Initiation of migration with withdrawal of feet and re-packaging of myofibrils, formation of lamellipodia, down regulation of ion channels, loss of contractility.
3. Migrating cell using actin based lamellipodial locomotion that is dependent on intracellular calcium stores.
4. Flattened migrating cells when the cells become confluent as wound is closed.
5. Muscle cell re-differentiation with re-organisation and extension of myofibres, up-regulation of ion channels, re-appearance of contractility.

Fig. 3.4. Diagram of the wound-healing process in the striated muscle cells of the medusa *Polyorchis penicillatus*.

REFERENCES

Bers, D. M. (1991). Excitation-contraction coupling and cardiac contractile force. Boston: Kluwer Academic.

Butcher, R. W. and Sutherland, E. W. (1962). Adenosine 3′, 5′-phosphate in biological materials. I. Purification and properties of cyclic 3′, 5′-nucleotide phosphodiesterase and the use of this enzyme to characterise adenosine 3′, 5′-phosphate in human urine. *J. Biol.Chem.* **237**, 1244-1250.

Freeman, G. (1981). The role of polarity in the development of the hydrozoan planula larva. *Rouxİs Arch. Dev. Biol.* **190**, 168-184.

Fye, W. B. (1987). The origin of the heart beat: a tale of frogs, jellyfish, and turtles. *Circulation* **76**, 493-500.

Grigoriev, N. G., Spafford, J. D., Przysiezniak, J., and Spencer, A. N. (1996). A cardiac-like sodium current in motor neurones of a jellyfish. *J. Neurophysiol.* **76**, 2240-2249.
Martin, P. Wound healing - aiming for perfect skin regeneration. *Science* **276**, 75-81 (1997).

Mitchison, T .J. and Cramer, L. P. (1996).Actin-based cell motility and cell locomotion. *Cell* **84**, 371-379.

Plickert, G. and Kroiher, M. (1988). Proliferation kinetics and cell lineages can be studied in whole mounts and macerates by means of BrdU/anti-BrdU technique. *Development* **103**, 791-794.

Romanes, G. J. (1876). Preliminary observations on the locomotor system of medusae. *Phil. Trans. Roy. Soc. London.* **166**, 269-313.

Romanes, G. J. (1877). Further observations on the locomotor system of medusae. *Phil. Trans. Roy. Soc. London.* **167**, 659-752.

Romanes, G .J. (1880). Concluding observations on the locomotor system of meduase. *Phil. Trans. Roy. Soc. London.* **171**, 161-202.

Schmid, V., Schmid, B., Schneider, B., Stidwill, R., and Baker, G. (1976). Factors effecting manubrium-regeneration in hydromedusae (coelenterata). *Roux's Arch. Dev. Biol.* **179**, 41-56.

Schmitt-Graff, A., Desmouliere, A., and Gabbiani, G. (1994). Heterogeneity of myofibroblast phenotypic features: an example of fibroblastic cell plasticity. *Virchows Archiv* **425**, 3-24.

Spencer, A. N. (1979).Neurobiology of *Polyorchis*. II. Structure of effector systems. *J. Neurobiol.* **10**, 95-117.

Spencer, A. N. and Satterlie, R. A. (1981).The action potential and contraction in subumbrellar swimming muscle of *Polyorchis penicillatus* (Hydromedusae). *J. Comp. Physiol.* **144**, 401-407.

Stenn, K. S. and DePalma, L. (1988). *in* The molecular and cellular biology of wound repair (eds. Clark, R.A.F. & Henson, P.M.) 321-336 (Plenum Press, New York).

Weber, K. T., Sun, Y., and Katwa, L. C. (1996). Wound healing following myocardial infarction. *Clin. Cardiol.* **19**, 447-455.

Weber, K. T., Sun, Y., Katwa, L. C., Cleutjens, J. P. M., and Zhou, G. (1996). Connective tissue and repair in the heart. *Ann. New York Acad. Sci.* **101**, 286-299.

Wolburg, H. and Rohlmann, A. (1995). Structure-function relationships in gap junctions. *Intl. Rev. Cytol.* **157**, 315-373.

Chapter 4

Characterization and localisation of a T-type calcium channel from a hydrozoan jellyfish, *Polyorchis penicillatus*

INTRODUCTION

Calcium ions play an important role in regulating a number of cellular processes, with the calcium ion concentration in various compartments determining the onset, speed and termination of various biochemical and biophysical events (Berridge 1993). Voltage-gated (Vg) calcium channels play a crucial role since their activity will influence the cytoplasmic concentration of calcium ions. Among the numerous examples of the regulatory activity of Vg Ca^{2+} channels are smooth and skeletal muscle contraction, transmitter release at synapses, signal transduction, development of vascular tone, release of hormones, and cellular growth (Hille 1992).

Voltage-gated calcium channels can be categorized into low voltage activated (LVA) and high voltage activated (HVA) channels. In general, LVA channels activate at around -70 to -40 mV, inactivate rapidly, and are sensitive to Ni^{2+} and mibefradil (Bean 1985, Akaike et al. 1989, Huguenard 1996, Ertel et al. 1997), while HVA calcium channels activate at > -40 mV. The activation and inactivation kinetics of HVA calcium channels are quite variable but they can be identified by their sensitivity to various pharmacological agents. They are categorized into at least 5 classes, namely L, N, P, Q, and R types. L-type channels are characterized by dihydropyridine sensitivity (Fox et al. 1987), N-type channels are blocked by ϖ-conotoxin (CTx)-GVIA (McCleskey et al. 1987), P-type channels by the funnel-web spider toxins FTX (Llinas et al. 1989) and by low concentration of ϖ-Agatoxin (AgaIVA) (2 nM; Mintz et al. 1992), and Q-type channels by high concentrations of AgaIVA (200 nM; Sather et al. 1993). The R-type channels are a class of HVA channels that are resistant to dihydropyridines, ϖ-conotoxin (CTx)-GVIA, ϖ-CTx-MVIIC, and ϖ-Agatoxin (AgaIVA) (Randall and Tsien 1995). It appears that most excitable cells express more than one type of calcium channel.

Muscle cells are recognized as being either striated or smooth depending on whether their contractile myofibrillar apparatus is in register or not. Smooth muscles with unaligned sarcomeres are usually responsible for tonic contraction while striated muscles are normally involved in phasic contraction. Cardiac muscle is one form of striated muscle.

Voltage-gated calcium channels are found in all muscle types, however, their roles in muscle contraction differ depending on the muscle type. Influx of external calcium ions is required to initiate contraction in both smooth and cardiac muscle but not in skeletal striated muscle of vertebrates (Bers 1991), where depolarisation of the membrane triggers release of calcium from the sarcoplasmic reticulum (Endo 1977). All cardiac myocytes possess L-type calcium channels while T-type channels are also present in cardiac cells that display primary or secondary pacemaker activity such as at the sinoatrial node, sinus venosus, and Purkinje fibres (Hagiwara et al. 1988, Hirano et al. 1989, Tseng and Boyden

1989, Bois and Lenfant 1991). However, T-type channels are absent or at low densities in ventricular myocytes (Bers 1991, Campbell and Strauss 1995). Thus, the primary role of L-type calcium channels appears to be the control and modulation of the electro-mechanical coupling process, while T-type channels are involved in pacemaker activity.

Several voltage-gated calcium currents have been recorded from neurons in jellyfish (Mackie and Meech, 1985; Anderson, 1987, Przysiezniak and Spencer, 1992), smooth muscles in ctenophores (Bilbaut et al. 1988, Dubas et al. 1988), and fertilized eggs in ctenophores (Barish 1984). The presence of calcium channels in the striated swimming muscle of the medusa *Polyorchis penicillatus* was shown by Spencer and Satterlie (1981). More recently, using isolated striated muscle strips from this jellyfish, we have shown that contraction depends on extracellular calcium and can be inhibited by the calcium channel blocker, nitrendipine (Chapter 3). Using both electrophysiological techniques and specific labelling, we report the presence of T-type calcium channels in striated myocytes of the hydrozoan jellyfish, *Polyorchis penicillatus*. A primary function of calcium currents through this channel population is to initiate muscle contraction. We have determined that the muscle feet have a far higher density of these channels than the somata.

MATERIALS AND METHODS

Medusae of *Polyorchis penicillatus* were collected in Bamfield Inlet or Pachena Bay, near Bamfield, B.C. Canada and maintained in an aquarium with running seawater at the Bamfield Marine Station, Bamfield, B.C. Canada.

Cell dissociation and electrophysiology

Subumbrellar areas were excised from the whole jellyfish and digested with 1 mg/ml of Pronase (Boehringer Mannheim) in ASW at 30°C or room temperature (20-22°C) for 15-20 minutes. Whole-cell, tight-seal recordings were made using borosilicate glass electrodes (TW-150-4, World Precision Instruments) which were pulled by a Sutter automatic puller, with resistances of 2-3 MΩ when filled with the electrode solution. Recordings were made at room temperature with an Axopatch-1D amplifier (Axon Instruments), low-pass filtered at 3 kHz using a 4-pole Bessel filter, and digitized using a Labmaster TL-125 acquisition board (Axon Instruments). Individual cells were viewed under phase contrast with a Nikon Diaphot inverted microscope. A piezo-electric driver (Burleigh) was used to manipulate the microelectrode onto the cell surface. Stimulus control, data acquisition, and analysis were performed with pCLAMP 6.0 software (Axon Instruments) on a Dell, IBM-compatible computer.

Leakage and capacitative currents were subtracted using -P/4 or -P/5 protocols (pCLAMP 6.0), from a holding potential of -80 mV, before test pulses eliciting active responses were applied. Series resistance (R_s) was compensated optimally to minimize voltage errors (R_s compensation was usually set to values of ≥ 80%). C_m (membrane capacitance) and R_s were obtained by minimizing the capacitative transient in response to a hyperpolarizing voltage step. All experiments were carried out at room temperature (20-22°C).

Solutions

All recording solutions were filtered through cellulose acetate membrane cartridges with a 0.2 µm pore size. Artificial seawater (pH 7.5) contained: NaCl: 376 mM, $Na_2(SO_4)$: 26 mM, $MgCl_2$: 41.4 mM, $CaCl_2$: 10 mM, KCl: 8.5 mM, and HEPES (hemisodium salt): 10 mM. The bath solution (pH 7.5) contained $MgCl_2$: 40 mM, $CaCl_2$ (or $BaCl_2$, or $SrCl_2$): 10 mM, KCl: 15 mM, NMG-Cl: 429 mM, HEPES free-acid: 10 mM.The electrode solution (pH 7.5) for total membrane currents contained: NaCl: 50 mM, $MgCl_2$: 2 mM, $CaCl_2$: 1 mM, ethylene glycol-bis(β-aminoethyl ether)-N,N,N',N'-tetraacetic acid: 11 mM, KCl: 350 mM, KOH: 30 mM, HEPES-free acid: 10 mM. The electrode solution (pH 7.5) for isolated Ca^{2+} currents contained NaCl: 50 mM, $MgCl_2$: 2 mM, $CaCl_2$: 1 mM, ethylene glycol-bis(β-aminoethyl ether)-N,N,N',N'-tetraacetic acid: 11 mM, CsCl: 350 mM, CsOH: 30 mM, HEPES-free acid: 10 mM, and TEA-Cl: 20 mM. All outward currents were totally blocked within the first minute after break-through.

Pharmacology of muscle contraction

Preliminary study indicated that both muscle strips from bell regions and vela had similar pharmacologies. Due to the thickness and elastic property of mesoglea in the bell region, recordings from muscle strips obtained from this region were extremely variable and it was difficult to measure contractile amplitude. Therefore, only muscle strips from vela were used in this study. The vela of medusae, anaesthetized in 1:1 isotonic $MgCl_2$ (0.33M) and artificial seawater (ASW), were excised so as to provide continuous strips of maximal width. Artificial seawater (pH 7.5) consisted of NaCl: 376 mM, $Na_2(SO_4)$: 26 mM, $MgCl_2$: 41.4 mM, $CaCl_2$: 10 mM, KCl: 8.5 mM, and HEPES (hemisodium salt): 10 mM. To avoid any contamination by nervous tissue, each velar strip was bisected lengthwise into two strips and only the strip free from any tissue from the inner nerve-ring was used in the study. The free ends of each velar strip were pinned to the Sylgard base of a 35 mm Petri dish which also contained a pair of embedded $Ag/AgCl_2$ stimulating electrodes connected to a Grass S44 stimulator. The velar strip ran between the two stimulating electrodes and around a small hook attached to a capacitative force transducer (Kent, Inc.). The tension on the strip was adjusted using a micromanupulator so as to remove any slack in the preparation and maximize tension excursions. The threshold for contraction was determined by increasing the stimulation voltage until a measurable contraction occurred. The rate of perifusion was controlled by a peristaltic pump at 1.5 ml/min and the perifusate was removed by a vacuum pump. All perifusates were kept at 12-14°C during the whole experiment by running the perfusion tubing through an ice bucket. The transduced tension was recorded on a digital Dash-IV pen-recorder (Astro-

Med Inc.). The amplitude of contractile tension for each condition (control, drug effect, and washed) was calculated from averaging 30 contractile tensions.

Localisation of calcium channels

Localisation of calcium channels with dihydropyridine-BODIPY (fDHP) followed Schild et al. (1995) with some modifications. Dissociated cells were incubated with both fDHP and a styryl dye RH414 at a final concentration of 10 μM and 5 μM, respectively. A laser scanning confocal microscope (Molecular Dynamic, Inc.) was used to examine the spatial distribution of T-type channels. The wavelength of the excitation beam was set to 488 and 568 nm (argon ion laser, 4.0 mW). The emitted fluorescence from labelled cells was split into two wavelength bands by a dichroic mirror (565 nm). The green and red fluorescence emissions, representing the labelling intensity of fDHP and RH414, respectively, were recorded by 2 photomultipliers with cut-off filters at 530 and 590 nm respectively.

For calculating the ratio of fluorescence intensity between green (fDHP) and red (RH414), each confocal image was split into two gray-scale images registering green and red fluorescence intensity. Images were then generated by determining the ratio of the intensity of green fluorescence (fDHP) to that of the red fluorescence (RH414) using the image math function in NIH image software. Only optical sections (1 μm) with sharp and definitive membrane labelling by RH414 (red images) were used for data analysis as it indicated a perpendicular section through the cell membrane. Data were collected and measured using the tool function in NIH image software by drawing lines along the membrane where RH414 showed sharp and definitive labelling.

RESULTS

Cell dissociation

The subumbrellar, muscle sheets of hydromedusae are formed by a monolayer of striated muscle cells. Each cell is polarized with contractile "feet" containing the myofibres attached to the cell soma by a narrow neck where the nucleus and other organelles are located (Spencer 1979). Cell dissociation conducted at room temperature resulted in cells with the feet retracted into the cell body, whereas, cell dissociation at 30°C retained the polarized morphology with about 53 ± 5% of muscle cells having 2 pairs of myofibres (Fig. 4.1a). Whole-cell recordings showed that cells dissociated at 30°C not only retained their polarized morphology but also retained more Vg channels as judged by current amplitude (Fig. 4.1b, c, d, e). Of the 87 heat-treated cells we recorded from, 75 had inward currents, whereas of the 20 cells dissociated at room temperature only 4 had inward currents.

Calcium-selective inward current

Calcium currents were isolated by blocking the outward potassium current with Cs^{2+} and TEA applied intracellularly through the patch pipette. Contamination by sodium currents was checked by using a calcium-free bath solution where Ca^{2+} ions and a portion of the NMG-Cl were replaced by 50 mM EDTA -Na_2 or 100 mM NaCl. In both cases the Na^+ concentration were raised to 100 mM. We only observed Na^+ current, passing through Ca^{2+} channels in EDTA containing solution while no current was recorded in the absence of EDTA (Ca^{2+} channels were blocked by Mg^{2+}).

Fig. 4.2a shows a typical trace of an isolated Sr^{2+} current. In this example the maximum current was elicited by a -40 mV test pulse from a holding potential of -80 mV. Fig. 4.2b is the average IV curve from 10 cells, showing that maximum Sr^{2+} current was produced at -30 mV. No reversal potential could be detected using test pulses up to +90 mV.

Permeability to divalent cations

The ionic permeability of calcium channels to barium and strontium was measured (data not shown). Channels were equally permeable to barium and strontium (P_{Ba}/P_{Ca} = 0.86 ± 0.08 (S.E.) and P_{Sr}/P_{Ca} = 0.85 ± 0.05 (S.E.), n = 4 cells in each case).

Electrical and Kinetic properties

The rate of activation was voltage-dependent (Fig. 4.3a) with the time to peak for maximal current of 1.49 ± 0.23 ms at -30 mV. The time course for inactivation was also voltage-dependent (Fig. 4.3b) with the inactivation time constant varying between app. 1.5 ms at +80 mV and 3.5 ms at -70 mV.

Fig. 4.4a is the steady-state inactivation curve for Sr^{2+} current. The current was almost fully available at -100 mV, half inactivated at -80 ± 3.5 mV, and completely inactivated at -45 mV. The time constant for recovery from inactivation was 51 ± 0.8 ms and complete recovery occurred in 200 ms (Fig. 4.4b).

Pharmacology

We encountered severe channel run-down during recording. In most cases no current could be recorded 5 min. after starting test protocols. For this reason the selectivity of Ca^{2+} channel blockers was first examined by evaluating their effect on contraction of muscle strips using field stimulation. When stimulated at 0.1 Hz at 12-14°C in artificial seawater these preparations could maintain a constant contractile force for several hours. Muscle contraction was sensitive to both dihydropyridines (DHP) and verapamil. The dihydropyridines, nicardipine and nifedipine, completely inhibited contraction at about 100 μM whereas other dihydropyridines, (+) and (-) Bay K 8644 and nitrendipine, completely inhibited contraction at less than 40 μM (Fig. 4.5). Diltiazem at 100 μM and DMSO at 0.5% did not produce any effect (data not shown).

The effect of dihydropyridines on dissociated cells was also examined to see if blockade of T-type calcium channels could account for the loss of contractility. Only the doses giving complete inhibition of muscle contraction were used. Fig. 4.6 shows typical traces of the inhibitory effects of (+) Bay K 8644 and nifedipine on T-type current. T-type channels were also inhibited by 50 μM $NiCl_2$ (64.1 ± 7.4%, mean ± S.E., n = 5 muscle stripes).

Localisation of T-channels by fDHP

Since larger amplitude membrane currents were recorded from dissociated cells that had been heat-treated and since they also retained muscle feet, we assumed that there was a differential pattern of channel distribution over the cell surface with channels being preferentially inserted in, or migrating to, the membrane overlying myofibres. We used fDHP to label calcium channels since we had determined they were blocked by DHPs. RH414 was used as a reference dye to correct for possible artifacts caused by membrane topology. Figure 4.7a shows double labelling of striated muscle cells dissociated at room temperature with fDHP (green) and RH414 (red). In cells dissociated at room temperature, which became spherical, RH414 labelled only the plasma membrane while fDHP labelled mostly small vesicles within the cytoplasm though occasionally fDHP labelling could be seen on the membrane. Figure 4.7b shows double labelling of striated muscle cells dissociated at 30°C, which always showed both RH414 and fDHP labelling. To analyse the differential distribution pattern of fDHP labelling the ratio of the intensity of green versus red fluorescence of images was measured pixel by pixel using NIH imaging software. Larger ratios indicated a higher density of fDHP labelling. The ratio of labelling intensity (fDHP to RH414) in the sarcolemma around myofibres is significantly higher than the somatal membrane (0.88 ± 0.03 and 0.67 ± 0.02, respectively, $p < 0.05$, $n = 20$ cells; fig. 4.7c).

DISCUSSION

Cell dissociation and channel localisation

Our data suggest that heat treatment “locks” the cytoskeleton thus retaining cell morphology after dissociation. Similar heat treatment has been used to dissociate tissues from other marine hydrozoan medusae and polyps for the purpose of cell identification (Schmid et al. 1981, Plickert and Kroiher 1988). Schmid and colleagues (1981) reported that although cell phenotype could be "fixed" by heat treatment, cells had a higher survival rate when heat-treated for a short period (30 min. vs. 60 min. at 28°C). We also noticed that there was a relatively short window of time and temperature for heat "fixation" of electrophysiologically competent cells. Prolonged treatment at 30°C (> 30 min.) or treatment at a higher temperature (37°C) for 15 min retained cell morphology, but ionic currents could not be recorded. Heat treatment did not apparently alter the kinetics of the inward current since similar kinetics were observed when compared with cells dissociated at room temperature, though current amplitude was reduced.

Since only cells with intact feet showed large currents, it is possible that most of the channels are located on the feet. Our fDHP data also support the proposition that DHP-sensitive ion channels are at a higher density on the feet. Several other systems also show a differential distribution pattern of ion channels that are obviously related to the excitability properties of the cell in question. For example, voltage-gated sodium channels are known to be clustered at the nodes of Ranvier in vertebrate myelinated axons and neuromuscular junctions (Ritchie and Rogart 1977, Ellisman and Levinson 1982, Lupa and Caldwell 1994), and L-type calcium channels are known to aggregate in T-tubules (Carl et al. 1995). Localisation of calcium channels on muscle feet in jellyfish striated muscle is further supported by the presence of membranous calcium stores just beneath the membrane of muscle feet (Chapter 5). A close association between calcium channels and calcium stores would allow for calcium-induced calcium release to augment the influx of calcium through Vg channels for regulation of muscle contraction. The precise way ion channel proteins and the cytoskeleton interact mechanically is not known, especially for jellyfish. Nevertheless, several adapter proteins have been reported to be associated with voltage and ligand-gated ion channels, which link them to the cytoskeleton. For example, ankyrin and spectrin immobilize sodium channels with actin filaments at presynaptic terminals and along axons (Srinivasan et al. 1988); rapsyn links nicotinic acetylcholine receptors to actin filaments at neuromuscular junctions (Apel et al. 1995); gephyrin links glycine receptors to microtubules at postsynaptic sites (Kirsch et al. 1993); $GABA_A$-receptor-associated protein (GABARAP) links $GABA_A$ receptors to microtubules at synapses (Wang et al. 1999).

Channel kinetics

The electrophysiological characteristics of the Ca^{2+} currents recorded from isolated muscle cells place them with T-type currents: activation occurred at low voltages (-70 mV), with both activation and inactivation being very rapid and voltage-dependent. Thus, this current shows the signature pattern of classical T-type channels (Randall and

Tsien 1998) in that with progressively stronger depolarisations, successive currents activated and inactivated faster. A noticeable difference between the current we recorded and T-type currents in other systems was the greater rate of both activation and inactivation in jellyfish muscle cells. Time to peak for maximum current at the membrane potential of -30 mV is 1.49 ± 0.23 ms and inactivation constant is 2.59 ± 0.38 ms for the T-type currents in jellyfish muscles compared with > 10 ms for time to peak and > 20 ms for inactivation constant for most reported T-type currents (Huguenard 1996, Randall 1998, Randall and Tsien 1998).

Pharmacology

Although our experiments examining the effects of various potential T-type channel blockers on muscle contraction were an indirect method for evaluating channel properties, they did provide us with estimates of the doses that might be effective when using whole-cell patch clamp recording. The sensitivity of the jellyfish T-type current to dihydropyridines, with an IC_{50} in the μM range, is similar to that reported for mouse spermatocytes (Arnoult et al. 1996, Lievano et al. 1996, Santi et al. 1996), hippocampal CA1 neurons (Takahashi and Akaike 1991), cerebellar Purkinje cells (Kaneda et al. 1990), amygdaloid neurons (Kaneda and Akaike 1989) and mouse sensory neurons (Richard et al. 1991). Also jellyfish T-type currents are sensitive to low concentrations of Ni^{2+} (<100 μM) which is similar to rat Purkinje cells (Regan 1991) and amygdaloid neurons (Kaneda and Akaike 1989). Based upon channel kinetics, activation and inactivation ranges, and pharmacology these channels are clearly within the subclass of T-type channels.

Possible function of T-type calcium channels in jellyfish striated muscle cells

Due to their low activation threshold and fast inactivation, T-type currents are generally believed to function in combination with other currents to produce pacemaker potentials where rhythmical activity is required (Randall 1998, Tsien 1998). In addition, T-type currents are implicated in regulation of cell growth and proliferation (Hermsmeyer 1998, Triggle 1998). As a T-type current appears to be the only significant inward current in jellyfish striated muscle cells, it is the first case reported of a T-type current being expressed in isolation without other inward currents. The action potential of these jellyfish muscles, which have been recorded in current clamp with sharp electrodes (Spencer 1978, Spencer and Satterlie 1981), are reminiscent of those in vertebrate cardiac muscle having large amplitudes (> 100 mV) and a long plateau phase (up to 170 ms). Although the ionic basis of the action potential was not clearly established by these authors they did demonstrate that most of the inward current was carried by calcium. However they also showed that some sodium was required externally to support an action potential. Our results contradict this study; nevertheless it is obvious that the rising phase of the action potential is mostly due to calcium influx through T-type channels and that the resulted increase in cytoplasmic calcium initiates muscle contraction.

Implications for channel evolution

Due to their phylogenetic position at the base of the metazoan radiations and being the first animal group to possess sodium currents, cnidarians have been a popular taxon to look for ancestral types of sodium channels or hybrid Ca^{2+}/Na^{+} channels (Anderson 1987, Spafford et al. 1996). Hille (1992) noted that T-type calcium channels could be the ancestor of sodium channels based on the similarity of their kinetics of activation and inactivation. Furthermore, sequence comparisons between Na^{+} and Ca^{2+} channels show the relatedness of domains in these two channel types (Spafford et al. 1998). Calcium selectivity of HVA channels is conferred by four negatively charged glutamate residues which form a high-affinity EDTA-like calcium-binding site in the pore region (Tsien 1998). This contrasts with Na^{+} channels where two of the negatively charged residues are replaced by a positively charged residue (lysine) and a neutral residue (alanine) (Heinemann et al. 1992, Ellinor et al. 1995). T-type channels might represent the transition state where these four critical residues are two glutamates and two aspartates (Tsien 1998). Measures of sequence similarity between L-type, non L-type, T-type and sodium channels also suggests that there was an early divergence of these channel types (Tsien 1998). However, the presence of a functionally undefined glycosylation-rich, extracellular loop between Segment 5 and 6, located just in front of the pore in domain I and found only in sodium channels and T-type calcium channels might indicate a remnant of their shared ancestry (Spafford 1998).

This jellyfish T-type current activates and inactivates much faster than most vertebrate T-type currents reported to date, with a kinetic property similar to sodium currents. This T-type calcium current is the major inward current of action potentials in striated swimming muscle, and it is tempting to speculate that this T-type calcium channel is closely related to the ancestral sodium channel.

Fig. 4.1. Dissociation of striated muscle cells from *Polyorchis penicillatus* at different temperatures and their associated membrane currents. a) Histogram to show that muscle cells dissociated with 1 mg/ml Pronase at 30°C retain their *in situ* morphology with more than 50% of cells having 2 or more pairs of muscle feet (myofibres). Error bars are S.E. b) Phase contrast micrograph of muscle cells dissociated at 20 to 22°C showing that cells lose muscle feet and round up. c) Voltage clamp recording of total membrane currents from a cell dissociated at 20 to 22°C showing that both inward and outward currents are reduced. Stimulus protocol was 25 ms test pulses incrementing in 10 mV steps from - 70 to + 90 mV from a holding potential of - 80 mV. d) Phase contrast micrograph of muscle cells dissociated at 30°C showing a muscle cell with 2 pairs of feet and a patch recording electrode attached. e) Voltage clamp recording of total membrane currents from a cell as shown in d) using the same stimulus protocol as in c).

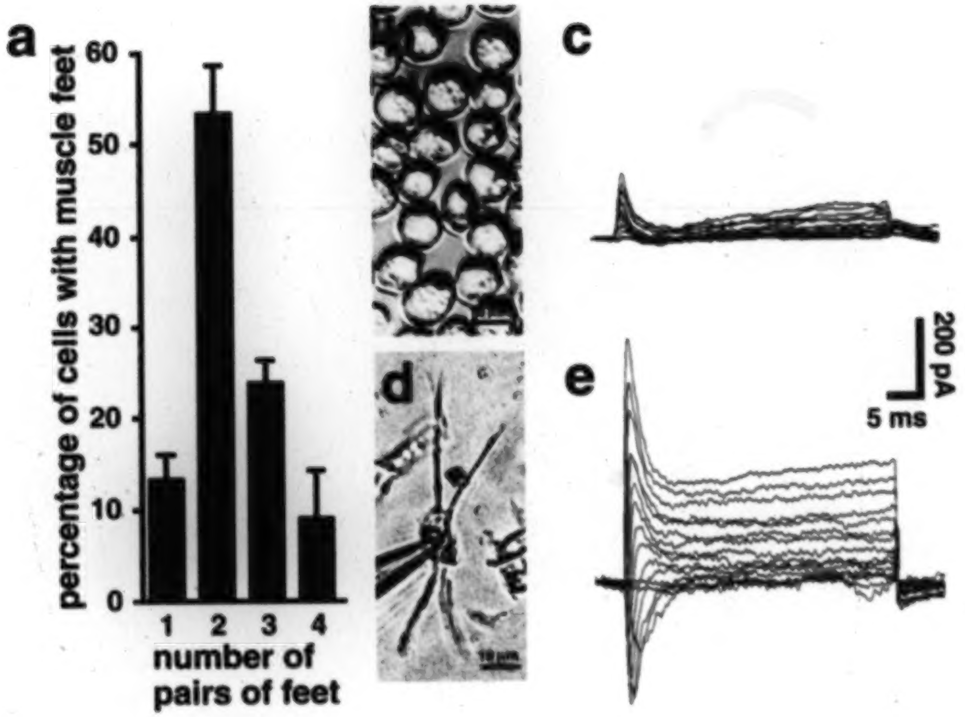
a
percentage of cells with muscle feet
0
10
20
30
40
50
60
1
2
3
4
number of pairs of feet
c
d
10 µm
e
200 pA
5 ms

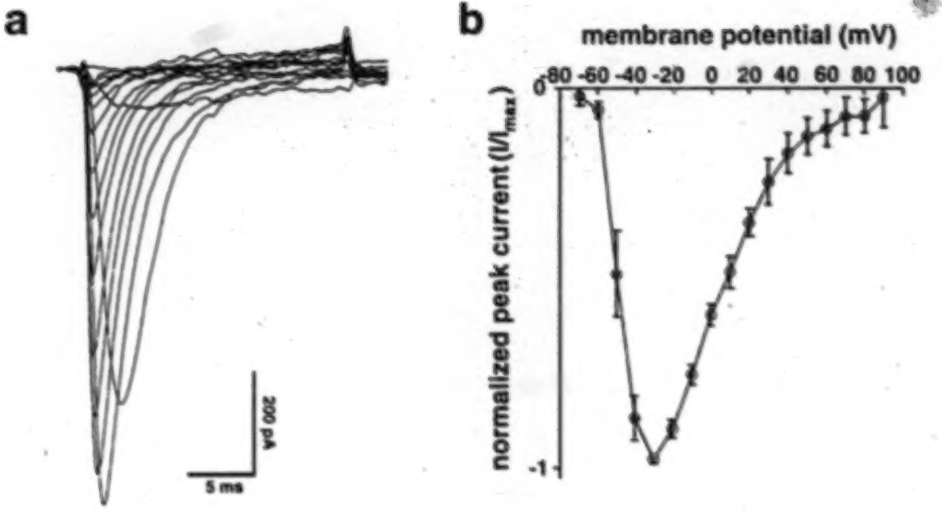

Fig. 4.2. T-type current recorded from a muscle cell dissociated at 30°C. a) Current traces recorded in whole-cell voltage clamp mode using a bath solution where Ca^{2+} was replaced by 50 mM Sr^{2+}. All potassium currents were blocked by cesium and TEA in the electrode solution (see Methods). The stimulus protocol was a series of 25 ms test potentials with increments of 10 mV from -70 to 90 mV using a holding potential of -80 mV. b) Mean I-V curve from 10 cells using the above protocols. Error bars are S.E.

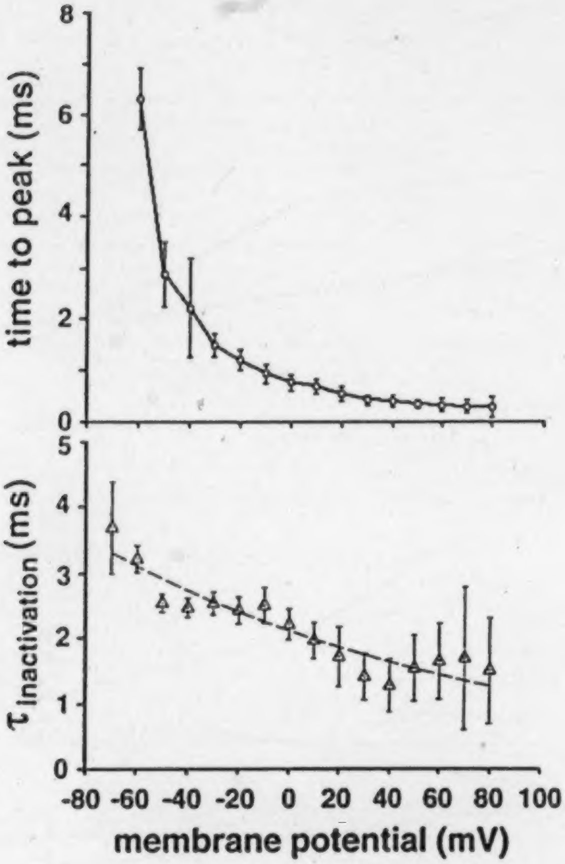

Fig. 4.3. Voltage dependence of time to peak (upper panel) and inactivation time constant (lower panel) of the T-type current. The stimulation protocol used to obtain the data for these graphs was a series of 25 ms test pulses incrementing in 10 mV from -70 to +90 mV for a holding potential of -80 mV. N = 10 cells, error bars are S.E.

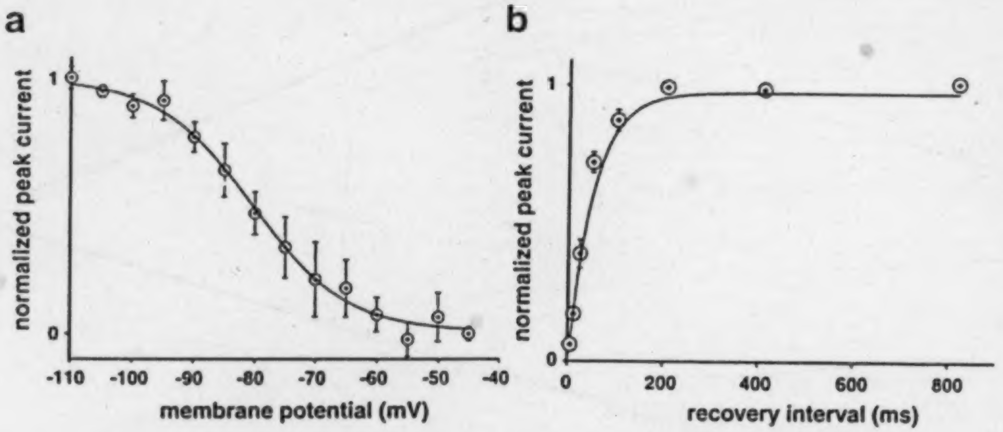

Fig. 4.4. Steady-state inactivation and recovery from inactivation of the T-type current. a) The steady-state inactivation curve was obtained from data generated using 20 ms test pulses to -30 mV immediately following 2 s conditioning prepulses from -110 to -30 mV in 5 mV increments. The holding potential prior to the conditioning pulse was - 80 mV. Steady-state inactivation data were normalized to averaged maximal current (I/Imax) and the means fitted with a Boltzman equation. Vh = -80 ± 3.5 mV, k = 7.7 ± 1.9 mV, n = 7. b) The curve for recovery from inactivation was generated from data obtained using 20 ms, inactivating prepulses to - 30 mV from a holding potential of -80 mV followed by a recovery period of variable duration from 6.4 to 800 ms at -80 mV, and a 25 ms test pulse to -30 mV. Peak currents obtained in response to test pulses were normalized to prepulse values (I/Imax) and fitted with exponential curves. Time constant (t) = 51.7 ± 0.8 ms. N = 10. Error bars are S.E.

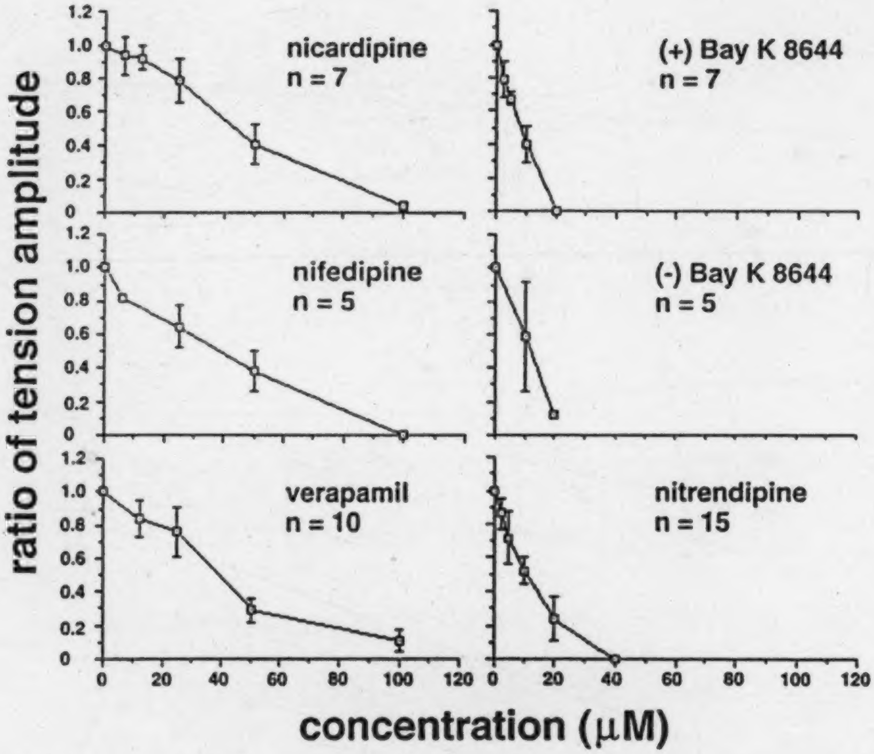

Fig. 4.5. Effect of various dihydropyridines and verapamil on swimming muscle contraction. Velar strips were stimulated by field stimulation at 0.2 Hz and mean peak tension was registered on a digital pen recorder through a capacitative force transducer. Peak tension was normalized to that in the ASW control. Perfusion rate was set at 1.5 ml/min and the temperature of the perfusate was 10 to 12°C. Error bars are S.E.

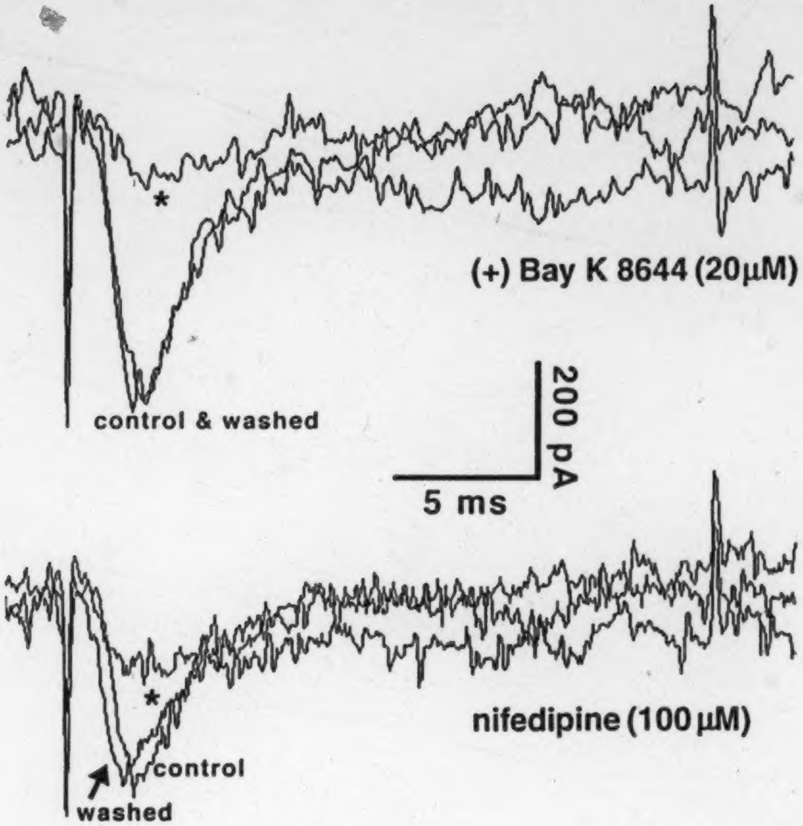

Fig. 4.6. Effect of two dihydropyridines on the T-type calcium current of swimming muscle. Both (+) Bay K 8644 (upper traces) and nifedipine (lower traces) inhibited the T-type calcium current. Current traces marked with an asterisk indicate those recorded with the drug applied. The stimulus protocol used was a single 20 ms voltage step to -30 mV from a holding potential of -80 mV. The early large phasic negative going current excursion is the uncompensated capacitative current.

Fig. 4.7. Labelling of striated muscle cells dissociated at room temperature a) and 30°C b) with RH414 and fDHP. Images were obtained using laser scanning confocal microscopy. The wavelengths of the excitation beam were set to 488 nm and 568 nm. The emitted fluorescence from labelled cells was collected at 530 nm for green fluorescence (fDHP) and 590 nm for red fluorescence (RH414). c) Ratio of labelling intensity of green (fDHP) versus red (RH414) fluorescence in the plasma membrane of myofibres (feet) and the cell soma. Data on the intensity of fluorescence (both green and red) were collected from those areas of the membrane showing sharp and definitive RH414 labelling (red), indicating that a perpendicular optical section through the cell membrane was being analyzed. The intensity of green fluorescence (fDHP) was divided by the intensity of red fluorescence (RH414) pixel by pixel using NIH image software. N = 20 cells, error bars are S.E.

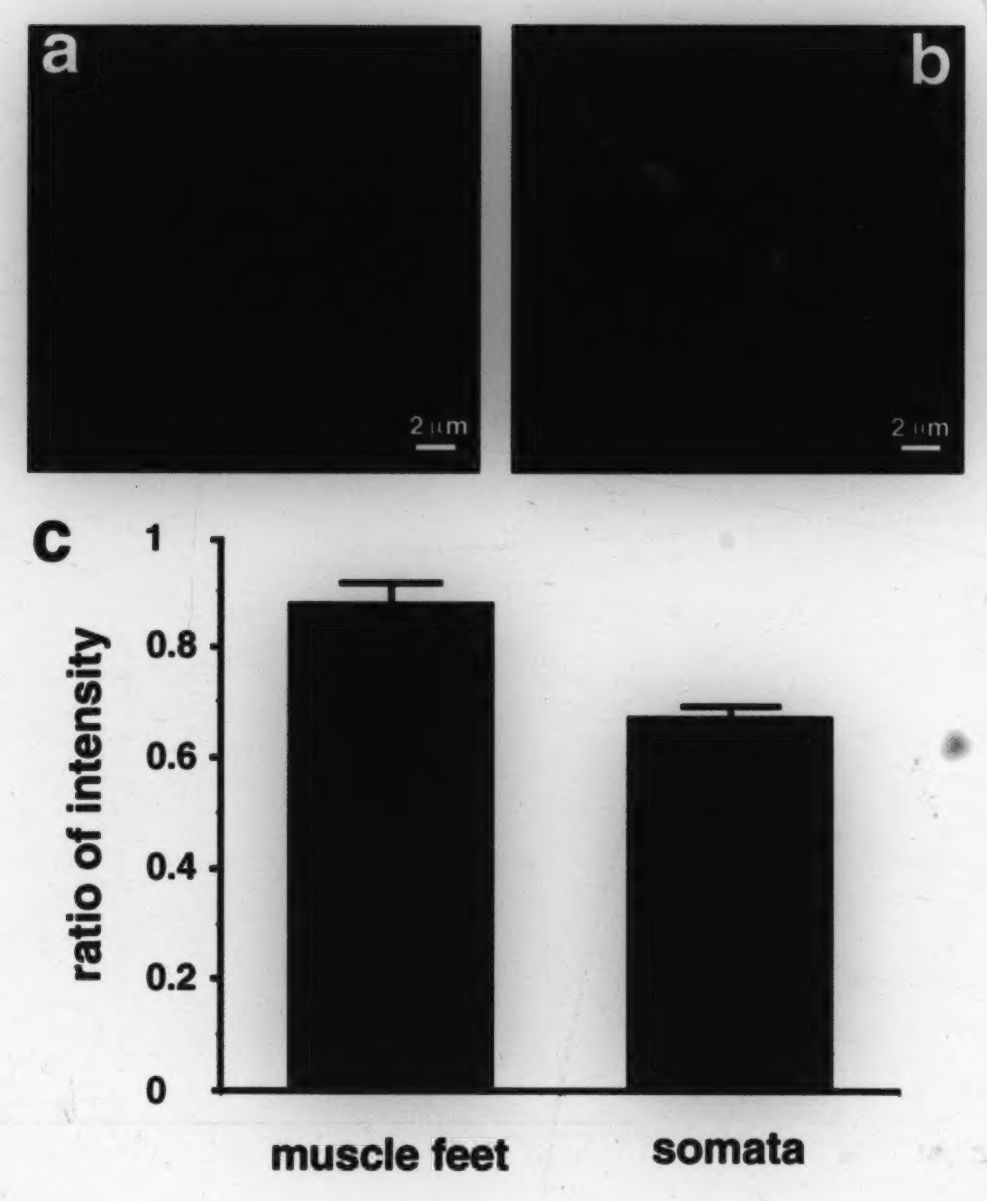
a
b
2 μm
2 μm
c
ratio of intensity
1
0.8
0.6
0.4
0.2
0
muscle feet
somata

REFERENCES

Akaike, N., Kostyuk, P. G., Osipchuk, Y. V. (1989). Dihydropyridine-sensitive low-threshold calcium channels in isolated rat hypothalamic neurons. *J. Physiol.* **412**, 181-195.

Anderson, P. A. V. (1987). Properties and pharmacology of a TTX-insensitive Na^+ current in neurons of the jellyfish, *Cyanea capillata. J. Exp. Biol.* **133**, 233-248.

Apel, E. D., Roberds, S. L., Campbell, K. P., and Merlie, J. P. (1995). Rapsyn may function as a linker between the acetylcholine receptor and the agrin-binding dystrophin-associated glycoprotein complex. *Neuron* **5**, 115-126.

Arnoult, C., Cardullo, R. A., Lemos, J. R., and Florman, H. M. (1996). Activation of mouse sperm T-type Ca^{2+} channels by adhesion to the egg zona pellucida. *Proc. Natl. Acad. Sci. USA* **93**, 13004-13009.

Barish, M. E. (1984). Calcium-sensitive action potential of long duration in the fertilized egg of the ctenophore *Mnemiopsis leidyi. Dev. Biol.* **105**, 29-40.

Bean, B. P. (1985). Two kind of calcium channels in canine atrial cells. *J. Gen. Physiol.* **86**, 1-30.

Berridge, M. J. (1993). Inositol trisphosphate and calcium signaling. *Nature* **361**, 315-325.

Bers, D. M. (1991). Excitation-contraction coupling and cardiac contractile force. Boston: Kluwer Academic Publishers.

Bilbaut, A., Hernandez-Nicaise, M. L., Leech, C. A., and Meech, R. W. (1988). Membrane currents that govern smooth muscle contraction in a ctenophore. *Nature* **331**, 533-535.

Bois, P. and Lenfant, J. (1991). Evidence for two types of calcium currents in frog cardiac sinus venosus cells. *Pflugers Arch.* **417**, 591-596.

Campbell, D. L. and Strauss, H. C. (1995). Regulation of calcium channels in the heart. *In* Advances in second messenger and phosphoprotein research, Vol. 30 (ed. A. R. Means). New York: Raven Press, Ltd.

Carl, S. L., Felix, K., Caswell, A. H., Brandt, N. R., Brunschwig, J. P., Meissner, G., and Ferguson, D. G. (1995). Immunolocalisation of triadin, DHP receptors, and ryanodine receptors in adult and developing skeletal muscle of rats. *Muscle &. Nerve* **18**, 1232-1243.

Dubas, F., Stein, P. G., and Anderson, P. A. (1988). Ionic currents of smooth muscle cells isolated from the ctenophore *Mnemiopsis*. *Proc. Roy. Soc. London B* **233**, 99-121.

Ellinor, P. T., Yang, J., Sather, W. A., Zhang, J. F., and Tsien, R. W. (1995). Ca^{2+} channel selectivity at a single locus for high-affinity Ca^{2+} interactions. *Neuron* **15**,1121-1132.

Ellisman, M. H. and Levinson, S. R. (1982). Immunocytochemical localisation of sodium channel distribution in the excitable membrane of *Electrophorus electricus*. *Proc. Natl. Acad. Sci. USA* **79**, 6701-6711.

Endo, M. (1977). Calcium release from the sarcoplasmic reticulum. *Physiol. Rev.* **57**, 71-108.

Ertel, S. I., Ertel, E. A. and Clozel, J. P. (1997). T-type Ca^{2+} channels and pharmacological blockade: potential pathophysiological relevance. *Cardiovas. Drugs Ther.* **11**, 723-39.

Fox, A. P., Nowycky, M., and Tsien, R. W. (1987). Kinetic and pharmacological properties distinguishing three types of calcium currents in chick sensory neurons. *J. Physiol. (London)* **394**, 149-172.

Hagiwara, N., Irisawa, H., and Kameyama, M. (1988). Contribution of two types of calcium currents to the pacemaker potential of rabbit sino-atrial node cells. *J. Physiol. (London)* **395**, 233-253.

Heinemann, S. H., Terlau, H., Imoto, K., and Numa, S. (1992). Calcium channel characteristics conferred on the sodium channel by single mutations. *Nature* **356**, 441-443.

Hermsmeyer, K. (1998). Role of T channels in cardiovascular function. *Cardiology* **89** (suppl 1), 2-9.

Hille, B. (1992). Ionic channels of excitable membranes. Sunderland: Sinauer.

Hirano, Y., Fozzard, H. A., and January, C. T. (1989). Characteristics of L- and T-type Ca^{2+} currents in canine cardiac Purkinje fibers. *Am. J. Physiol.* **256**, H1478-H1492.

Huguenard, N. J. (1996). Low-threshold calcium currents in central nervous system neurons. *Ann. Rev. Physiol.* **58**, 329-348.

Kaneda, M. and Akaike, N. (1989). the low-threshold Ca current in isolated amygdaloid neurons in the rat. *Brain Res.* **497**, 187-190.

Keneda, M., Wakamori, M., Ito, C., and Akaike, N. (1990). Low-threshold calcium current in isolated Purkinje cell bodies of rate cerebellum. *J. Neurophysiol.* **63**, 1046-1051.

Kirsch, J., Wolters, I., Triller, A., and Betz, H. (1993). Gephyrin antisense oligonucleotide prevents glycine receptor clustering in spinal neurons. *Nature* **366**, 745-748.

Lievano, A., Santi, C. M., Serrano, C. J., Trevino, C. L., Bellve, A. R. Hernandez-Cruz, A., and Darszon, A. (1996). T-type Ca^{2+} channels and alpha 1E expression in spermatogenic cells, and their possible relevance to the sperm acrosome reaction. *Febs Lett.* **388**, 150-154.

Llinas, R., Sugimori, M., Lin, J.-W. and Cherskey, B. (1989). Blocking and isolation of a calcium channel from neurons in mammals and cephalopods utilizing a toxin fraction (FTX) from funnel-web spider poison. *Proc. Natl. Acad. Sci. USA* **86**, 1689-1693.

Lupa, M. T. and Caldwell, J. M. (1994). Sodium channels aggregate at former synaptic sites in innervated and denervated regenerating muscles. *J. Cell Biol.* **124**, 139-147.

Mackie, G. O., and Meech, R. W. (1985). Separate sodium and calcium spikes in the same axon. *Nature* **313**, 791-3.

McCleskey, E. W., Fox, A. P., Feldman, D. H., Cruz, L. J., Olivera, B. M., Tsien, R. W., and Yoshikami, D. (1987). ϖ-Conotoxin: direct and persistent blockade of specific types of calcium channels in neurons but not muscle. *Proc. Natl. Acad. Sci. USA* **84**, 4327-4331.

Mintz, I. M., Venema, V. J., Swiderek, K. M., Lee, T. D., Bean, B. P., and Adams, M. E. (1992). P-type calcium channels blocked by the spider venom toxin ϖ-Aga-IVA. *Nature* **355**, 827-829.

Plickert, G. and Kroiher, M. (1988). Proliferation kinetics and cell lineages can be studied in whole mounts and macerates by means of BrdU/anti-BrdU technique. *Development* **103**, 791-794.

Przysiezniak, J. and Spencer, A. N. (1992). Voltage-activated calcium currents in identified neurons from a hydrozoan jellyfish, *Polyorchis penicillatus*. *J. Neurosci.* **12**, 2065-2078.

Randall, A. D. (1998). The molecular basis of voltage-gated Ca^{2+} channel diversity: is it time for T? *J. Memb. Biol.* **161**, 207-213.

Randall. A. D. and Tsien, R. W. (1995). Pharmacological dissection of multiple types of Ca^{2+} channel currents in rat cerebellar granule neurons. *J. Neurosci.* **15**, 2995-3012.

Randall, A. D. and Tsien, R. W. (1998). Distinctive biophysical and pharmacological features of T-type calcium channels. *In* Low-voltage-activated T-type calcium channels (eds. R. W. Tsien, J.-P. Clozel, and J. Nargeot). England: Adis International.

Regan, L.J. (1991). Voltage-dependent calcium currents in Purkinje cells from rat cerebellar vermis. *J. Neurosci.* **11**, 2259-2269.

Richard, S., Diochot, S., Nargeot, J., Baldy-Moulinier, M., and Valmier, J. (1991). Inhibition of T-type calcium currents by dihydropyridines in mouse embryonic dorsal root ganglion neurons. *Neurosci. Lett.* **132**, 229-234

Ritchie, J. M. and Rogart, R. B. (1977). Density of sodium channels in mammalian myelinated nerve fibers and nature of the axonal membrane under the myelin sheath. *Proc. Natl. Acad. Sci. USA* **74**, 211-215.

Santi, C. M., Darszon, A., and Hernandez-Cruz, A. (1996). A dihydropyridine-sensitive T-type Ca^{2+} current is the main Ca^{2+} current carrier in mouse primary spermatocytes. *Am. J. Physiol.* **271**, C1583-1593.

Sather, W. A., Tanabe, T., Zhang, J.-F., Mori, Y., Adams, M. E., and Tsien, R. W. (1993). Distinctive biophysical and pharmacological properties of class (B1) calcium channel a_1 subunits. *Neuron* **11**, 291-303.

Schmid, V., Stidwill, R., Bally, A., Marcum, B., and Tardent, P. (1981). Heat dissociation and maceration of marine cnidarians. *Roux's Arch. Dev. Biol.* **190**, 143-149.

Schild, D., Geiling, H., and Bischofberger, J. (1995). Imaging of L-type Ca2+ channels in olfactory bulb neurones using fluorescent dihydropyridine and a styryl dye. *J. Neurosci. Meth.* **59**, 183-190.

Spafford, J. D. (1998). The evolution of voltage-gated sodium channels as interpreted from a study of sodium currents and channels from the hydrozoan jellyfish, *Polyorchis penicillatus*. Ph.D. thesis. University of Alberta.

Spafford, J. D., Grigoriev, N. G., and Spencer, A. N. (1996). Pharmacological properties of voltage-gated sodium currents in motor neurons from a jellyfish *Polyorchis penicillatus*. *J. Exp. Biol.* **199**, 941-948.

Spafford, J. D., Spencer, A. N., and Gallin, W. J. (1998). A putative voltage-gated sodium channel α subunit (PpSCN1) from the hydrozoan jellyfish, Polyorchis penicillatus:

structural comparisons and evolutionary considerations. *Biochem. Biophys. Res. Comm.* **244**, 772-780.

Spencer, A. N. (1978). Neurobiology of *Polyorchis*. I. Function of effector systems. *J. Neurobiol.* **9**, 143-157.

Spencer, A. N. (1979). Neurobiology of *Polyorchis*. II. Structure of effector systems. *J. Neurobiol.* **10**, 95-117.

Spencer, A. N. and Satterlie, R. A. (1981). The action potential and contraction in subumbrellar swimming muscle of *Polyorchis penicillatus* (Hydromedusae). *J. Comp. Physiol.* **144**, 401-407.

Srinivasan, Y., Elmer, L. W., Davis, J. Q., Bennett, V., and Angelides, K. J. (1988). Ankyrin and spectrin associate with voltage-dependent sodium channels in brain. *Nature* **333**, 177-180.

Takahashi, K. and Akaike, N. (1991). Calcium antagonist effects on low threshold (T-type) calcium current in rat isolated hippocampal CA1 pyramidal neurons. *J. Pharm. Exp. Ther.* **256**, 169-175.

Triggle, D. J. (1998). The physiological and pharmacological significance of cardiovascular T-type, voltage-gated calcium channels. *Am. J. Hyper.* **11**, 80S-87S.

Tseng, G.-N.. and Boyden, P. A. (1989). Multiple types of Ca^{2+} currents in single canine Purkinje cells. *Circ. Res.* **65**, 1735-1750

Tsien, R. W. (1998). Key clockwork component cloned. *Nature* **391**, 839-841

Wang, H., Bedford, F. K., Brandon, N. J., Moss, S. J. and Olsen, R. W. (1999). $GABA_A$-receptor-associated protein links $GABA_A$ receptors and the cytoskeleton. *Nature* **397**, 69-72.

Chapter 5

Localisation of intracellular calcium stores putatively involved in excitation-contraction coupling

INTRODUCTION

Muscle contraction is initiated by an increase in the intracellular free calcium concentration. This increase in intracellular calcium may occur as a result either of direct calcium influx through calcium channels in the plasma membrane, or of calcium release from intracellular stores (i.e. the sarco/endoplasmic reticulum), or both. In striated muscles, the requirement for extracellular calcium influx for muscle contraction is inversely correlated to the development of the sarcoplasmic reticulum (Bers 1991). For example, in the tunicate *Doliolum*, contraction of striated muscle is completely dependent on calcium influx through the sarcolemma since no sarcoplasmic reticulum has been observed (Bone et al. 1997). By contrast, in vertebrate skeletal muscles, which have a very extensive and well-organized sarcoplasmic reticulum, contraction depends almost exclusively on calcium release from the sarcoplasmic reticulum (Armstrong et al. 1972). Most invertebrate striated muscle and vertebrate cardiac muscle have a less pronounced sarcoplasmic reticulum compared to vertebrate skeletal muscle. In many invertebrates, contraction depends both on calcium influx through the sarcolemma and calcium release from sarcoplasmic reticulum with varied relative importance (Bers 1991, Ashley et al. 1993, Palade and Györke 1993, Paniagua et al. 1996).

The sarcoplasmic reticulum of striated muscle is an intracellular tubular network with different, functionally discrete units that respond differently to various types of cellular stimulation (Golovina and Blanstein 1997). The terminal cisternae of sarcoplasmic reticulum have been identified as the calcium release and storage site. They contain the calcium release channels (ryanodine receptors) (Winegrad 1965, Inui et al. 1987, Lai et al. 1988) and high-capacity and low-affinity calcium binding proteins (calsequestrin) (Meissner et al. 1973, Jorgensen et al. 1983). Calcium uptake by sarcoplasmic reticulum is mediated by Ca^{2+}/Mg^{2+}-ATPase pumps which are a family of transmembrane proteins (Carafoli 1991) with each pump molecule transporting two calcium ions from the cytoplasm into the lumen of the SR during each catalytic cycle at the expense of a single molecule of ATP (Tada et al. 1982, Inesi 1987).

Myoepithelial cells in cnidarians represent some of the most "primitive" types of muscle (Prosser 1982), and are formed by an apical soma attached by a narrow neck to several contractile feet. Myoepithelial cells of polyps are non-striated while the subumbrellar myoepithelial cells of medusae have striated myonemes (Chapman et al. 1962, Fautin and Mariscal 1991, Thomas and Edwards 1991). The myofibres of *Polyorchis penicillatus*, like other hydromedusae (Spencer and Satterlie 1981) contain thick and thin myofilaments arranged in a hexagonal array of one thick filament surrounded by 6 thin filaments (Singla 1978a, b) and are joined end-on by desmosomes and laterally by gap junctions (Spencer 1979). Despite their structural similarity to other striated muscles, little is known about the mechanism of excitation-contraction coupling in cnidarian striated muscle. In this study, we present data on muscle contraction to show that calcium released from intracellular calcium stores plays a role in the contraction of jellyfish swimming muscle and we also localize putative calcium stores by cytochemical labelling of Ca^{2+}-ATPase and calcium.

MATERIALS AND METHODS

Medusae of *Polyorchis penicillatus* were collected from Bamfield Inlet or Pachena Bay, near Bamfield, British Columbia, Canada.

Field stimulation of muscle strips

Preliminary study indicated that both muscle strips from bell regions and vela had similar pharmacologies. Due to the thickness and elastic property of mesoglea in the bell region, recordings from muscle strips obtained from this region were extremely variable and it was difficult to measure contractile amplitude. Therefore, only muscle strips from vela were used in this study. The vela of medusae, anaesthetized in 1:1 isotonic $MgCl_2$ (0.33M) and artificial seawater (ASW), were excised so as to provide continuous strips of maximal width. Artificial seawater (pH 7.5) consisted of NaCl: 376 mM, $Na_2(SO_4)$: 26 mM, $MgCl_2$: 41.4 mM, $CaCl_2$: 10 mM, KCl: 8.5 mM, and HEPES (hemisodium salt): 10 mM. To avoid any contamination by nervous tissue, each velar strip was bisected lengthwise into two strips and only the strip free from any tissue from the inner nerve-ring was used in the study. The free ends of each velar strip were pinned to the Sylgard base of a 35 mm Petri dish which also contained a pair of embedded $Ag/AgCl_2$ stimulating electrodes connected to a Grass S44 stimulator. The velar strip ran between the two stimulating electrodes and around a small hook attached to a capacitative force transducer (Kent, Inc.). The tension on the strip was adjusted using a micromanupulator so as to remove any slack in the preparation and maximize tension excursions. The threshold for contraction was determined by increasing the stimulation voltage until a measurable contraction occurred. The rate of perifusion was controlled by a peristaltic pump at 1.5 ml/min and the perifusate was removed by a vacuum pump. All perifusates were kept at 12-14°C during the whole experiment by running the perfusion tubing through an ice bucket. The transduced tension was recorded on a digital Dash-IV pen-recorder (Astro-Med Inc.). The amplitude of contractile tension for each condition (control, drug effect, and washed) was calculated by averaging 10 contractions. Caffeine was dissolved in ASW at 10 mM.

Localisation of Ca^{2+}-ATPase

Small pieces of the subumbrellar muscle sheet were washed and relaxed in Ca^{2+}-free ASW and then fixed with 2% paraformaldehyde and 0.25% glutaraldehyde in cacodylate-buffered saline at pH 7.8 (Na cacodylate/HCl: 100 mM, NaCl: 300 mM, KCl: 10 mM) for 30 min. on ice. Glutaraldehyde was added to provide better preservation of the ultrastructure (Ueno and Mizuhira 1984). After three washes (30 min. each) in ice-cold cacodylate-buffered saline and two brief rinses in glycine/NaOH buffer (250 mM, pH 9.0), tissues were incubated at either 12°C or 37°C for 45 min. in a solution containing glycine/NaOH buffer: 250 mM (pH 9.0), ATP-Na: 3 mM, $CaCl_2$: 10 mM, $MgCl_2$: 5 mM, lead citrate: 4 mM (Ando et al. 1981). Levamisole was added at 8 mM to exclude any contribution of non-specific alkaline phosphatase to ATP hydrolysis (Van-Noorden and Jonges, 1987). Oubain (10 mM) was added to the incubation medium to inhibit Na^+-K^+-ATPase (Maggio et al., 1991). To examine ATP, calcium, and substrate dependence of the histochemical reaction, the following controls were performed with incubation in: a. ATP-free medium; b. in Ca^{2+}-free medium with 10 mM EGTA; c. lead citrate-free medium. After incubation, samples were rinsed sequentially in glycine buffer and cacodylate-buffered saline, post-fixed in 1% OsO_4 in cacodylate-buffered saline for 1 h, and then processed for conventional TEM examination. Sections of 70 - 90 nm were collected on nickel grids and examined without staining.

Ultrastructural localisation of calcium

Calcium stores were localized using the method of Probst (1986). Tissue samples were fixed with 4% paraformaldehyde and 2% glutaraldehyde in 0.1 M phosphate buffer (pH 7.4) for 2 h at 4°C and post-fixed in 1% osmium tetroxide and 2.5% potassium dichromate in 0.1 M phosphate buffer at 4°C for 24 h. After incubation, samples were rinsed in phosphate-buffered saline then processed for conventional TEM examination. Sections of 70 - 90 nm were examined without staining.

Electron energy-loss spectroscopy (EELS)

Unstained ultrathin sections of 30 to 50 nm were used for EELS on an energy-filtering transmission electron microscope (EM 902, Zeiss, Germany) and examined at an accelerating voltage of 80 kV. The inelastically scattered electrons with element-specific energy losses were used to obtain high resolution imaging of calcium distribution in the section. For calcium element mapping, energy-filtered images (energy width 20 eV) were recorded above and below the edge of electron absorption specific for calcium ($Ca_{L2,3}$ edge

346 eV) at 355 eV and 330 eV, respectively. The image taken at 330 eV served as a reference image for background levels. Net calcium distribution images were obtained by computer-assisted image processing of the difference between image taken at 355 and 330 eV.

RESULTS

Field stimulation of muscle strips

Velar strips rarely contracted spontaneously after being mounted in the perfusion chamber and consistent responses to field stimulation without significant changes in amplitudes could be maintained for 3 - 4 hours. Figure 5.1 a, b shows that the maximum contractile tension increased stepwise as stimulation frequency was increased from 0.1 to 0.8 Hz. Note that the increase in stimulation frequency led to a contractile tension increase in a progressive “staircase”. This force-frequency relationship suggested the presence of calcium stores and calcium release that was induced by influx of extracellular calcium (Bers 1991). Caffeine was used to examine if calcium stores were involved in muscle contraction. At the onset of bath-application of caffeine at 10 mM, caffeine immediately increased the amplitudes of several contractions higher than ASW control (Fig. 5.1c, d). The subsequent mean amplitude of contraction was reduced to 75.87 ± 3.57% of control at 0.1 Hz in the presence of 10 mM caffeine. These data show that caffeine-sensitive intracellular calcium stores are involved in muscle contraction. Caffeine also abolished the frequency dependent increase in tension (Fig. 5.1 c, d), indicating that the force-frequency relationship is mainly mediated by the caffeine-sensitive, calcium stores. Together, these data show that calcium influx through voltage-gated calcium channels is sufficient to evoke contraction and suggest that calcium released from caffeine-sensitive intracellular calcium stores plays an additive role in excitation-contraction coupling.

Localisation of Ca^{2+}-ATPase

The ultrastructure of *Polyorchis* swimming muscle has been well documented in two previous studies (Singla 1978b, Spencer 1979). Figure 5.2 shows the ultrastructure of the swimming muscle where each cell is separated into somal and myofibrillar regions. No T-tubular structures have been observed in *Polyorchis* myofibres (Singla 1978b, Spencer 1979), however several membrane-bound vesicles in the sub-sarcolemmal cytoplasm were found to be close to contractile filaments. The distribution of these vesicles did not show any specific pattern. To establish if these subsarcolemma vesicles are sarcoplasmic reticulum and possibly involved in excitation-contraction coupling in swimming muscle cells, we used a cytochemical method to test the presence of Ca^{2+}-ATPase activity in these vesicles, which is the calcium pump of calcium stores (Ando et. al. 1981). The indicator, lead phosphate precipitate, was localized to a number of intracellular membranous sites in tissues incubated in media containing calcium and magnesium ions and ATP (Fig. 5.3 and 5.4). No precipitates were observed in the following negative control solutions: a medium lacking ATP, a calcium-free medium with 10 mM EGTA, and a medium lacking lead citrate (Fig. 5.5). No differences were noticed between tissue samples incubated at 12°C and 37°C. Together these data suggest that ATPase activity is specific and calcium dependent. Presumably some of these sites, particularly vesicles underneath the sarcolemma, are acting as Ca^{2+} stores for muscle excitation-contraction coupling. Granular precipitates were found in the nucleus, Golgi stacks, vesicular structures in somal regions probably representing the endoplasmic reticulum, and both apical and lateral plasma membrane (Fig. 5.3). In general, little or no precipitates were found in mitochondria and if present they were not intense. Precipitates were found on both sides of the membrane in the apical and lateral plasma membrane (Fig. 5.3), those precipitates on the outer side of the membrane presumably arose from non-specific ecto-ATPase activity (Ogawa et al. 1986, Nasu and Inomata 1990). Intense precipitation was seen at the inner side of the sarcolemma surrounding the myofibrils. Precipitation was particularly dense at the junction of adjacent myofibrils where the plasma membrane from both cells was folded and interdigitated. Precipitates were also found amongst the myofibrils which were probably associated with myosin filaments. Lead precipitates were also found in sub-sarcolemmal vesicles which were distributed sparsely along the myofibrils (Fig. 5.4). A somewhat surprising finding was that calcium-dependent ATPase activity was found in the mesoglea close to the myofibres, although the activity could not be attributed to any organelles (Fig. 5.4).

Ultrastructural localisation of calcium

We used potassium dichromate to precipitate calcium as another indicator for the presence of calcium stores (Probst 1986). This histochemical method localizes loosely bound calcium and hence it indicates calcium-binding sites. In somata, electron dense precipitates (EDPs) were found in the nucleus, mitochondria, and endoplasmic reticulum-like structures/vesicles (Fig. 5.6). In myofibrils, EDPs were found in the sub-sarcolemmal vesicles, as well as lining the inner side of the sarcolemma (Fig. 5.6). Fine EDPs were also found in mesoglea adjacent to myofibrils.

We used electron energy loss spectroscopy to establish if the EDPs contained calcium. The net calcium distribution image (Fig. 5.7a) was generated by subtracting the image taken below the absorption edge specific for calcium (served as a background level reference image) from the image taken above the calcium edge. The bright spots on the image represent the calcium signals which were almost identical to the position of the EDPs on the image taken at zero energy loss (Fig. 5.7b, conventional TEM mode), indicating that EDPs contained calcium.

DISCUSSION

While it has been shown that the generation of action potentials and contraction in the swimming muscles of *Polyorchis* are dependent on the availability of extracellular calcium (Spencer and Satterlie 1981), the findings in this report suggest that an intracellular source(s) of calcium may also play a role in muscle contraction. Caffeine was applied to determine whether calcium stores were directly involved in mediating contraction. In most tissues, caffeine empties intracellular stores by making the store leaky to calcium (Weber and Herz 1968). In our experiments, caffeine reduced the steady-state peak tensions (0.1 Hz) to about 75% of the control and abolished the progressive tension increase that normally accompanies increased stimulation frequency (Fig. 5.1). These data imply that calcium released from caffeine-sensitive, calcium stores is only responsible for a small portion of contractile tension and the increased contraction tension resulting from increased stimulation frequency is mediated by the caffeine-sensitive intracellular stores.

At least three characteristics are necessary for an intracellular compartment to act as a "calcium store" involved in muscle contraction: 1) the presence of membrane pumps to replenish Ca^{2+} in the store; 2) calcium-release channels which release calcium into the cytoplasmic space; and 3) calcium-binding proteins which bind calcium in the store. In vertebrate striated muscles the calcium stores are known to be the sarcoplasmic reticulum. In large diameter muscle cells, however, these stores may be distant from the external plasma membrane which provides the initial influx of external Ca^{2+} to trigger calcium release. To ensure efficient triggering of calcium-induced calcium release, larger muscle cells have T-tubules that are invaginations of the plasma membrane, thus bringing this triggering signal close to sarcoplasmic reticulum deep within the muscle. T-tubules are obviously specialized for providing the external Ca^{2+} signal because their membranes have a high density of voltage-gated calcium channels (Carl et al. 1995). Small muscle cells, such as those in frog and lizard hearts, however, do not posses T-tubules and all compartments of the sarcoplasmic reticulum are relatively close to the external plasma membrane. Similarly, T-tubules have never been observed in electron micrographs of *Polyorchis* swimming muscle, presumably because there is only one layer of myofibrils and each is about 2 µm in diameter (Singla 1978b, Spencer 1979, this study).

To localize calcium stores at high resolution, we chose to map Ca^{2+}-ATPase activity since this family of enzymes is known to participate in sequestering calcium into stores as well as pumping calcium into extracellular space (Carafoli 1991). At least two types of Ca^{2+}-ATPase have been identified, one is located on the sarcolemma or plasmalemma and the other type is located on sarcoplasmic reticulum (Carafoli 1991). The method used in this study does not distinguish between these two types of Ca^{2+}-ATPases, nor the non-specific ecto-ATPase activity (Ogawa et al. 1986, Nasu and Inomata 1990). This latter activity is characterized by its location which is at the outer surface of the plasma membrane (Ando et al. 1981).

The plasmalemmal Ca^{2+}-ATPase functions to remove calcium from intracellular space during the relaxation phase of the muscle contraction cycle (Carafoli 1991). The sarcolemmal region of *Polyorchis* swimming muscle is more heavily labelled by Ca^{2+}-ATPase specific precipitates than the apical region. This polarized distribution of Ca^{2+}-ATPase activity is to be expected and parallels the functional polarization of the cells into somal and contractile compartments. A polarised distribution of Ca^{2+}-ATPase has been reported for vertebrate epithelium, pancreatic and salivary gland cells, photoreceptors (Seguchi et al 1982, Lee et al. 1997, Krizaj and Copenhagen 1998) and crustacean posterior caecal epithelium (Meyran and Graf 1986). Plasmalemmal Ca^{2+}-ATPase has been localised to the caveolae or uncoated plasma membrane invaginations in mouse endothelial cells, smooth muscle cells, cardiac muscle cells, epidermal keratocytes and mesothelial cells by using specific antibody generated against erythrocyte membrane Ca^{2+}-ATPase (Fujimoto 1993). Although we did not see caveolae-like structures in the sarcolemma, the plasma membrane surrounding myofibres is heavily invaginated and ruffled, especially at the junctions between adjacent myofibres where Ca^{2+}-ATPase activity is very high.

Another type of Ca^{2+}-ATPase is located on the sarcoplasmic reticulum membrane and pumps calcium into the sarcoplasmic reticulum during the relaxation phase of muscle contraction (Lytton and Nigam 1992), and is considered to be an indicator protein for calcium stores. In *Polyorchis* muscle, the presence of Ca^{2+}-ATPase activity in sub-sarcolemmal vesicles close to myofilaments indicates these vesicles indeed perform the function of sarcoplasmic reticulum.

The calcium precipitation method revealed a similar distribution pattern as Ca^{2+}-ATPase localisation, however, it should be noted that although calcium precipitates were present in mitochondria there was no associated Ca^{2+}-ATPase activity. This is to be expected for although mitochondria can act as calcium sinks, calcium ion influx is via a calcium uniporter into mitochondria instead of using the Ca^{2+}-ATPase pump (Crompton 1985). Calcium precipitates also outlined the inner leaflet of the sarcolemma of *Polyorchis* swimming muscle. Similar findings for membrane-bound calcium have been reported in a large variety of cell types in which calcium ions were suggested to be bound by negatively charged glycoproteins (Carafoli 1987). Lullman and Peters (1977, 1979) proposed that these membrane-bound calcium ions could be released during depolarisation of the sarcolemma and participate in cardiac myocyte contraction. However, further studies showed that neither intracellular calcium concentration, nor muscle contraction increases during depolarisation without calcium influx (Rich et al. 1988, Nabauer et al. 1989). Thus the inner leaflet of the sarcolemma might simply serve as a calcium-buffering site.

Calcium precipitates were also found in similar vesicular structures in the soma and beneath the sarcolemma of myofibrils. As is implied by the Ca^{2+}-ATPase activity, these vesicles underneath the sarcolemma may function as calcium stores during excitation-contraction coupling, since they are adjacent to the myofibrils. Calcium channels are more abundant on the sarcolemma of myofibres than on the somal plasmalemma (Chapter 4) to ensure rapid excitation-contraction coupling. Thus cytochemical localisation of Ca^{2+}-ATPase and calcium indicates the presence of a poorly organized sarcoplasmic reticulum and the physiological actions of caffeine on muscle contraction indicate that calcium influx through voltage-gated calcium channels is sufficient for muscle contraction. Therefore, the weakly developed sarcoplasmic reticulum may only play a minor role in muscle contraction. For example, when *Polyorchis* swims in a bout the amplitude of the first contraction is less than succeeding ones (Spencer and Satterlie 1981). This facilitation in the amplitude of contractile tension can be the result of refilling calcium stores after a period of rest.

The presence of Ca^{2+}-ATPase activity and calcium precipitates in the mesoglea close to myofibres is intriguing. One possible function for calcium and Ca^{2+}-ATPase in mesoglea could be similar to the opacification (blanching) in the mesoglea of the siphonophore *Hippopodius* which is a calcium dependent process (Bassot et al. 1979). Opacification in mesoglea is due to a temporary formation of light-scattering granules in response to the propagation of action potentials in epithelia and is calcium dependent, however, such a functional role for mesoglea Ca^{2+}-ATPase is improbable in *Polyorchis*, since the opacification process has not been observed in this jellyfish. Nevertheless it is attractive to suppose that the mesoglea can act as a long-term store for calcium and that there is dynamic exchange with the epithelia surrounding it.

Fig. 5.1. Force-frequency relationship of the swimming muscle. a) a typical force trace of muscle contraction at stimulation frequencies of 0.1, 0.2, 0.4, and 0.8 Hz. The increase in stimulation frequency led to a contractile tension increase in a progressive positive "staircase". b) Quantitative data for the force-frequency relationship. All maximal contraction forces were normalized to the mean force at 0.1 Hz in ASW. Data were collected from 8 muscle strips. Error bars = S.E. c) a typical trace of the effect of 10 mM caffeine on the force-frequency relationship. Arrow indicates the beginning of 10 mM caffeine perfusion. d) Quantitative data for the force-frequency relationship when caffeine was present in the perfusate at 10 mM. All maximal contraction forces were normalized to the mean force at 0.1 Hz in ASW. Data were collected from 3 muscle strips. Caffeine significantly inhibited the maximal tension developed at all frequencies ($p < 0.05$). Error bars = S.E.

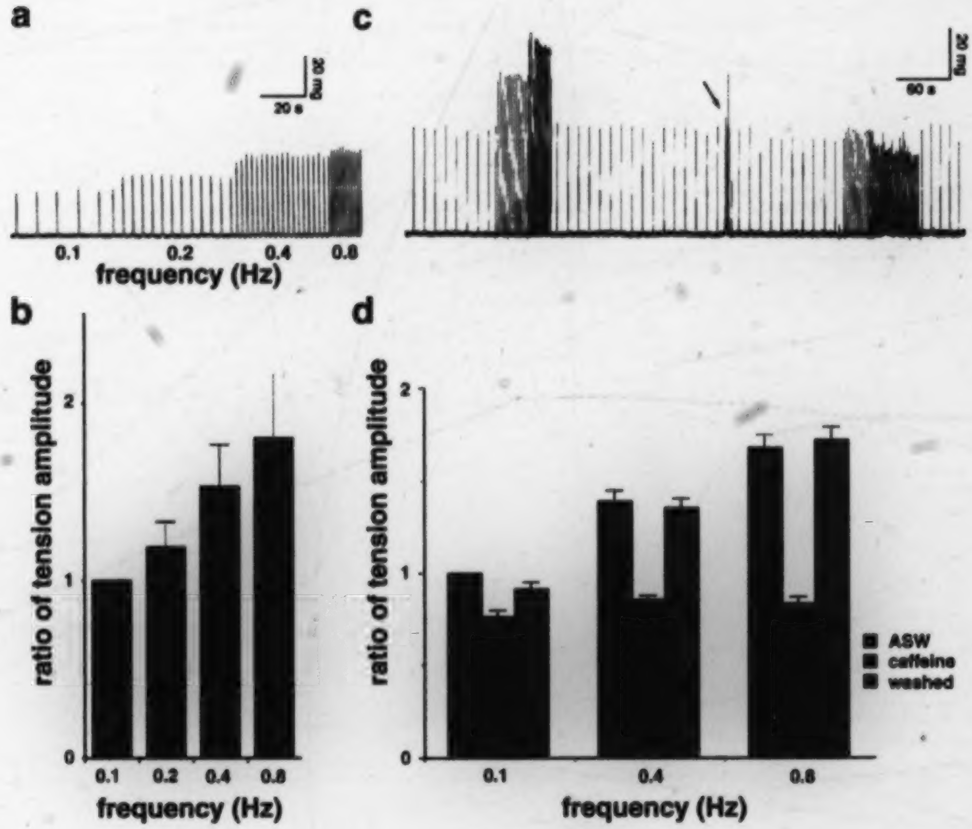
a
20 mg
20 s
0.1
0.2
0.4
0.8
frequency (Hz)
c
20 mg
60 s
b
ratio of tension amplitude
0
1
2
0.1
0.2
0.4
0.8
frequency (Hz)
d
ratio of tension amplitude
0
1
2
0.1
0.4
0.8
frequency (Hz)
ASW
caffeine
washed

Fig. 5.2. The ultrastructure of the swimming muscle of the *Polyorchis* medusa. Each muscle cell is separated into soma and feet. The somal region contains the nucleus (N), vacuoles, Golgi complex, and mitochondria (M). Note the larger number of mitochondria (M) lying along the striated myofibrils. Arrows indicate the vesicles in the subsarcolemma region. Me: mesoglea.

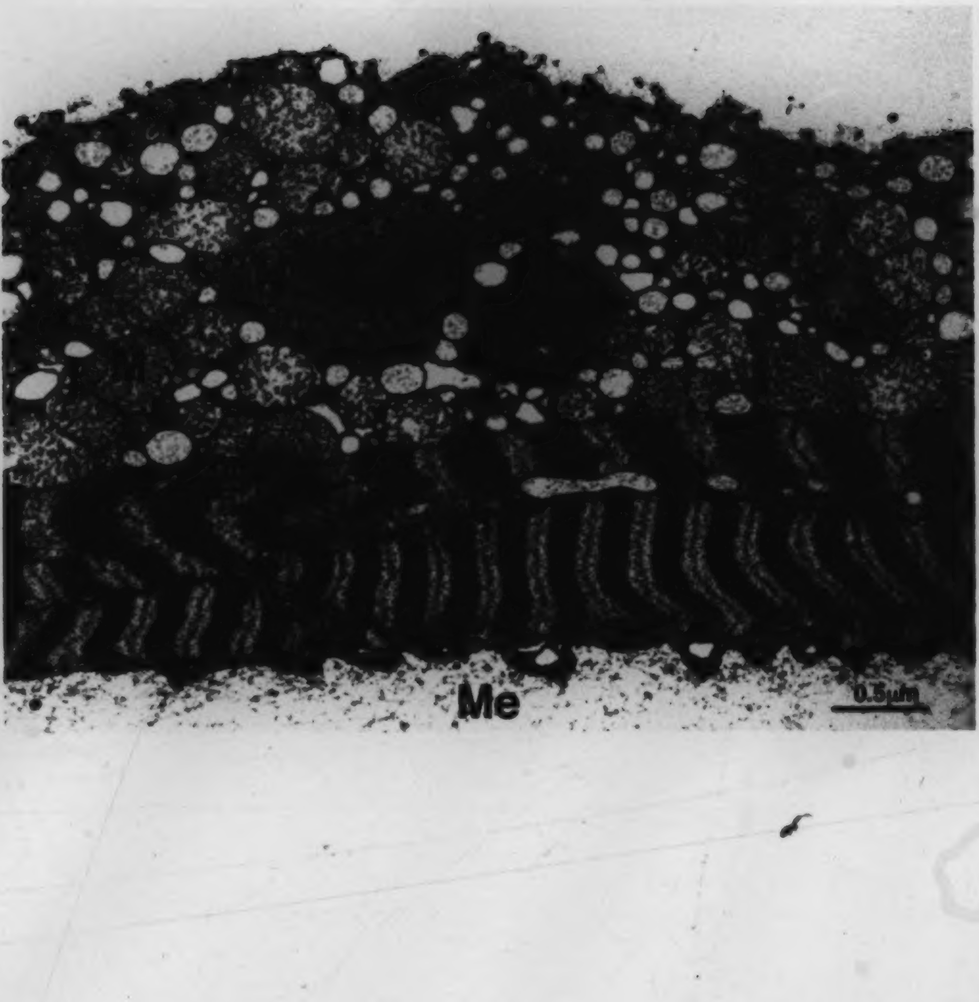
Me
0.5µm

Fig. 5.3. Ca^{2+}-ATPase activity in the soma of the *Polyorchis* swimming muscle. The reaction products (lead phosphate precipitates) of Ca^{2+}-ATPase activity are located in a) the nucleus; b) Golgi stacks; c) lateral plasma membrane and vesicles. Note in c) the absence of reaction products in the mitochondria (M) whereas there are precipitates in the sarcoplasmic reticulum (arrow). The arrowhead indicates the lateral plasma membrane. Most of the precipitates are located on the outer leaflet of this membrane. The apical region which is at the top of panel does not show heavy precipitation.

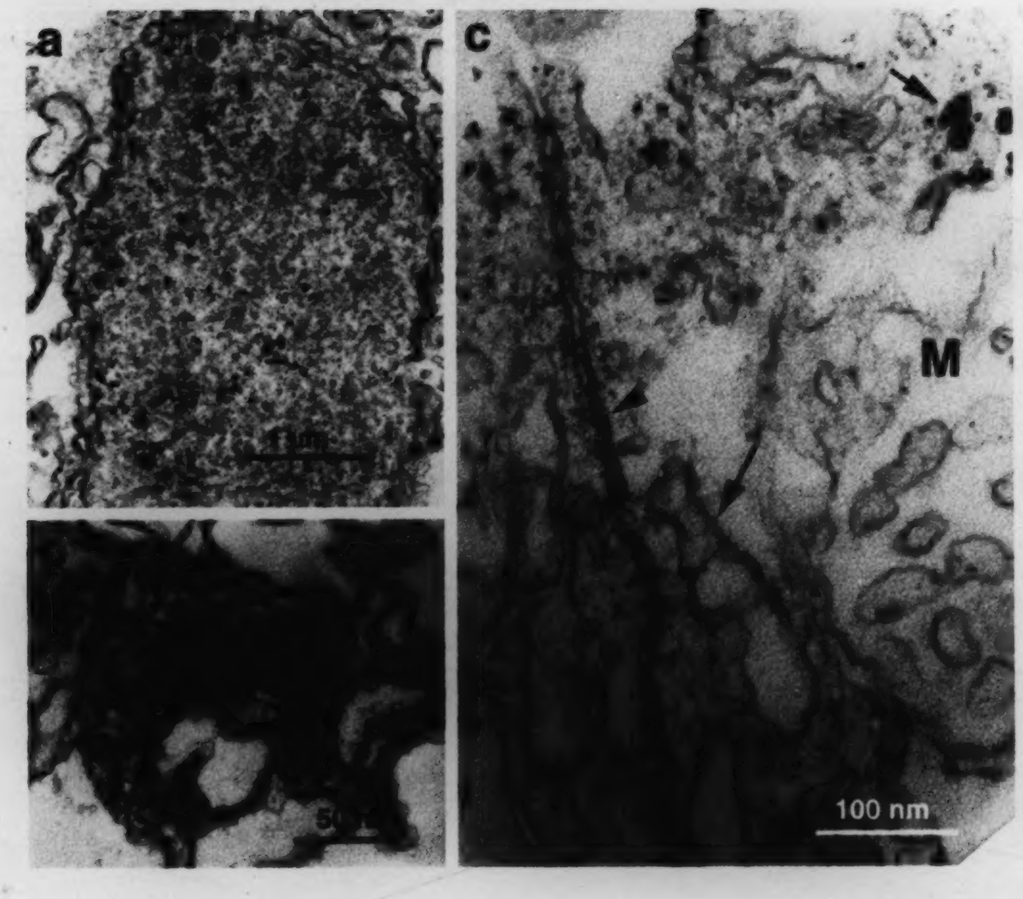
a
1 µm
50
c
M
100 nm

Fig. 5.4. A cross section of the myofibrils showing the Ca^{2+}-ATPase activity in the myofibrils of the *Polyorchis* swimming muscle. Precipitates are found along both sides of sarcolemma. No precipitates are found in mitochondria (M). Arrows point to the subsarcolemmal vesicles showing Ca^{2+}-ATPase activity. Arrowhead indicates a tubular structure which does not have any precipitate.

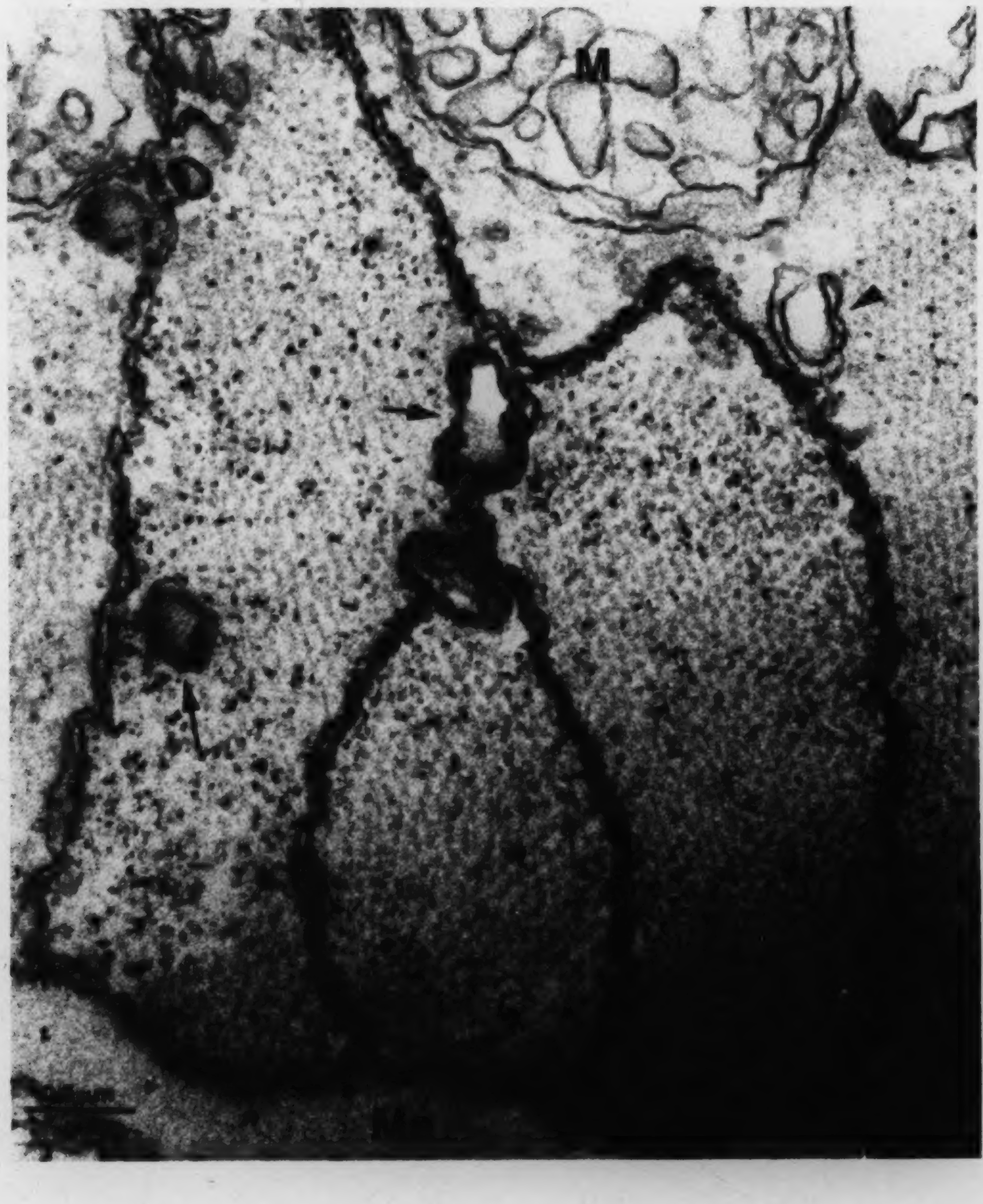
M

Fig. 5.5. Negative control for the Ca^{2+}-ATPase activity. Note no lead phosphate precipitation when tissues are incubated in a calcium-free medium with 10 mM EGTA. Arrow indicates the vesicle strueture and the arrowhead indicates sarcolemmal membrane which is free of precipitate. M: mitochondria; Me: mesoglea.

Me

Fig. 5.6. Localisation of calcium in the swimming muscle of *Polyorchis* by potassium dichromate. a) Nucleus; grainy electron dense precipitates (EDPs) are found inside the nucleus. b) Vesicles in the somal region showing high calcium content. Arrowhead indicates the plasma membrane showing EDPs located on the inner side of membrane. c) Vesicles (arrowed) in the subsarcolemma contain EDPs. Arrowhead indicates the sarcolemma. d) Large vesicles sitting between mitochondria (M) and myofilaments in the subsarcolemma contain EDPs (arrowed). Arrowhead indicates the sarcolemma membrane, note the EDPs are on the inner side of membrane. Me: mesoglea.

a

Fig. 5.7. Electron energy loss spectroscopy of calcium localisation in *Polyorchis* swimming muscle. a) Net calcium distribution image. This image is generated by computer subtraction of a background image taken at dE = 330 eV from the image taken at dE = 355 eV which is above the edge of electron absorption specific for calcium (CaL2,3 edge 346 eV. The bright spots indicate the calcium signal. b) Corresponding image taken using conventional TEM mode (zero energy loss). In both images the arrowhead indicates a hemidesmosome; the arrow indicates subsarcolemmal vesicles.

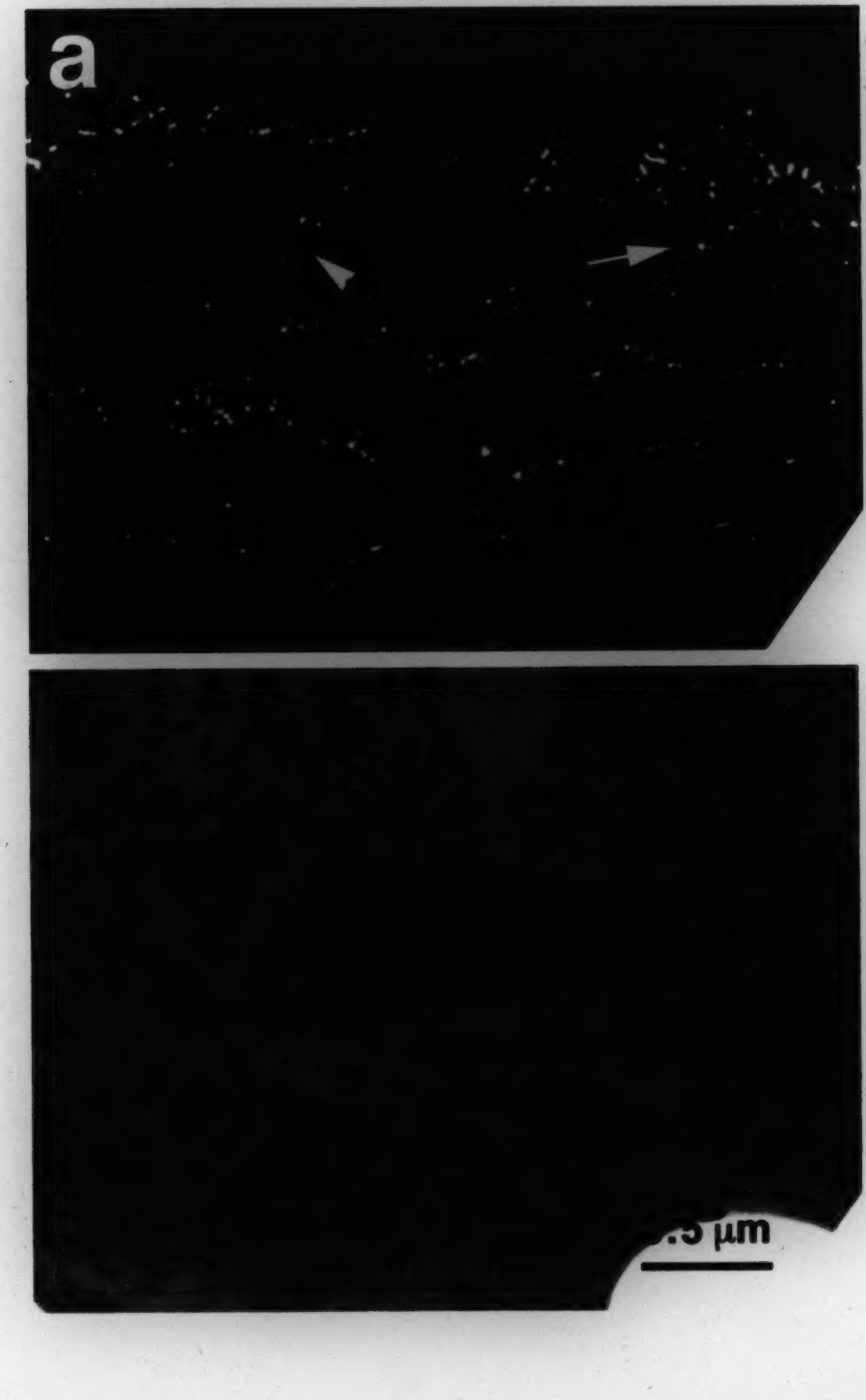
a
.5 µm

REFERENCES

Armstrong, C. M., Bezanilla, F. M., and Horowicz, P. (1972). Twitches in the presence of ethylene glyco bis(-aminoethyl ether)-N,N'-tetraacetic acid. *Biochim. Biophys. Acta* **267**, 605-608.

Ando, T., Fujimoto, K., Mayara, H., and Ogawa, K. (1981). A new one step method for histochemistry and cytochemistry of calcium ATPase activity. *Acta Histochem Cytoch* **14**, 705-734.

Ashley, C. C., Griffiths, P. J., Lea, T. J., Mulligan, I. P., Palmer, R. E., and Simnett, S. J. (1993). Barnacle muscle: Ca2+, activation and mechanics. *Rev. Physiol. Biochem. Pharm.* **122**, 149-258.

Bassot, J. M., Bilbaut, A., Mackie, G. O., Passano, L. M., and Pavans de Ceccatty, M. (1979). Bioluminescence and other responses spread by epithelial conduction in the siphonophore *Hippopodius*. *Biol. Bull.* **155**, 473-98.

Bers, D. M. (1991). Excitation-contraction coupling and cardiac contractile force. Boston: Kluwer Academic.

Bone, Q., Inoue, I., and Tsutsui, I. (1997). Contraction and relaxation in the absence of a sarcoplasmic reticulum: muscle fibres in the small pelagic tunicate Doliolum. *J. Mus. Res. Cell. Motil.* **18**, 375-380.

Carafoli, E. (1987). Intracellular calcium homeostasis. *Annu. Rev. Biochem.* **56**, 395-433.

Carafoli, E. (1991). Calcium pump of the plasma membrane. *Physiol. Rev.* **71**, 129-153.

Carl, S. L., Felix, K., Caswell, A. H., Brandt, N. R., Brunschwig, J. P., Meissner, G., and Ferguson, D. G. (1995). Immunolocalisation of triadin, DHP receptors, and ryanodine receptors in adult and developing skeletal muscle of rats. *Muscle & Nerve* **18**, 1232-1243.

Chapman, D. M., Pantin, C. F. A., and Robson, E. A. (1962). Muscle in coelenterates. *Rev. Canad. Biol.* **21**, 267-278.

Crompton, M. (1985). The regulation of mitochondria calcium transport in heart. *Curr. Top. Memb. Transp.* **25**, 231-276.

Fautin, D .G. and Mariscal, R. N. (1991). Cnidaria: Anthozoa. *In* Placozoa, Porifera, Cnidaria, and Ctenophora, Vol. 2 (eds. F. W. Harrison and J. A. Westfall). New York: Wiley-Liss, Inc.

Fujimoto, T. (1993). Calcium pump of the plasma membrane is localized in caveolae. *J. Cell Biol.* **120**, 1147-1157.

Golovina, V. and Blaustein, M. P. (1997). Spatially and functionally distinct Ca^{2+} stores in sarcoplasmic and endoplasmic reticulum. *Science* **275**, 1643-1648.

Inesi, G. (1987). Sequential mechanism of calcium binding and translocation in sarcoplasmic reticulum adenosine triphosphatase. *J. Biol. Chem.* **262**, 16338-16342

Inui, M., Saito, A., Fleischer, A. (1987). Purification of the ryanodine receptor and identity with feet structure of junctional terminal cisternae of sarcoplasmic reticulum from skeletal muscle. *J. Biol. Chem.* **262**, 1740-1747.

Jorgensen, A. O., Shen, A. C., Campbell, K. P., and MacLennan, D. H. (1983). Ultrastructural localisation of calsequestrin in rat skeletal muscle by immunoferritin labelling of ultrathin frozen sections. *J. Cell Biol.* **97**,1573-1581.

Krizaj, D. and Copenhagen, D. R. (1998). Compartmentalization of calcium extrusion mechanisms in the outer and inner segments of photoreceptors. *Neuron* **21**, 249-256.

Lai, F. A., Erickson, H. P., Rousseau, E., Liu, Q. Y., and Meissner, G. (1988). Purification and reconstitution of the calcium release channel from skeletal muscle. *Nature* **331**, 315-319.

Lee, M. G., Xu, X., Zeng, W., Diaz, J., Kuo, T. H., Wuytack, F., Racymaekers, L., and Muallem, S. (1997). Polarized expression of Ca^{2+} pumps in pancreatic and salivary gland cells. *J. Biol. Chem.* **272**, 15771-15776.

Lullmann, H. and Peters, T. (1977). Plasmalemmal calcium in cardiac excitation contraction coupling. *Clin. Exp. Pharm. Physiol.* **4**, 49-57.

Lullmann, H. and Peters, T. (1979). Action of cardiac glycosides on the excitation-contraction coupling in the heart muscle. *Prog. Pharm.* **2**, 3-58.

Lytton, J. and Nigam, S. K. (1992). Intracellular calcium: molecules and pools. *Cur. Opin. Cell Biol.* **4**, 220-226.

Mackie, G. O. (1970). Neuroid conduction and the evolution of conducting tissues. *Q. Rev. Biol.* **45**, 319-332.

Maggio, K., Watrin, A., Keicher, E., Nicaise, G., and Hernandez-Nicaise, M. (1991). Ca^{2+}-ATPase and Mg^{2+}-ATPase in *Aplsia* glia and interstitial cells: an EM cytochemical study. *J. Histo. Cyto.* **39**, 1645-1658.

Meissner, G., Conner, G. E., and Fleischer, S. (1973). Isolation of sarcoplasmic reticulum by zonal centrifugation and purification of Ca^{2+}-pump and Ca^{2+}-binding proteins. *Biochim. Biophys. Acta.* **298**, 246-269.

Meyran, J. C. and Graf, A. (1986). Ultrahistochemical localisation of Na^{+}/K^{+}-ATPase, Ca^{2+}-ATPase and alkaline phophatase activity in a calcium-transporting epithelium of a crustacean during moulting. *Histochem* **85**, 313-320.

Nabauer, M., Callewart, G., Cleemann, L., and Morad, M. (1989). Regulation of calcium release is gated by calcium current, not gating charge, in cardiac myocytes. *Science* **244**, 800-803.

Nasu, F. and Inomata, K. (1990). Ultracytochemical demonstration of Ca^{2+}-ATPase activity in the rat saphenous artery and its innervated nerve terminal. *J. Electron Microsc.* **39**, 487-491.

Ogawa, K. S., Fujimoto, K., and Ogawa, K. (1986). Ultracytochemical studies of adenosine nucleotidases in aortic endothelial and smooth muscle cells-Ca^{2+}-ATPase and Na^{+}, K^{+}-ATPase. *Acta Histochem. Cytochem.* **19**, 601-620.

Palade, P., and Györke, S. (1993). Excitation-contraction coupling in crustacea: do studies on these primitive creatures offer insights about EC coupling more generally? *J. Mus. Res. Cell Motil.* **14**, 283-287.

Paniagua, R., Royuela, M., Garcia-anchuelo, R. M., and Fraile, B. (1996). Ultrastructure of invertebrate muscle cell types. *Histol. Histopathol.* **11**, 181-201.

Probst, W. (1986). Ultrastructural localisation of calcium in the CNS of vertebrates. *Histochem.* **85**, 231-239.

Prosser, C. L. (1982). Diversity of narrow-fibered and wide-fibered muscles. *In* Basic biology of muscle: a comparative approach (eds. B. M. Twarog, R. J. C. Levine, and M. M. Dewey). New York: Raven Press.

Rich, T. L., Langer, G. A., and Klassen, M. G. (1988). Two components of coupling calcium in single ventricular cell of rabbits and rats. *Am. J. Physiol.* **254**, H937-H946.

Seguchi, H., Okada, T., and Ogawa, K. (1982). Localisation of Ca^{2+}-activated adenosine triphosphatase activities in the transitional epithelium of the rabbit urinary bladder. *Acta Histochem. cytochem.* **15,** 76-89.

Singla, C. L. (1978a). Locomotion and neuromuscular system of *Aglantha digitale*. *Cell Tiss. Res.* **188,** 317-27.

Singla, C. L. (1978b). Fine structure of the neuromuscular system of *Polyorchis penicillatus* (Hydromedusae, Cnidaria). *Cell Tiss. Res.* **193,**163-74.

Spencer, A. N. (1979). Neurobiology of *Polyorchis*. II. Structure of effector systems. *J. Neurobiol.* **10,** 95-117.

Spencer, A. N. and Satterlie, R. A. (1981). The action potential and contraction in subumbrellar swimming muscle of *Polyorchis penicillatus* (Hydromedusae). *J. Comp. Physiol.* **144,** 401-407.

Tada, M., Yamada, M., Kadoma, M., Inui, M., and Ohmori, F. (1982). Calcium transport by cardiac sarcoplasmic reticulum and phosphorylation of phospholamban. *Mol. Cell Biochem.* **46,** 74-95.

Thomas, M. B. and Edwards, N. C. (1991). Cnidaria: Hydrozoa. *In* Placozoa, Porifera, Cnidaria, and Ctenophora, Vol. 2 (eds. F. W. Harrison and J. A. Westfall). New York: Wiley-Liss, Inc.

Ueno, S. and Mizuhira, V. (1984). Calcium transport mechanism in crayfish gastrolith epithelium correlated with the molting cycle. II cytochemical demonstration of Ca^{2+} ATPase and Mg^{2+} ATPase. *Histochem.* **80,** 213-230.

Van-Noorden, C. J. And Jonges, G. N. (1987). Quantification of the histochemical reaction for alkaline phosphatase activity using the indoxyl terranitro BT method. *Histoch. J.* **19,** 93-101.

Weber, A. and Herz, R. (1968). The relationship between caffeine contrature of intact muscle and the effect of caffeine on reticulum. *J. Gen. Physiol.* **52,** 750-759.

Winegrad, S. (1965). Autoradiographic studies of intracellular calcium in frog skeletal muscle. *J. Gen. Physiol.* **48,** 455-479.

Chapter 6

General conclusion

Neuroanatomy and monoclonal antibodies

The anatomy of nervous system revealed by the monoclonal antibody 5C6 (mAb 5C6) represents the most complete anatomical description of the nervous system of the hydromedusa *Polyorchis penicillatus*. In a single whole mount preparation, it contains all known nervous network described by different histological and electrophysiological techniques and some previously undescribed network elements. The mAb 5C6 staining reveals that each swimming muscle quadrant is encircled by the swimming motor neuron network. Thus, the synchronized excitation in the muscle field can be achieved by the changes in the duration of action potentials to compensate conduction delay (Spencer 1982, Spencer et al. 1989).

The monoclonal antibody staining not only provides the most complete nervous system described in *Polyorchis,* it also reveals the complexity of the nervous systems at the bell margin. There are several networks at the bell margin, including swimming motor neuron network, "B" system, "O" system, accessory nerve network (Spencer 1981, 1982, Spencer and Arkett 1984) and some unnamed networks (Chapter 2). To further elucidate the complexicity of the nervous system in the bell margin, different histological and electrophysiological techniques, including peptide-specific antibody staining, intracellular recording, and Lucifer yellow and carboxyfluoroscein iontophoresis can be combined with mAb 5C6 staining to show where the particular network in study is located related to the whole nervous system.

The hybridoma technique proves to be very useful in generation of antibodies against specific cell types. Only one of the 156 positive hybridoma cultures was described here; preliminary screening indicates that there are several other clones of hybridomae producing antibodies against nervous systems of *Polyorchis*. To produce different antibodies against specific nervous networks, screening and cloning the present hybridoma collection is the first step. Another approach is to isolate specific neuronal fractions by PERCOLL step gradient. This approach includes cell dissociation by heat treatment which preserves the cell morphology (Chapter 4), mAb 5C6 staining for identifying interstitial cells and all their derivatives (Chapter 2), and toluidine blue staining for interstitial cells. After the first PERCOLL step gradient separation the neuron-enriched fractions can be identified and can be further separated by another run of PERCOLL step gradient and each fraction collected can be used to inoculate mice for the production of mAbs. This approach might provide a better chance of producing mAbs specific for different neuronal types.

Wound healing

Wound healing process in vertebrate system generally involves several different cell types and different trophic factors (Lawrence 1998). In the striated muscle sheet of jellyfish, the wound healing process described in chapter 3 only involves a single cell type: the striated muscle cells. When the swimming muscle layer is damaged the nearby undamaged muscle cells begin to migrate. Before the initiation of migration, junctional connections (including hemidesmosomes and desmosomes) are removed from the striated muscle and myofibrils are withdrawn and lamellipodia are formed in readiness for migration. Cells migrate as a whole sheet and retain gap junction connections. This process is very similar to the process of re-epithelization in vertebrate wound healing (Stenn and DePalma 1988). The presence of gap junction connections in the migratory epithelial cell sheet can also be found in vertebrate epidermal keratinocytes and cornea keratocytes (Gabbiani et al.1978, Watsky 1995a). It is believed that the function of these gap junctions is to regulate the synchronized locomotion of the migratory cell sheet (Stenn and DePalma 1988). The ability of striated muscle cells to behave like epithelial cells during wound-healing process might be related to their developmental origin. Striated muscle cells of medusae are derived from epithelial cells during asexual reproduction of polyps. These striated muscle cells only appear in medusae stage of cnidarian life cycle and under certain primary culture condition these striated muscle cells can lose their striated pattern in their myofibres (Schmid and Reber-Muller 1995). Therefore, the striated muscle cells might be considered as the most advanced developmental stage of epithelial cells. Molecular cloning experiments in the jellyfish *Podocoryne carnea* indicates some specific genes are activated during the development of medusae (Schuchert et al. 1993, Aerne et al. 1995). For the striated muscle cells in the jellyfish *Polyorchis penicillatus* the T-type calcium channels and A-type potassium channels might be considered as specific features associated with the differentiated status, since these ion channels are removed prior to, or during, migration when cells are becoming more epithelial cell-like (Chapter 3). The phenomena of losing ion channels in the process of migration can also be found in the vertebrate corneal keratocytes that are also derived from epithelial cells (Watsky 1995b).

The initiation of migration process in striated muscle cells of jellyfish does not require the production of new proteins, since cycloheximide does not interfere with this process (Chapter 3). The initiation of migration process might simply be a result of the disruption in the connections among cell-cell junctional proteins, since the disruption in the connection of junctional proteins is known to evoke a cascade of cellular events (Clark and Brugge 1995, Schwartz et al. 1995). Cell migration requires a sophisticated regulation of the interaction between cytoskeleton and extracellular matrix. In general the interaction between cytoskeleton and extracellular matrix is carried out through integrin receptors (Hynes 1992, Huttenlocher et al. 1996). For mammalian epithelial cells the onset of migration requires the expression of different set of integrins to interact with extracellular matrix (Cavani et al. 1993). The exact nature of integrins present in cnidarians has never been looked at. The only available information is that an anti-human β1-integrin antibody shows cross reactivity with the nerve cells of the jellyfish *Turritopsis nutricula* (Piraino et al. 1996) and the attachment of Hydra nematocytes to fibronetin can be inhibited by peptides containing Arg-Gly-Asp (RGD) sequence (Ziegler and Stidwill 1992), which suggesting the presence of integrin receptors in cnidarians. Since the onset of migration in jellyfish striated muscle cells does not require synthesis of new proteins, this suggests that the same receptors for extracellular matrix in the intact muscle cells might be used for cell migration. To address the function of extracellular matrix receptors in wound healing process in jellyfish, one might have to look for what kind of extracellular receptors are present on the striated muscle cells. Integrins can bind to several different extracellular matrix elements and are involved in most cell migration studied (Hynes 1992). Therefore integrins should be the first candidates to look for in the striated muscle cells. To identify what integrins are present in muscle cells immunohistochemistry and western blotting will be the first step. After identifying which extracellular receptors are present in the striated muscle, the antibody perturbation of receptor function will be next step to establish the role of identified receptors in the migration of muscle cells. Receptors for extracellular matrix relay their message through different signalling pathways which contain kinases, GTPases and other molecules (Clark and Brugge 1995). Although some kinases has been identified in cnidarians (DePetrocellis et al. 1993, Chan et al. 1994, Hassel 1998), their role in the signalling pathways for extracellular metrix receptors have not been explored in cnidarians.

Cytoskeleton plays a major role in cell migration. In the jellyfish striated muscle cells, cell migration can be inhibited by disrupting actin filaments with cytochalasin B (Chapter 3). Another cytoskeleton component known to be important in regulating cell shape is microtubule. However, the importance of microtubule in cell migration seems to be cell-type specific. Mammalian endothelial cells require microtubules for cell migration whereas fish keratocytes do not (Schliwa and Honer 1993). The requirement of microtubules for cell migration in jellyfish can be verified by using pharmacological drugs to interfere microtubule structures and antibodies staining to visualize the effect on microtubules.

One interesting observation during the wound healing process in jellyfish is that cell proliferation did not occur to make up the loss in cell number, although cell proliferation might occur in larger wounds (Chapter 3). The closure of the wound is actually governed by the traction force generated during cell migration and re-polarization that deformed the mesoglea. In vertebrate systems, the force generated by myofibroblasts is believed to cause the closure of wound (Gabbiani 1998). Thus, in addition to the normal function of epithelial cells, myoepithelial cells play a similar role to that of myofibroblasts during wound healing.

T-type calcium currents in muscle contraction

The only inward ionic component recorded from dissociated swimming muscles is a T-type calcium current (Chapter 4). This jellyfish current shares all the characteristics of T-currents described elsewhere (Huhuenard 1996, Randall 1998, Randall and Tsien 1998), including activation at low membrane potential, fast activation and inactivation, similar permeability to calcium, strontium, and barium, and sensitivity to nickel ions. Although its sensitivity to dihydropyridines is not a common characteristic among all T-type currents, the concentration of inhibition falls within the range reported for some T-type currents.

T-type calcium channels have been suggested as the ancestor of sodium channels (Hille 1992). Recent molecular cloning experiments support this notion by comparing sequences from the pore region of high-voltage-activated (HVA) calcium channels, sodium channels, and T-type calcium channels. At the pore region, HVA calcium channels have 4 negatively charged glutamate residues, whereas in the sodium channels two negatively charged residues have been replaced by one positively charged lysine residue and one neutral alanine residue. T-type calcium channels from human heart and brain have two glutamates and two aspartates in their sequences at this critical pore region (Tsien 1998). As mentioned in the Chapter 4, activation kinetics of the T-type calcium current recorded from jellyfish striated muscle cells are very fast and comparable to the kinetics of sodium channels. Due to the particular phylogenetic position of cnidarians, it might be worthwhile to clone the sequence of T-type calcium channels and compare its sequence to the other reported sequences of T-type calcium channels.

Some preliminary current-clamp recordings from these heat-treated striated muscle cells indicate that action potential can be evoked with the presence of only T-type calcium channel, A-type potassium channels, and delayed-rectifier potassium channels. The shape of action potential from heat-treated muscle cells is a sharp peak without any shoulder plateau phase. However, previous studies showed that the action potential recorded from striated muscle sheets of *Polyorchis* depends on both extracellular calcium and sodium and is square-shaped with a plateau phase after depolarization (Spencer and Satterlie 1981). The square-shaped action potenitials from jellyfish muscle sheet is reminant of action potential shape in vertebrate cardiac myocytes. The ionic composition of vertebrate cardiac myocytes is consisted of sodium channel, T-type and L-type calcium channels, and A-type and delayed-rectifier potassium channels. The T-type currents activate at low membrane potential (-70 mV) and bring the membrane potential to the activation threshold of sodium channels for the generation of an action potential (Ertel et al. 1997, Triggle 1998). The plateau phase of action potentials is maintained by the calcium entrance through L-type calcium, since T-type calcium channels inactivate very fast (Bers 1991). Potassium channels function to regulate the activation, duration, and firing frequency of action potentials. The discrepancy between these two results might be the difference of methodology. Indeed, there is no evidence that heat treatment preserves the full suite of ion channels on striated muscle cells. It is possible that heat treatment somehow only preserves the T-type calcium channels but not the sodium channels and L-type calcium channels. On the other hand, the formation of plateau phase of action potential in striated muscle sheet can be a result of summation of action potentials from individual cells, since striated muscle cells are heavely interconnected by gap junctions. To address this question, intracellular recording should be performed in the presence of reagents which will disrupt the gap junction connection, for example, tamoxifen or heptanol (Verrecchia and Herve 1997, Wolosin et al. 1997). The other problem to be addressed is whether the sodium channel is present in striated muscle cells or not. To address this question, intracellular recording should be performed under different conceentrations of extracellular sodium to see if the amplitudes of action potentials very with different concentrations of extracellular sodium.

Putative calcium stores involved in excitation-contraction coupling

The presence of sarcoplasmic reticulum-like structures has been observed using TEM in striated myoepithelial cells in cnidarians, ctenophores, echinoderms, and annelids (Chapman 1974, Paniagua et al. 1996). However, the participation of this sarcoplasmic reticulum in excitation-contraction coupling has not been examined. In jellyfish swimming muscle, caffeine suppresses contraction and abolishes the frequency-dependent increase in tension (Chapter 5) indicating that calcium stores participate in excitation-contraction coupling. Although caffeine is known to have other effects on muscle contraction, these all increase, rather that suppress the amplitude of contraction. My ultrastructural observations confirm the presence of Ca^{2+}-ATPase and calcium in the sarcoplasmic reticulum under the sarcolemma, which are in turn indicators of calcium stores. Together with the higher concentration of T-channels on the sarcolemma of myofibrils (Chapter 4), this gives strong support for the proposition that a calcium induced calcium release mechanism is involved in the excitation-contraction coupling of jellyfish striated muscle.

In the chapter 5 where localization of calcium and calcium ATPase activity was used to establish the subsarcolemmal vesicles as putative calcium stores the third criteria (the presence of calcium releasing channel on the subsarcolemmal vesicles) was not addressed. To examine the presence of calcium releasing channels on the subsarcolemmal vesicles, activators or inhibitors for calcium releasing channels, for example ryanodine (Hisayama and Takayanagi 1988), should be tested by the field stimulation of muscle contraction to establish their potency. Further localization of the calcium releasing channels can be achieved by using TEM immunogold techniques, if there is antibody available or TEM autoradiography techniques, if the isotope-labelled channel inhibitors or activators are available.

Further evidence that a calcium-induced calcium released mechanism participates in muscle contraction of jellyfish could be obtained by using muscle cells with perforated cell membranes (Bers 1991). Perforated muscle cells can be induced to contract by increasing the calcium concentration in the bath solution. The direct effects of various pharmacological agents, such as caffeine, on putative calcium stores in the cytosolic compartment could be examined using such a system.

Calcium dependence of cell migration

The contraction of jellyfish swimming muscle depends on extracellular calcium through voltage gated calcium channels (Chapters 3, 4, 5). The contribution of calcium from the sarcoplasmic reticulum to muscle contraction plays an additive role during contraction. However, when the muscle cells are induced to migrate, the morphological changes are accompanied with a change in the dependence on calcium of cell motility. Muscle cells migrate normally under low extracellular calcium (1 µM) and migration is slowed in the presence of caffeine or thapsigargin. Caffeine and thapsigargin deplete calcium stores by making the stores leaky and inhibiting calcium reuptake through inhibiting Ca^{2+}-ATPases respectively (Lytton and Nigam 1992). Thus, cell migration is largely dependent on intracellular calcium (Chapter 3). To further investigate the role of calcium in the migration of striated muscle cells one good approach is to use calcium imaging techniques, such as fura-2, to study spatial and temporal distribution of calcium in the migrating cells. My preliminary study using the fura-2 as calcium indicator has not been successful. One major obstacle was the inability to load fura-2 AM into striated muscle cells. This could be related to different composition of jellyfish cell membrane (Schetz and Anderson 1993, 1995) or the lack of enzyme to cleave the AM residue. Alternative loading method such as microinjection of fura-2 salt should be used.

To date, there is no evidence to show which calcium stores regulate the migration process. Do calcium stores in the somal region regulate cell migration? Alternatively, is this role fulfilled by the sarcoplasmic reticulum in the myofibillar region? Further studies are needed to address these questions.

Conclusion

The present study demonstrates that the mAb 5C6 gives the most complete picture of the nervous system in the jellyfish, *Polyorchis penicillatus*. Thus, this antibody will be a useful tool for future study on circuitry mapping and behaviour control. In addition, the present study clearly demonstrates multifunction in tissues of animals with few identifiable cell types. The myoepithelial cells in the subumbrellar area of jellyfish clearly have plural functions. First, the single layer of cells functions as epithelium, separating the interior environment from the exterior. Second, the long myofibrils of the myoepithelial cells have the same arrangement of filament as vertebrate striated muscle cells and generate phasic contraction in movement. Third, the myoepithelial cells generate traction force during migration and repolarization to close the wound in a similar manner to myofibroblasts of vertebrates. Thus, the wound healing process illustrates the plasticity of cellular functions and thereby provides a convenient experimental model of the mechanisms regulating switching between different functions. Furthermore, the present study also demonstrates the presence of a T-type calcium current and putative calcium stores involved in muscle contraction. The close proximity of calcium store and T-type calcium channels ensures the efficiency of excitation-contraction coupling.

REFERENCES

Aerne, B. L., Baader, C. D., and Schmid, V. (1995). Life stage and tissue-specific expression of the homeobox gene cnox 1-Pc of the hydrozoan *Podocoryne carnea*. *Dev. Biol.* **169**, 547-556.

Bers, D. M. (1991). Excitation-contraction coupling and cardiac contractile force. Boston: Kluwer Academic.

Chapman, D. M. (1974). Cnidarian Histology. *In* Coelenterate biology: review and new perspectives (ed. L. Muscatine and H. M. Lenhoff). New York: Academic Press, Inc.

Cavani, A., Zambruno, G., Marconi, A., Manca, V., Marchetti, M., and Gianetti, A. (1993). Distinctive integrin expression in the newly forming epidermis during wound healing in humans. *J. Invest. Dermatol.* **101**, 600-604.

Chan, T. A., Chu, C. A., Rauen, K. A., Kroiher, M., Tatarewicz, S. M., and Steele, R. E. (1994). Identification of a gene encoding a novel protein-tyrosine kinases containing SH2 domains and ankyrin-like repeats. *Oncogene* **9**, 1253-1259.

Clark, E. A. and Brugge, J. S. (1995). Integrins and signal transduction pathways: the road taken. *Science* **268**, 233-239.

De Petrocellis, L., Di Marzo, V., and Cimino, G. (1993). The possible involvement of protein kinase C and phospholipase A2 in Hydra tentacle regeneration. *Experientia* **49**, 57-64.

Ertel, S. I., Ertel, E. A., and Clozel, J. P. (1997). T-type Ca^{2+} channels and pharmacological blockade: potential pathophysiological relevance. *Cardioves. Drugs Ther.* **11**, 723-39.

Gabbiani, G. (1998). Evolution and clinical implications of the myofibroblast concept. *Cardiovas. Res,* **38**, 545-548.

Gabbiani, G., Chapponnier, C., and Huttner, I. (1978). Cytoplasmic filaments and gap junctions in epithelial cells and myofibroblasts during wound healing. *J. Cell Biol.* **76**, 561-580.

Grigoriev, N. G., Spafford, J. D., Przysiezniak, J., and Spencer, A. N. (1996). A cardiac-like sodium current in motor neurons of a jellyfish. *J. Neurophysiol.* **76**, 2240-2249.

Hassel, M., Bridge, D. M., Stover, N. a., Kleinholz, H., and Steele, R. E. (1998). The level of expression of a protein kinase C gene may be an important component of the patterning process in *Hydra*. *Dev. Genes Evol.* **207**, 502-514.

Hisayama, T and Takayanagi, I. (1988). Ryanodine: its possible mechanism of action in the caffeine-sensitive calcium store of smooth muscle. *Pflugers Archiv* **412**, 376-381.

Huguenard, N. J. (1996). Low-threshold calcium currents in central nervous system neurons. *Ann. Rev. Physiol.* **58**, 329-348.

Huttenlocher, A., Ginsberg, M., and Horwitz, A. (1996). Modulation of cell migration by integrin-mediated cytoskeletal linkage and ligand-binding affinity. *J. Cell Biol.* **134**, 1551-1562.

Hynes, R. O. (1992). Integrins: versatility, modulation, and signalling in cell adhesion. *Cell* **69**, 11-25.

Lytton, J. and Nigam, S. K. (1992). Intracellular calcium: molecules and pools. *Cur. Opin. Cell Biol.* **4**, 220-226.

Nuss, H. B. and Houser, S. R. (1993). T-type Ca^{2+} current is expressed in hypertrophied adult feline left ventricular myocytes. *Circ. Res.* **73**, 777-782.

Paniagua, R., Royuela, M., Garcia-Anchuelo, R. M., and Fraile, B. (1996). Ultrastructure of invertebrate muscle cell types. *Histol. Histopathol.* **11**, 181-201.

Piraino, S., Boero, F., Aeschbach, B., and Schmid, V. (1996). Reversing the life cycle: medusae transforming into polyps and cell transdifferentiation in *Turritopsis nutricula* (cnidaria, Hydrozoa). *Biol. Bull.* **190**, 320-312.

Przysiezniak, J. and Spencer, A. N. (1989). Primary culture of identifies neurons from a cnidarian. *J. Exp. Biol.* **142**, 97-113.

Przysiezniak, J. and Spencer, A. N. (1992). Voltage-activated calcium currents in identified neurons from a hydrozoan jellyfish, *Polyorchis penicillatus*. *J. Neurosci.* **12**, 2065-2078.

Przysiezniak, J. and Spencer, A. N. (1994). Voltage-activated potassium currents in isolated motor neurons from the jellyfish *Polyorchis penicillatus*. *J. Neurophysiol.* **72**, 1010-1019.

Randall, A. D. (1998). The molecular basis of voltage-gated Ca^{2+} channel diversity: is it time for T? *J. Memb. Biol.* **161**, 207-213.

Randall, A. D. and Tsien, R. W. (1998). Distinctive biophysical and pharmacological features of T-type calcium channels. *In* Low-voltage-activated T-type calcium channels (eds. R. W. Tsien, J.-P. Clozel, and J. Nargeot). England: Adis International.

Schetz, J. A. and Anderson, P. A. V. (1993). Investigations of lipid components of neurone-enriched membranes of the jellyfish *Cyanea capillata*. *J. Exp. Biol.* **177**, 23-39.

Schetz, J. A. and Anderson, P. A. V. (1995). Glycosylation patterns of membrane proteins of the jellyfish *Cyanea capillata*. *Cell Tiss. Res*. **279**, 315-321.

Schliwa, M. and Honer, B. (1993). Microtubules, centrosomes and intermediate filaments in directed cell movement. *Trends Cell Biol.* **3**, 377-380.

Schmid, V. and Reber-Muller, S. (1995). Transdifferentiation of isolated striated muscle of jellyfish in vitro: the initiation process. *Sem. Cell Biol.* **6**, 109-116.

Schuchert, P., Reber-Muller, S., and Schmid, V. (1993). Life stage specific expression of a myosin heavy chain in the hydrozoan Podocoryne carnea. *Differentiation* **54**, 11-18.

Schwartz, M., Schaller, M., and Ginsberg, M. (1995). Intergrins: emerging paradigms of signal transduction. *Annu. Rev. Cell Dev. Biol.* **11**, 549-599.

Sen, L. and Smith, T. W. (1994). T-type Ca2+ channels are abnormal in genetically determined cardiomyopathic hamster hearts. *Circ. Res.* **75**, 149-155.

Spafford, J. D., Grigoriev, N. G., and Spencer, A. N. (1996). Pharmacological properties of voltage-gated Na+ currents in motor neurons from a hydrozoan jellyfish *Polyorchis penicillatus*. *J. Exp. Biol.*199, 941-948.

Spencer, A. N. (1981). The parameters and properties of a group of electrically coupled neurons in the central nervous system of a hydrozoan jellyfish. *J. Exp. Biol.* **93**, 33-50.

Spencer, A. N. (1982). The physiology of a coelenterate neuromuscular synapse. *J. Comp. Physiol.* **148**, 353-363.

Spencer, A. N. and Arkett, S. A. (1984). Radial symmetry and the organization of central neurones in a hydrozoan jellyfish. *J. Exp. Biol.* **110**, 69-90.

Spencer, A. N., Przysiezniak, J., Acosta-Urquidi, J., and Basarsky, T. A. (1989). Presynaptic spike broadening reduces junctional potential amplitude. *Nature* **340**, 636-8.

Spencer, A. N. and Satterlie, R. A. (1981). The action potential and contraction in subumbrellar swimming muscle of *Polyorchis penicillatus* (Hydromedusae). *J. Comp. Physiol.* **144**, 401-407.

Stenn, K. S. and DePalma, L. (1988). Re-epithelialization. *In* The molecular and cellular biology of wound repair (ed. R. A. F. Clark and P. M. Henson). New York: Plenum Press.

Triggle, D. J. (1998). The physiological and pharmacological significance of cardiovascular T-type, voltage-gated calcium channels. *Am. J. Hyper.* **11**, 80S-87S.

Verrecchia, F. and Herve, J. (1997). Reversible inhibition of gap junctional communication by tamoxifen in cultured cardiac myocytes. Pflugers Archiv 434(1), 113-116.

Watsky, M. A. (1995a). Loss of Keratocyte ion channels during wound healing in the rabbit cornea. *Invest. Ophthalmol. Vis. Sci.* **36**, 1095-1099.

Watsky, M. A. (1995b). Keratocyte gap junctional communication in normal and wounded rabbit corneas and human corneas. *Invest. Ophthalmol. Vis. Sci.* **37**, 1001-1005.

Wolosin, J. M., Candia, O. A., Peteerson-Yantorno, K., Civan, M. M., and Shi, X. P. (1997). Effect of heptanol on the short circuit currents of corea and ciliary body demonstrates rate limiting role of heterocellular gap junction in active ciliary body transport. *Exp. Eye Res.* **64(6)**, 945-952.

Ziegler, U. and Stidwill, R. P. (1992). The attachment of nematocytes from the primitive invertebrate Hydra to fibronectin is specific and RGD-dependent. ***Exp. Cell Res.*** **202**, 281-286.

Appendix

Isolation and culture of interstitial cells

To culture interstitial cells, bell margins of jellyfish were dissociated using 1000 units/ml of collagenase type I (Sigma) in artificial seawater (ASW - NaCl: 376 mM, $Na_2(SO_4)$: 26 mM, $MgCl_2$: 41.4 mM, $CaCl_2$: 10 mM, KCl: 8.5 mM, and HEPES (hemisodium salt): 10 mM), for 1 to 2 h at room temperature (Przysieziak and Spencer, 1989). In some later experiments tissue was dissociated with 1 mg/ml of Pronase (Boehringer Mannheim) in ASW at 30°C for 30 min. Dissociated cells were layered onto a Percoll step gradient which has 15% to 40% of Percoll stock solution with an increment of 5% each (Pharmacia, LKB, Biotechnology) and centrifuged at 2000 x *g* for 30 min at 12°C. The Percoll stock solution was prepared by diluting pure Percoll 9:1 with 10 x ASW. The 10 x ASW was NaCl: 3760 mM, $Na_2(SO_4)$: 260 mM, $MgCl_2$: 414 mM, $CaCl_2$: 100 mM, KCl: 85 mM, and HEPES (hemisodium salt): 100 mM. After centrifugation, an enriched interstitial cell population (over 80% purity) can be obtained between 25% and 30% of Percoll stock solution gradient. Interstitial cells were collected after the separation by Percoll step gradient, washed 3 times, 15 minutes each with sterilized ASW in which either Penicillin G (100 U/ml) and Streptomycin sulfate (100 mg/ml) or Gentamicin sulfate (50 mg/ml) was added.

Since interstitial cells did not attach to either glass or plastic Petri-dish, I tested different substrates for cell attachment. I have used native mesoglea with or without homogenization, poly-L-lysine, laminin, fibronectin, collagen type I and IV, and gelatin. Dissociated interstitial cells did not attach to any of these substrates, however, some epithelial cells and nerve cells attached to mesoglea. Therefore mesoglea was used and prepared as in Przysiezniak and Spencer (1989).

I tested the ability of different culture media to support cell survival and proliferation. The media tested were DMEM, RPMI1640, Williams' medium E, medium 199, NCTC 135, Waymouth medium MB 752/1, and Grace's insect medium. Of those commercial media, inorganic salts were added to provide the osmolarity to seawater. One medium was formulated according to the analysis of free amino acids in cnidarians (Table A1, Lane and Pringle 1965, Webb and Schimpf 1972, Shick 1976). Sera from different hosts were also tested. Conditioned media from cultures of dissociated jellyfish cells or pieces of jellyfish tissues were also tested. Homogenates of jellyfish tissues (either heat-treated at 100°C for 10 minutes or not) were also added into culture media to test if they would support cell proliferation or induce cell differentiation. The pH of the above media were adjusted to 7.5 or 8.0. No visible cell proliferation has been observed when PERCOLL-separated interstitial cells were maintained in these media. Seeded cells died out gradually in 2-3 months and cells did not attach to the mesoglea-coated substrate. Cells obtained from different sources, i.e. young vs. old jellyfish and wounded vs. intact tentacles, did not show any difference in their ability to survive or proliferate *in vitro*. Alternatively, tissues without enzyme dissociation were used to initiate cultures. No visible cell proliferation was observed in this kind of preparation.

Some possible mitogens were also tested for their ability to stimulate cell proliferation *in vitro*. I have used *Hydra* Head Activator (HHA)(Schaller 1973) and Proportion Altering Factor (PAF)(Plickert 1987) as possible mitogens in my system. These two factors are known to promote cell proliferation or neuronal differentiation in *Hydra* and *Hydractinia* (Schaller 1976, Plickert 1989). Unfortunately, no significant effects were observed with cultured cells from *Polyorchis*. The reason for this may be because these two factors are the priming factors which drive pluripotent interstitial cells into the neuronal pathway, but they are not mitogens. One transdifferentiation study in the jellyfish, *Podocoryne carnea,* showed that PAF increased the number of RFamide positive neurons only when PAF was applied to cells prior to or during entrance into S phase (Schmid and Plickert 1990). Thus one may need to apply a mitogen with the differentiation factor.

Some chemicals involved in second messenger systems, such as TPA (phorbol 12-myristate 13-acetate) and DAG (diacylglycerol) have been shown to interfere with morphogenesis in *Hydra* and jellyfish (Greger and Berking 1991, Kurz and Schmid1991). I have tested the effects of these chemicals on isolated *Polyorchis* interstitial cells with no significant effect being observed.

Table A1. Components of the jellyfish culture medium*#

Component	Concentration (mg/l)
Inorganic Salts	
NaCl	17600
Na2SO4	2953
MgCl2	3153
KCl	506
CaCl2	888
Other components	
Glucose	2000
Lactalbumin	1600
Bovine Serum Albumin	1000
Taurine	200
Hepes	5958
Phenol Red	5
Amino Acids	
L-Arginine	252
L-Alanine	89
L-Asparagine	150
L-Aspartic acid	133
L-cystine	48
L-Glutamine	584
L-Glutamine Acid	147
Glycine	75
L-Histidine.HCl.H2O	84
L-Hydroxyproline	20
L-Isoleucine	105
L-Leucine	105
L-Lysine.HCl	145
L-Methionine	30
L-Phenylalanine	66
L-Proline	115
L-Serine	105
L-Threonine	95
L-Trytophan	20
L-Tyrosine	72
L-Valine	94
Vitamins	
D-Ca Pantothenate	2
Choline Chloride	2

Table A1. Continued

Component	Concentration (mg/l)
Folic Acid	2
i-Inositol	4
Nicotinamide	2
Pyridoxal.HCl	2
Riboflavin	0.2
Thiamine.HCl	2

*Concentrations of amino acids are formulated in according to studies on free amino composition of cnidarians (Lane and Pringle 1965, Webb and Schimpf 1972, Shick 1976).
#Fetal bovine serum is added at final concentration of 2% and lipid concentrate (Gibco RBL) is added at final concentration of 1%.

REFERENCES

David, C. N. and Hager, G. (1994). Formation of a primitive nerveous system: nerve cell differentiation in the polyp of hydra. *Perspect. Dev. Neurobiol.* **2**: 135-140.

Greger, V. and Berking, S. (1991). Nerve cell production in Hydra is deregulated by tumour-promoting phorbol ester. *Roux's Arch. Dev.l Biol* **200**, 234-236.

Kurz, E., and Schmid, V. (1991). Effects of tumor promoters and diacylglycerol on the transdifferentiation of striated muscle cells of the medusa *Podocoryne carnea* to RF-amide positive nerve cells. *Hydrobiologia* **216/217**, 11-17.

Lane, C. E.and Pringle, E. (1965). Amino acids in extracellular fluids of *Physalia physalis* and *Aurelia aurita*. *Comp. Biochem. & Physiol.* **15(2)**, 259-62.

Plickert, G. (1987). Low-molecular-weight factors from colonial hydroids affect pattern formation. *Roux's Arch. Dev.l Biol.* **196**, 248-256.

Plickert, G. (1989). Proportion-altering factor (PAF) stimulates nerve cell formation in *Hydractinia echinata*. *Cell Diff & Dev* **26**, 19-27.

Przysiezniak, J. and Spencer, A. N. (1989). Primary culture of identifies neurons from a cnidarian. *J. Exp. Biol.* **142**, 97-113.

Schaller, H. C. (1973). Isolation and characterization of a low-molecular-weight substance activating head and bud formation in hydra. *J. Embryol. & Exp. Morph.* **29**, 27-38.

Schaller, H. C. (1976). Action of the head activator on the determination of interstitial cells in hydra. *Cell Diff* **5**, 13-25.

Schmid, V. (1992). Transdifferentiation in medusae. Intl. Rev. Cyto. 142: 213-261.

Schmid, V. and Plickert, G. (1990). The proporttion altering factor (PAF) and the in vitro transdifferentiation of isolated striated muscle of jellyfish into nerve cells. *Differentiation* **44**, 95-102.

Shick, J. M. (1976). Free amino aicds in *Aurelia aurita* scyphistomae from Corpus Christi, Texas. *Comp. Biochem. and Physiol.* **53B**,1-2.

Webb, K. L. and Schimpf, A. L. (1972). Free amino acid composition of scyphozoan polyps of *Aurelia aurita*, *Chrysaora quinquecirrha* and *Cyanea capillata* at various salinities. *Comp. Biochem. and Physiol.* **43B**, 653-663.